Battelle

Final Report No. 12-180

Final Report

Track Record of In-Line Inspection as a Means of ERW Seam Integrity Assessment

J. F. Kiefner, K.M. Kolovich, C.J. Macrory-Dalton, D.C. Johnston, C.J. Maier, and J.A. Beavers

November 15, 2012

Kiefner & Associates, Inc.
585 Scherers Court ***(614) 888-8220***
Worthington, Ohio 43085 ***www.kiefner.com***

Det Norske Veritas (U.S.A.), Inc.
5777 Frantz Road ***(614)761-1214***
Dublin, Ohio 43017 ***www.dnv.com***

0533-1101

Intentionally blank

Final Report No. 12-180

Final Report

on

TRACK RECORD OF IN-LINE INSPECTION AS A MEANS OF ERW SEAM INTEGRITY ASSESSMENT

to

BATTELLE

AS THE DELIVERABLE OF SUBTASK 1.3 ON
U.S. DEPARTMENT OF TRANSPORTATION
OTHER TRANSACTION AGREEMENT NO. DTPH56-11-T-000003

November 15, 2012

by

J. F. Kiefner, K.M. Kolovich, C.J. Macrory-Dalton, and D.C. Johnston

Kiefner and Associates, Inc.
585 Scherers Court
Worthington, Ohio 43085

C.J. Maier and J.A. Beavers

Det Norske Veritas (U.S.A.), Inc.
5777 Frantz Road
Dublin, Ohio 43017

0533-1101

DISCLAIMER

EXECUTIVE SUMMARY

The purpose of this project was to determine the reliability of in-line inspection (ILI) crack-detection tools with respect to characterizing the nature and severity of ERW line pipe seam anomalies. Anomaly characterization results from 13 ILI crack-tool runs in segments of ERW pipelines were compared to findings from excavations and direct examinations of samples of the anomalies located by the tools. The 13 cases of ERW seam integrity assessments described in this document involved three different types of in-line inspection (ILI) technologies:

- Nine cases involved ultrasonic angle-beam inspections for crack detection (2 vendors).
- Three cases involved circumferential magnetic-flux leakage (CMFL) inspections for detecting axially-oriented anomalies (2 vendors).
- One case involved an Electromagnetic Acoustic Transducer (EMAT) inspection for crack detection (1 vendor).

The inspections covered 741 miles of liquid, highly volatile liquid (HVL), and natural gas pipelines comprised of low-frequency-welded ERW (LF-ERW) pipe, direct-current-welded ERW (DC-ERW) pipe, and/or high-frequency-welded ERW (HF-ERW) pipe.

In some of the cases examined herein, the effectiveness of the ILI was investigated not only by means of field-NDE techniques but also by direct means such as a subsequent hydrostatic test, removal of anomalies and breaking them open to reveal their nature and dimensions, and/or burst testing of removed samples of pipe. In the remaining cases discussed herein, verification of the effectiveness of the ILI was accomplished solely by the use of field non-destructive examination (NDE) to characterize the dimensions of anomalies located by the tools.

Among the 13 cases examined, there was no case for which the investigating team is willing to say that the inspection provided full confidence in the seam integrity of the assessed segment. There are various reasons for this.

1. For Cases 1, 2, and 4-6, the verification of the ultrasonic crack detection ILI effectiveness was solely dependent on field NDE. Field NDE as typically practiced (that is without any blind calibration) is not reliable. In Cases 1 and 2, the Field-NDE-predicted anomaly depths exceeded the ILI-predicted anomaly depths. In contrast, in Cases 4-6 the ILI-predicted anomaly depths were often twice the depths predicted by Field-NDE. Therefore, without knowing which if either depth predictions are correct these attempts to verify ILI performance via Field NDE only are insufficient to provide confidence in seam integrity.

2. For Cases 3, 7, and 12, metallurgical examinations or follow-up hydrostatic tests revealed the existence of anomalies that were missed by the ultrasonic crack detection ILI even though the lengths and depths of the anomalies exceeded the threshold detection limits of the tools. The metallurgical examinations in Case 3 suggested that the Field NDE depths and lengths in that case reasonably matched the actual lengths and depths and that the ILI tended to overcall the depths by as much as 2 to 1. Field NDE revealed one anomaly that was missed by the ILI even though the depth and length of the anomaly exceeded the threshold values for detection. The hydrostatic test in Case 7 resulted in the failures of two anomalies not detected by the ILI at stress levels below 100% of SMYS suggesting that the anomalies were large enough to have been detected by the ILI. The metallurgical examinations of several anomalies following the ILI in Case 12 revealed an anomaly that had been missed by the ILI even though its depth and length exceeded the detection thresholds of the ILI tool.
3. For Case 8, a service failure that occurred 2 years after an ILI, appeared to have originated at a seam anomaly large enough to have been detected by the ultrasonic crack tool. This occurrence clearly shows that the seam integrity was not assured by the ILI.
4. For Cases 9, 10, and 13, where a CMFL tool was used, it is clear that the CMFL ILI could not reliably find some crack-like defects that would likely impair the integrity of the ERW seam[1].
5. For Case 11, although the EMAT tool was shown able to find some ERW seam anomalies, there was insufficient information to evaluate the tool let alone prove its effectiveness.
6. The results of some of the burst tests and hydrostatic tests show that the failure-stress-prediction models that are typically used by ILI vendors and pipeline operators to predict failure stresses for anomalies in or adjacent to LF-ERW or DC-ERW seams do not give reliable predictions of the actual failure stresses.

This study did not systematically examine the reasons why the various inspections did not correctly identify some of the anomalies in the ERW seams. In a few cases, the answer was obvious. In the one case where EMAT technology was used, the primary purpose of the run was to detect SCC not to detect ERW seam anomalies. In this case, the EMAT tool did identify ERW seam anomalies, but the vendor declined to categorize the depths of the anomalies. In the cases where the CMFL technology was used, the vendors do not claim to be able to detect tight cracks. Many ERW seam anomalies would tend to have widths well below the CMFL tool's width detection threshold of 0.004 inch (one vendor) or 0.008-inch (another vendor). In the remaining cases, where ultrasonic crack detection technology was used, the reasons for the ILI missing or mischaracterizing some important anomalies are not clear. The reviews of these 13

[1] These CMFL tool runs were done without "enhanced filtering" a technique which has been introduced by one pipeline operator. The presentation entitled "KMAP™ for Longitudinal Weld Threat Analysis" given by Noel Duckworth on behalf of Kinder Morgan at the PHMSA Pipeline Seam Weld Workshop in Arlington, VA on July 20, 2011 introduced a new procedure for improved analysis of CMFL data. The results mentioned in that presentation suggest the CMFL technology used with enhanced filtering could be significantly more effective than was demonstrated by the cases reviewed in this document.

cases consistently point to two significant weaknesses in the use of ILI crack-detection tools for ERW seam assessment. One weakness relates to the ILI itself. The sizing accuracies for anomaly length and depth leave something to be desired. More importantly, defects with sizes exceeding the threshold detection limits of the tools were missed. The other significant weakness is related to the fact that field NDE measurements of the lengths and depths of anomalies are unreliable and should not be considered as a sufficient means to "prove-up" ILI crack-detection tool results unless the NDE methods have been carefully calibrated for the pipeline being inspected.

A third weakness in the use of ILI crack-detection tools for ERW seam integrity assessment that may not be obvious from the reviews of these 13 cases has to do with calculating failure stress levels and predicting remaining lives of anomalies found and sized by the ILI. In several instances, the failure stresses predicted by often-used ductile fracture initiation models did not agree with the actually observed failure stresses in burst tests conducted in conjunction with some of the cases examined herein. Because of this and because of the previously mentioned weaknesses, the operator of an ERW pipeline really cannot have confidence that the seam integrity has been validated even though the lengths and depths of the detected anomalies are given, the failure stress levels and remaining lives have been calculated, and the ostensibly injurious anomalies indicated thereby have been repaired.

The inability of a failure-stress prediction model to consistently predict the failure stress of an ERW seam anomaly means that, even if the tools could accurately describe the sizes of anomalies, a reliable means of predicting the failure stresses of the pipes containing the anomalies would have to be discovered or developed. Most likely, this deficiency results from the inability to accurately characterize the strength and toughness of the material in the vicinity of an ERW seam, particularly, near defects in LF-ERW and DC-ERW seams.

The results of the inspections described herein should not discourage the use of these ILI technologies for ERW seam integrity assessment. Even as the technology exists at this time, the tools clearly are useful for finding and eliminating some seam defects. Only by continuing to use the tools can pipeline operators expect to see the technologies improve to the point where they can have a high degree of confidence in the ERW seam integrity of an inspected pipeline.

The facts that ILI technology continues to improve and that continued use of the tools is one of the best ways to evaluate them, strongly suggest that ILI crack-detection technology should continue to be accepted as one component of an f ERW seam-integrity assessment. However, more rigorous verification of tool performance is needed. For future use of ILI tools for ERW seam integrity inspection, the use of one or more of the following verification procedures is recommended.

- A hydrostatic test of the pipeline can be conducted to assess the integrity of the ERW seams.
- A field-NDE calibration program can be carried out. This could consist of blind examinations of ERW seams on pieces of ERW pipe either taken from the pipeline to be inspected or from pipe of the same manufacturer and vintage. The inspection results on these samples should be calibrated based on destructive metallurgical examinations of the located anomalies. After all located anomalies have been examined and compared to the NDE findings, the remaining pipe samples should be subjected to pressure testing to a level of at least 100% of SMYS to assure that no injurious defects were missed. By doing this, the pipeline operator can have some assurance that the dimensions of anomalies found by the ILI tool that are evaluated by field NDE will be believable.
- Samples of pipe containing anomalies found by the tool can be removed and subjected to metallurgical examination and/or burst testing. Direct examination of the dimensions of defects allows calibration of the dimensional accuracy of both the ILI and the field NDE. Samples not used for metallurgical examination can be subjected to burst testing to prove that no injurious anomaly was missed.

Eventually, as confidence in the capabilities of the technologies grows, the need for these verification procedures will diminish.

For a pipeline operator to have a high degree of confidence in the seam integrity of a pipeline comprised of ERW pipe, it will be necessary to demonstrate that the tools will reliably find and characterize any injurious seam anomaly. The first necessary improvement is for the technologies to be able to correctly classify the anomalies as cold welds (or lack of fusion), hook cracks, selective seam weld corrosion, an anomaly that has been enlarged by fatigue crack growth, or some combination of these. These different kinds of defects have different impacts on pipeline integrity. Hook cracks and defects enlarged by fatigue tend to behave in a relatively ductile manner and usually have to be relatively large to cause a pipeline to fail in service. Cold weld defects or selective seam corrosion defects, on the other hand, tend to cause brittle fracture, and they do not necessarily have to be large for that to occur. Even, without improved sizing capabilities, this improvement could lead to more efficient screening of anomalies. Ultimately, of course, full confidence in such tools will only come when it can be shown that they give reasonably accurate representations of the dimensions of anomalies.

Finally, there is the question of what to do about the apparent inability of typical failure stress prediction models to accurately predict the failure stress levels of flaws in or adjacent to ERW seams. The problem may not be the models themselves; they certainly have been well-validated for flaws in ductile pipe parent metal. The problem is that the strength and toughness of the ERW weld zone are usually quite different from the parent metal, and notoriously difficult to measure. No model will be satisfactory until or unless the applicable strength and toughness are known and the model is capable of predicting failure stresses for anomalies that may fail in a brittle manner. Efforts are underway on other tasks within this research project that may shed light on how to get the applicable strength and toughness and reveal models that may be better suited to predicting the failure stress levels of anomalies in brittle materials. In the meantime, pipeline operators utilizing ILI crack-tool technology for ERW seam assessment should continue to use available models to prioritize excavations, but once the anomalies have been characterized, the focus should be on consideration of the dimensions and type of anomalies. Conservative repair criteria should be followed in the absence of certainty about the strength and toughness of the ERW seam.

Intentionally blank

Table of Contents

LIST OF FIGURES

LIST OF TABLES

Intentionally blank

Track Record of In-Line Inspection as a Means of ERW Seam Integrity Assessment

J. F. Kiefner, K.M. Kolovich, C.J. Macrory-Dalton, D.C. Johnston, C.J. Maier, and J.A. Beavers

INTRODUCTION

This report presents the results of evaluations of ERW seam integrity assessments conducted by means of in-line inspection (ILI). The objective is to assess the effectiveness of ILI crack-tool inspections as a means of assessing seam integrity for pipelines comprised of ERW pipe and flash-welded pipe.

Acknowledgement

The authors are grateful for the contributions of data from numerous pipeline operators. In many cases, we adopted or modified their spreadsheets of data for use in this document.

BACKGROUND

The value of an ILI crack-tool seam-integrity inspection depends on the ability of the tool to detect and characterize ERW seam anomalies to the extent that the pipeline operator can find and eliminate those anomalies that could threaten the integrity of the pipeline. The value of the inspection also depends on being able to quantify the effects of anomalies on pipeline integrity so as to identify anomalies that threaten integrity immediately or in the near term and to assess the remaining life of those anomalies that do not immediately threaten the integrity of the pipeline.

In theory, ILI tool-reported depths and lengths of crack-like anomalies and wall thicknesses of the pipe allow one to calculate the effects of a given anomaly on the remaining strength of the pipe. That can be done if the applicable level of fracture toughness is known and if the algorithm used to calculate the remaining strength accurately reflects the properties of the material and the characteristics of the anomalies. The local fracture toughness of any given piece of pipe is generally not available. Usually, the best that can be done is to assume a conservative value based on measurements made on samples of the pipe or based on historic data for similar pipe. The validity of the calculations of remaining strength also depends on the accuracy of the model used to calculate remaining strength.

A major factor to be established for any given ILI tool run is the level of accuracy of the tool with respect to detecting, characterizing, and sizing the anomalies. Vendors' websites provide stated accuracies of their ILI tools as shown in the following table. The abbreviation "CMFL" stands for circumferential magnetic flux leakage. The abbreviation "t" stands for wall thickness of the pipe.

Type of Tool	**Number of Cases Discussed Herein**	**Minimum Length Detection Threshold**	**Minimum Depth Detection Threshold**	**Crack Opening Detection Limit**
Ultrasonic Vendor 1	8	30 mm (1.2 inch)	1 mm (0.04 inch)	<0.1 mm (<0.004 inch)
Ultrasonic, Vendor 2	1	30 mm (1.2 inch)	1 mm (0.04 inch) pipe body 2 mm (0.08 inch) in long seam	Not stated
CMFL Vendor 1	1	50 mm (2 inches)	0.25t	>0.1 mm (>0.004 inch)
CMFL Vendor 2	2	Not stated	0.2t with 90% certainty if width > 1 mm (0.04 inch)	>0.2 mm (>0.008 inch)
EMAT	1	40 mm (1.57 inch)	1 mm (0.04 inch) pipe body 2 mm (0.08 inch) in long seam	Not stated

In addition to providing detection, location, and sizing of anomalies, the vendors attempt to identify the "type" of anomaly. For ultrasonic tools including the EMAT tool, the types of anomalies most commonly called out are "weld anomaly", "notch-like", "crack-like", and "crack field". Firm definitions of these terms may or may not be provided in the vendor's report, but the terms are generally regarded to mean the following.

- Weld anomaly A seam irregularity involving wall thickness such as excess trim, grooving corrosion, or mismatched edges.
- Notch-like A groove along or in the weld such as grooving corrosion, a contact burn or gouge.
- Crack-like An anomaly such as a hook crack, cold weld or lack of fusion, or a weld-area crack.
- Crack field An anomaly comprised of more than one crack.

For the CMFL tool, the type of anomalies called out are Type A anomalies (those having all of the characteristics of crack-like anomalies), Type B anomalies (those having some of the characteristics of crack-like anomalies, and Seam anomalies which are seam irregularities involving wall thickness such as excess trim, grooving corrosion, or mismatched edges.

"Effective" tool accuracy, for a given tool run, must be established by comparisons between the called attributes of the anomalies and the actual attributes of the anomalies as determined by direct examinations consisting of one or more of the following: field examinations using non-destructive examination (NDE) methods of various types, a hydrostatic test conducted to adequate levels either just prior to or shortly after the ILI tool run, removal of samples containing ILI-tool-called anomalies that are subjected either to burst tests or metallurgical examinations or both.

Pipeline operators typically prioritize anomalies by their predicted failure stress levels or remaining lives or both based upon the ILI vendor's listings of lengths and depths of the anomalies. In most cases, the vendor makes the calculations of failure stresses and remaining lives for the operator using a predictive model of choice such as the API 579 Level 2 approach, the Modified LnSec Equation, Corlas™, or PAFFC. The models are based on the assumption that the material will behave in a relatively ductile manner in the presence of a longitudinally-oriented anomaly subjected to hoop stress, and they tend to give similar answers for a given anomaly and particular values of flow strength and toughness. For the 13 cases discussed herein, the flow strength values were based on specified minimum yield strength (SMYS), specified minimum ultimate strength, or a combination of the two. The toughnesses of the ERW seam welds were assumed to correspond to full-size Charpy V-notch upper shelf energy levels, and levels of 20 ft lb, 7 ft lb, and 1 ft lb were used in different situations as will be explained.

The 13 case studies evaluated in this report provide insight into how well ILI crack-tools are working in terms of providing confidence in the seam integrity of a pipeline. Before these cases are discussed, however, it is important to note that there are at least three cases known to the investigating team where in-service pipeline failures occurred within two years after ILI crack-tool runs. These three failures are as follows.

Table 1. ERW Seam Failures That Occurred Within 2 Years of an ILI Seam Inspection

Failure Number	Year of Failure	Failure Stress, %SMYS	Type of Anomaly	Length of Anomaly, inches	Depth of Anomaly, % of Wall	Type of Tool	Year of Tool Run	As Called on the Basis of the Tool Data
1	2007	71.0	hook crack	2.4	27%	Ultrasonic crack-detection tool	2005	no indication
2	2006	59.8	hook crack + fatigue	9.5	hook crack 45% extended by fatigue to 80%	Circumferential MFL tool	2005	non-injurious indication
						Ultrasonic crack-detection tool	2005	non-injurious indication
3	2011	61.0	damaged skelp edge + fatigue	damaged skelp edge 27 fatigue 8.5	damaged skelp edge 46% extended by fatigue to 86%	Circumferential MFL tool	2009	evaluated as metal gain
						Ultrasonic crack-detection tool	2010	no crack-like indications

The attributes of the three pipelines involved in these failures are as follows.

Table 2. Attributes of Pipelines Where ERW Seam Failures Occurred After an ILI Seam Inspection

Failure Number	Fluid	Pipe Diameter, inches	Wall Thickness, inch	Grade	Seam Type
1	HVL	12.75	0.250	X52	LF-ERW
2	Liquid	12.75	0.203	X52	LF-ERW
3	Liquid	18	0.219	X52	DC-ERW

SPECIFIC CASES OF ILI CRACK-TOOL INSPECTIONS

Presented below are thirteen cases of ILI crack-tool runs where extensive follow-up work was done. In 12 of the 13 cases, the results were made available in confidence by pipeline operators. In the remaining case, the results are based on a technical paper available in the public domain. A summary of the cases is provided in Table 3.

Table 3. Cases of ERW Seam Inspections Discussed in This Document

Case Number	Year Installed	Manufacturer	Liquid or Gas	Diameter, inch	Wall Thickness, inch	Grade	Seam Type	Miles	Year of ILI	Type of ILI
1	1953	Youngstown	Liquid	16	0.281	X52	DC ERW	29.9	2007	Ultrasonic crack-detection tool
2	1966	Bethlehem	Liquid	16	0.312	X52	LF ERW	53.9	2007	Ultrasonic crack-detection tool
3	1961	Page Hersey	Liquid	12.75	0.219 & 0.250	X52	LF ERW	54	2008	Ultrasonic crack-detection tool
4	1986	Stelco	Liquid	12.75	0.25 & 0.375	X56	HF ERW	64	2008	Ultrasonic crack-detection tool
5	1961	Alberta Phoenix	Liquid	12.75	0.250	X52	LF ERW	40	2008	Ultrasonic crack-detection tool
6	1961	Prairie Pipe	Liquid	12.75	0.250	X52	LF ERW	16	2008	Ultrasonic crack-detection tool
7	1953	Youngstown	Liquid	16	0.250	X42	DC ERW	21.8	2007	Ultrasonic crack-detection tool
8	1961	Lone Star	HVL	12.75	0.250	X52	LF ERW	120.3	2005	Ultrasonic crack-detection tool
9	1961	Lone Star	HVL	12.75	0.250	X52	LF ERW	120.3	2008	Circumferential MFL
10	1956	Lone Star/A.O. Smith	Gas	16	0.250	X52	LF ERW	64	2007	Circumferential MFL
11	1960	Lone Star	Gas	16	0.260	X52	LF ERW	18	2009	EMAT
12	1968	Youngstown/U.S. Steel	Liquid	20	0.230/0.219	X52	DC ERW/HF ERW	139	2009	Ultrasonic crack-detection tool
13	1943	Youngstown	Gas	20	0.375	Grade B	DC ERW	23	1999	Circumferential MFL

The total mileage covered by these cases is 741 miles.

Case 1

Pipeline Attributes and Inspection Parameters

A 30-mile segment of a liquid pipeline comprised of 16-inch-OD, 0.281-inch-wall, X52 direct-current-welded ERW pipe manufactured by Youngstown Sheet and Tube Company installed in 1953 was inspected by means of an ultrasonic crack-detection tool. The maximum operating pressure of the pipeline corresponds to 54% of SMYS. The year of inspection was 2007. This segment had experienced no in-service failures. The seam integrity of this segment was assessed by means of hydrostatic testing in 1994 and 2012. The 1994 hydrostatic test was carried out at stress levels ranging from 69% to 71% of SMYS. No test failures occurred. The 2012 hydrostatic test was carried out to a minimum stress level of 88% of SMYS. No test failures occurred.

As a result of the 2007 ILI crack-tool run, 60 seam anomalies (average of 2 per mile) were reported and 12 of these were subjected to examination in the field. The field examinations consisted of visual inspection and magnetic particle inspection (MT) to characterize the type and length of the anomaly and ultrasonic inspection (UT) to measure the depth of the anomaly or, in the case of an internal anomaly, to characterize the length of the anomaly as well. None of the anomalies was removed for either burst testing or metallurgical examination. The history of the segment since the inspection involves no seam failure incident.

The breakdown of the 60 anomalies indicated by the ILI by type of anomaly is: Weld Anomaly (8), Notch-Like (25), Crack-Like (25), and Crack Field (2). The breakdown of the 12 anomalies subjected to field examination by type of anomaly is: Weld Anomaly (5), Notch-Like (2), Crack-Like (4), and Crack Field (1). The rationale for choosing anomalies to examine appeared to have been based both on the lowest predicted failure stresses and the type of anomaly. All 12 field-examined anomalies were repaired by means of Type B sleeves.

Comparisons between ILI Dimensions and Field-Measured Dimensions

Comparisons between the ILI anomaly dimensions and those measured in the field are presented in Table 4. The first two columns in Table 4 present comparisons between the types of anomalies indicated by ILI and the nature of the anomaly as it appeared to the field investigators. The other columns present comparisons between ILI size parameters and the size parameters that field investigators were able to measure. As seen in the table, some elements of data are missing from the field measurements. In these cases, the missing elements were depths of the field-examined anomalies. In one case no anomaly was found. Apparently, because the other three anomalies in question were not cracks, no depths were recorded.

Table 4. Comparison between ILI and Field-Measured Parameters for Case 1

Anomaly Number	Type of Anomaly		Length, inches		Depth, % Wall Thickness		Wall Thickness, inch	
	ILI	Field	ILI	Field	ILI	Field	ILI	Field
1	Weld Anomaly	No anomaly found	5.1		25.0		0.256	0.270
2	Weld Anomaly	Seam Misalignment	15.1		25.0		0.268	0.375
3	Weld Anomaly	Seam Misalignment	11.3		25.0		0.268	
4	Notch-Like	Undercut	23.8		25.0		0.287	0.290
5	Weld Anomaly	Metal Loss in Seam	2.6	2.2	40.0	54	0.287	0.280
6	Crack-Like	OD Crack	4.0	4.7	25.0	15	0.287	0.300
7	Weld Anomaly	ID seam Crack	1.4	2.9	25.0	37	0.287	0.313
8	Crack Field	OD Crack	1.2	3.4	40.0	62	0.287	0.292
9	Crack-Like	OD seam Crack	1.8	4.8	12.5	27	0.287	0.270
10	Crack-Like	ID seam Crack	5.8	5.8	25.0	27	0.287	0.316
11	Crack-Like	two OD cracks	2.9	8.4	25.0	42	0.268	0.283
12	Notch-Like	OD seam Crack	8.8	14.8	12.5	70	0.268	0.286

In terms of type of anomaly, the field-observed type probably depends somewhat on the field investigator's personal preference. Terms such as undercut or metal loss in the seam may not adequately describe the anomaly. The term undercut is usually associated with a weld involving electric arc welding. Undercut occurs where the electric arc has melted base metal but has not filled the gap with deposited weld metal. It is difficult for an individual not present at the field site to picture what undercut means in terms of an ERW seam. It could mean "over-trim" which refers to a situation where trimming of the weld flash by the manufacturer removed too much material. Similarly, metal loss in the seam could mean that selective seam weld corrosion had occurred, but it could also refer to over-trim. Other terms used by the field investigator such as seam misalignment, OD crack and OD seam crack are more easily pictured by an individual not present at the field site.

An interesting and possibly significant aspect of the anomaly-type comparisons is that, aside from the fact that no anomaly was found corresponding to Anomaly 1, weld-anomaly calls (except in one case) tended to be non-crack features whereas cracks tended to be present when the anomaly had been called crack-like or crack field.

The comparisons between field-measured and ILI anomaly dimensions listed in Table 4 are illustrated in Figure 1, Figure 2, and Figure 3 for anomaly depth, anomaly length, and pipe thickness, respectively.

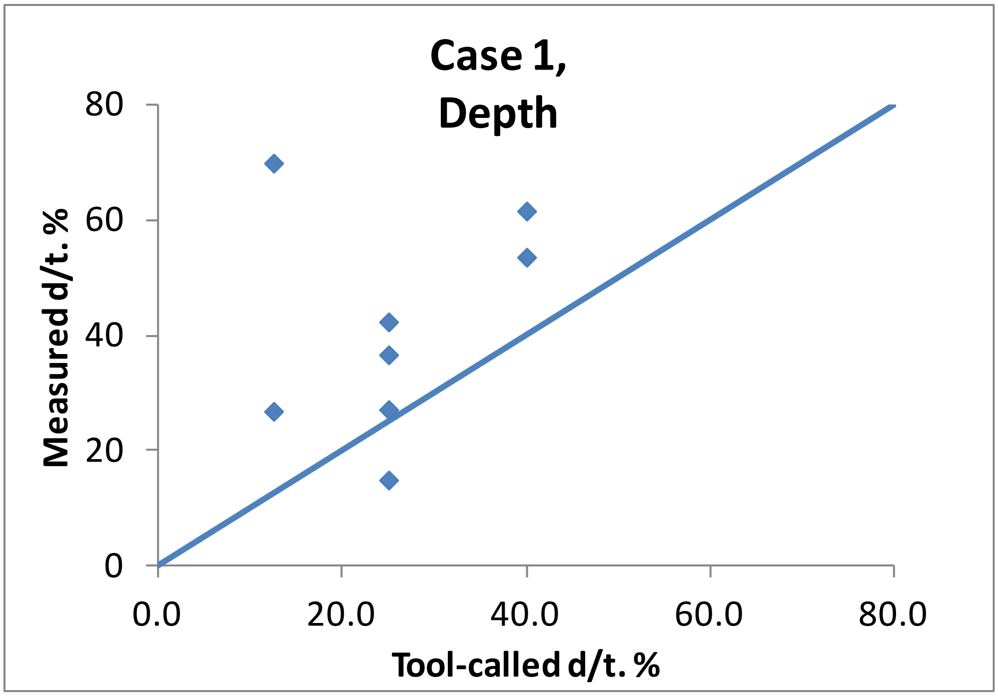

Figure 1. Comparisons between Field-determined Anomaly Depth and ILI Anomaly Depth, Case 1

It is seen in Figure 1 that the ILI dimensions are clustered at values of 12.5%, 25%, and 40%. That is because the depth-sizing capability of the tool was such that depth could only be categorized as being between 0% and 12.5% of the wall thickness, between 12.5% and 25% of the wall thickness, between 25% and 40% of the wall thickness, or greater than 40% of the wall thickness. In each case, the investigating team member took the depth of the anomaly to be the highest value in the particular range.

It is also seen in Figure 1 that one value of measured depth (Anomaly No. 12) is way out of line with the ILI depth (d/t of 70% as field-measured versus d/t of 12.5% from ILI). Otherwise the field-measured and ILI depths seem to be aligned within some reasonable scatter band.

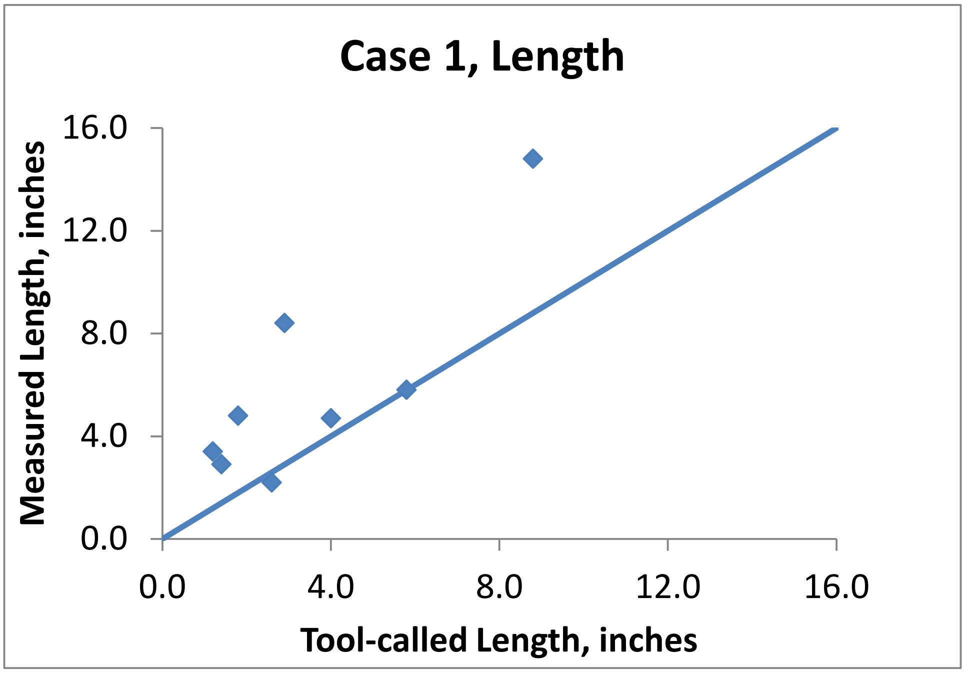

Figure 2. Comparisons between Field-determined Anomaly Length and ILI Anomaly Length, Case 1

The ILI lengths were almost always shorter than the field-measured lengths as shown in Figure 2. This is believed to be at least partly the result of the tool not being able to detect the very shallow parts of a crack where it tapers back to zero depth at its ends. In any case, the lack of match-up in length is less of a concern than an inability to get accurate depths because the failure stress of an axially-oriented defect in a pressurized pipe is much more depth-dependent than length-dependent for defect lengths greater than the square root of the quantity diameter times wall thickness.

Figure 3 illustrates the degree to which the wall thicknesses by ILI aligned with those measured in the field. When one considers the small range of thicknesses over which the comparisons are made, the relationship shown in Figure 3 reflects a reasonable comparison between ILI and field-measured wall thickness. Note that the ILI wall thickness at Anomaly No. 2. (0.268 inch) is out of line with the field-measured value of 0.375 inch. The scale of Figure 3 is too limited to allow this value to be plotted. This may be a case where the anomaly was in a short segment of heavier-wall pipe at a road crossing.

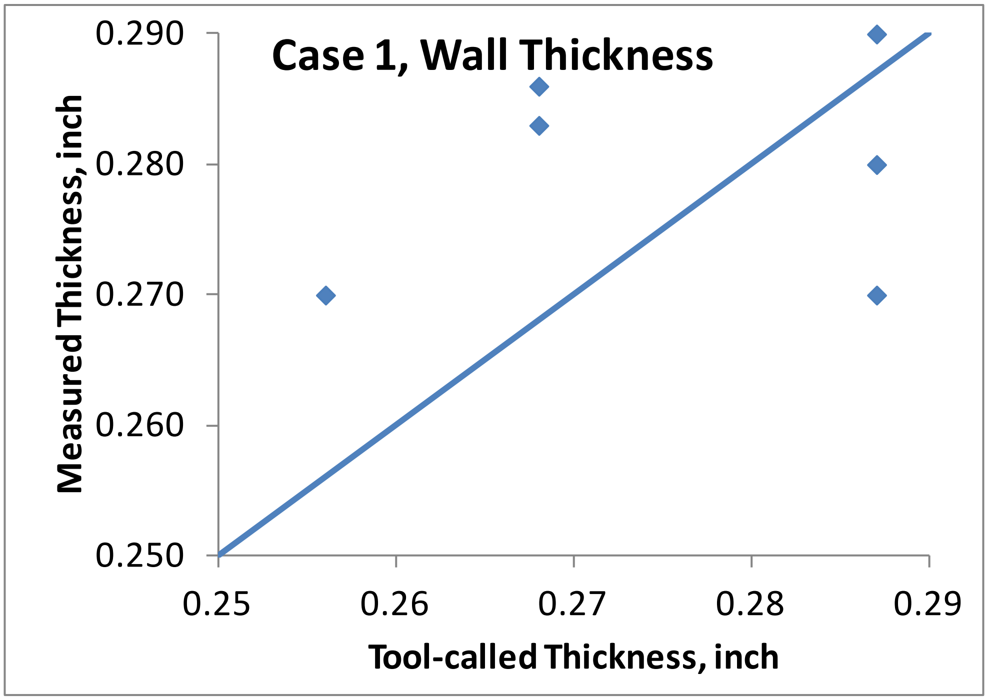

Figure 3. Comparisons between Field-determined Wall Thickness and ILI Wall Thickness, Case 1

A comparison between failure stresses of the anomalies calculated on the basis of ILI dimensions and those calculated on the basis of field-measured dimensions is presented in Figure 4. Failure stress levels for these anomalies were calculated using the Modified Ln-Sec Equation Elliptical C-Equivalent model with a full-size-equivalent Charpy upper shelf energy of 20 ft-lb[2]. In one case (Anomaly No. 12), the calculated failure stress based on the ILI dimensions was 105% of SMYS. In contrast, the calculated failure stress based on the field-measured dimensions was 33% of SMYS. The disparity is largely the result of the large difference between the ILI depth (12.5% of wall thickness) and the field-measured depth (70% of wall thickness).

Because the calculated failure stress based on the field-measured depth is well below the maximum operating pressure of the pipeline (54% of SMYS), and because the pipeline was hydrostatically tested to a stress level of 69 to 71% of SMYS in 1994, the calculated failure stress and the field depth measurement on which it largely depends are suspect.

[2] A Charpy energy of 20 ft lb was used by the vendor in several of the cases for reasons not clear to the investigating team. In many cases, the team retained the 20 ft lb value because it is not out of line with the levels one typically measures in the base metal of most 1950s and 1960s vintage line pipe materials

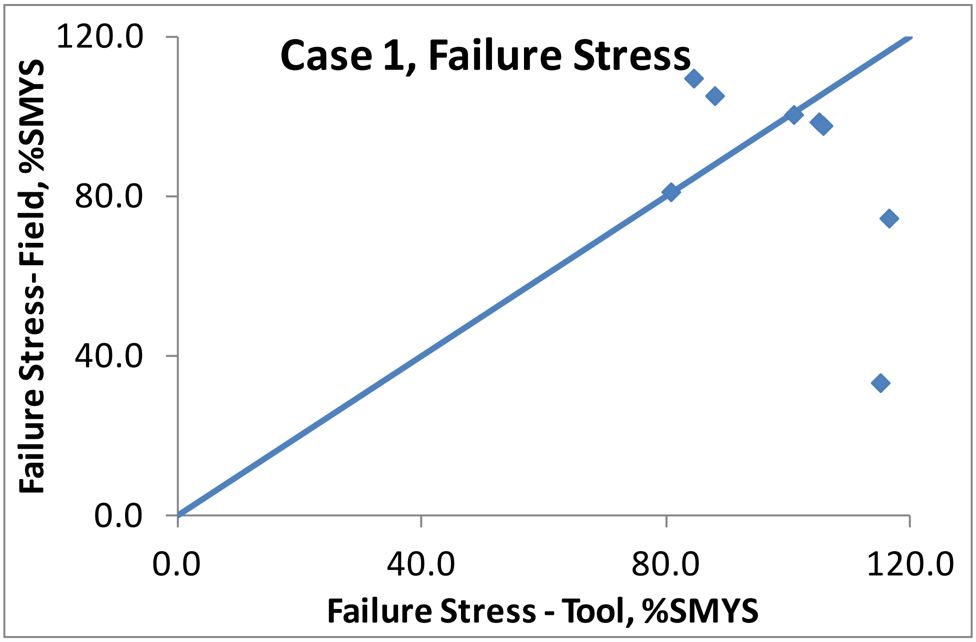

Figure 4. Comparisons between Predicted Failure Stresses Based on Field-Measured Anomaly Dimensions and Those Based on ILI Dimensions, Case 1

Comparisons between ILI Findings and Subsequent Service History

As noted previously, at the time this report was being prepared (5 years after the ILI crack-tool inspection), no in-service seam leaks or ruptures have occurred. Note that the maximum operating stress of this segment is 54% of SMYS.

Comparisons between ILI Findings and Hydrostatic Test Results

Assessments of seam integrity of the Case 1 segment by means of hydrostatic testing consist of the manufacturer's (mill test) hydrostatic test (most likely to 85% of SMYS for 5 or 10 seconds in 1953), a 49 CFR 195, Subpart E hydrostatic test in 1994 to a minimum of 69% of SMYS, and a spike test to 88% of SMYS followed immediately by a 49 CFR 195, Subpart E test in 2012. A pre-service pressure test may have been performed, but no record of it was made available to the investigating team. The mill test was conducted too long ago to be relevant. In the 1994 test, there were no test breaks or leaks. However, the relatively low stress level employed and the age of the test tend to render any comparison between its results and the results of the 2007 ILI tool run unproductive. The 2012 spike test to 88% of SMYS which produced a hoop stress level of 1.63 times the maximum operating stress level of 54% of SMYS establishes a high degree of confidence in the integrity of this 30-mile segment. It shows, the 2007 ILI crack-tool run did not miss any significant defects, and that, if any significant defects did exist at the time, they were repaired.

Comparisons between ILI Findings and Burst Test Results

No samples of pipe containing ILI anomalies were available for the purposes of burst testing.

Comparisons between ILI Findings and Metallurgical Examinations

No samples of pipe containing ILI anomalies were available for the purposes of metallurgical examination.

Conclusions Regarding the Case 1 ILI Crack-Tool Run

Twelve comparisons between ILI anomalies and field measurements confirm that anomalies were found by the tool. The comparisons further show that the ILI (except in one case) was able to distinguish crack-like anomalies from non-crack-like anomalies. In one case, the field examination could not find the anomaly that had been indicated by ILI.

The comparisons of ILI versus field-measured anomaly dimensions indicate some degree of correlation, but one comparison of anomaly depth suggests that either the tool inspection or the field inspection was considerably inaccurate regarding the depth of the anomaly. Unfortunately, without the benefit of a burst test or a metallurgical examination, one cannot ascertain whether it was the ILI or the field measurement that was inaccurate. The overall conclusion is that the Case 1 ILI tool run results cannot be regarded as having proved the seam integrity of the segment to be adequate, although the integrity of the segment was adequately demonstrated by the fact that the segment survived a spike hydrostatic test to 88% of SMYS conducted in 2012.

The Case 1 example shows that trying to evaluate the quality of inspection for a given ILI run cannot always be done merely through field NDE. In this example, there is just as much reason to doubt the accuracy of the field NDE as there is to doubt the accuracy of the ILI inspection results, so the ILI results were not adequately validated. Hence, the operator really cannot have confidence that the seam integrity was validated by the 2007 ILI crack-tool inspection alone even though the failure stress levels of all detected anomalies were calculated, and their remaining lives were calculated.

Case 2

Pipeline Attributes and Inspection Parameters

A 54-mile segment of a liquid pipeline, comprised of 16-inch-OD, 0.312-inch-wall, X52 low-frequency-welded ERW pipe manufactured by Bethlehem Steel Corporation installed in 1966 was inspected by means of an ultrasonic crack-detection tool. The maximum operating stress of the pipeline corresponds to 71% of SMYS. The year of inspection was 2007. This segment had experienced no in-service failures. The seam integrity of this segment was last assessed by means of hydrostatic testing at the time of construction in 1966. The 1966 hydrostatic test was carried out at a stress level of 90% of SMYS. Twelve seam failures occurred, all of which initiated at seam manufacturing defects. The only information made available to this project concerning the 12 test failures is that all were in the seam, all fractures were brittle, and the anomalies that appeared to have initiated the failures were said to have been too small to have met the rejection criteria of API Standard 5L.

As a result of the 2007 ILI crack-tool run, 73 crack-like seam anomalies (average of 1.4 per mile) were reported and 12 of these were subjected to examination in the field. The field examinations mentioned in the documentation consisted of visual inspection and ultrasonic inspection. Four of the 12 anomalies were examined by a second NDE vendor. None of the anomalies was removed for either burst testing or metallurgical examination. The history of the segment since the inspection involves no seam failure incidents.

The 73 anomalies indicated by ILI were said to be crack-like. The rationale for choosing anomalies to examine appeared to have been based on the lowest values of predicted failure pressure. All field-examined anomalies appear to have been repaired, but the means of repair were not stated.

Comparisons between ILI Dimensions and Field-Measured Dimensions

Comparisons between the ILI anomaly dimensions and those measured in the field are presented in Table 5. The first two columns in Table 5 present comparisons between the type of anomaly indicated by ILI and the nature of the anomaly as it appeared to the field investigators. The other columns present comparisons between ILI size parameters and the size parameters that field investigators were able to measure. As seen in the table, some elements of data are missing from the field measurements for reasons that were not apparent to the investigating team (i.e., KAI, DNV, or Battelle).

Table 5. Comparison between ILI and Field-Measured Parameters for Case 2

Anomaly Number	Type of Anomaly		Length, inches		Depth, % Wall Thickness		Location (External or Internal)	
	ILI	Field	ILI	Field	ILI	Field	ILI	Field
1	Crack-Like	Lack of Fusion	2.6	2.6	25	39	Ext	Int
2	Crack-Like	Lack of Fusion	7.0	5.5	25	69	Ext	Ext
3	Crack-Like	Lack of Fusion	3.3	9.2	25	46	Ext	Int
4	Crack-Like	Lack of Fusion	9.3	9.5	25	49	Ext	Int
5	Crack-Like	Lack of Fusion	7.7	8.7	25	85	Ext	Int
6	Crack-Like	Lack of Fusion	6.3	6.3	25	65	Ext	Int
7	Crack-Like	Lack of Fusion	4.4	6.0	25	50		
8	Crack-Like	Lack of Fusion	5.0	4.3	25	7	Ext	Mid
9	Crack-Like	Lack of Fusion	4.7	4.0	25	60	Ext	Int
10	Crack-Like	Mismatched Seam	5.0	4.8	25	21	Ext	Ext
11	Crack-Like	Lack of Fusion	6.3	7.0	25	16	Ext	Int
12	Crack-Like	Lack of Fusion	3.7	4.3	25	17		Int

In terms of type of anomaly, 11 of the 12 anomalies were interpreted by field NDE to have been lack-of-fusion defects in the seam. One anomaly was said to have been a mismatched seam. Note that neither the wall thicknesses indicated by ILI nor those measured in the field were given. However, the locations (external or internal) of the anomalies were given as indicated by ILI and as observed in the field. The ILI indicated all flaws to be external except for two where the discrimination was not made. The field personnel called all but one of the lack-of-fusion defects as either internal or mid-wall. The ILI and field locations were in agreement only for one of the lack of fusion anomalies (Anomaly 2) and the seam mismatch (Anomaly 10).

The comparisons between field-measured and ILI anomaly dimensions listed in Table 5 are illustrated in Figure 5 and Figure 6 for anomaly depth and anomaly length, respectively.

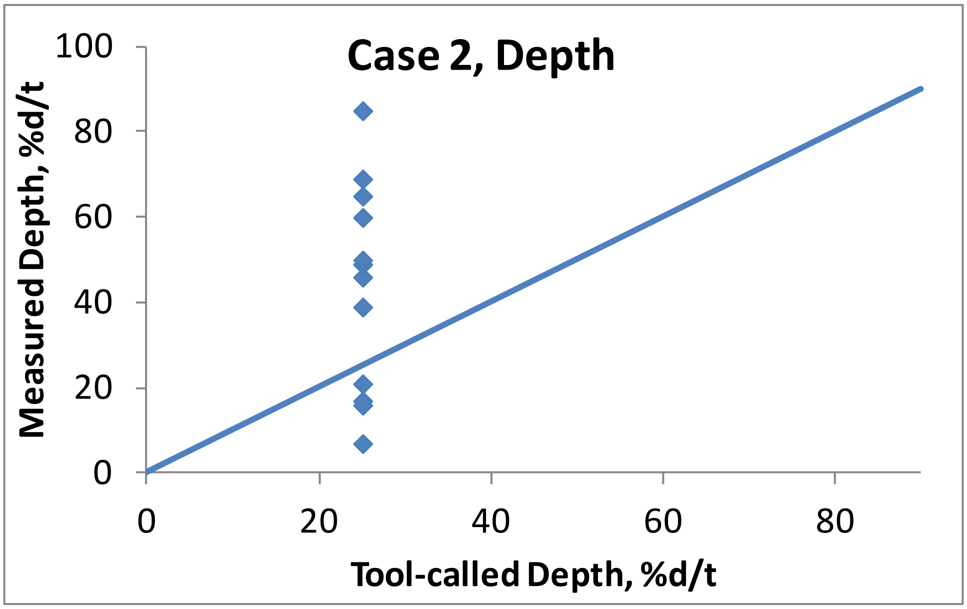

Figure 5. Comparisons between Field-determined Anomaly Depth and ILI Anomaly Depth, Case 2

It is seen in Figure 5 that the ILI dimensions are clustered at a value of 25%. That is because the depth-sizing capability of the tool was such that depth could only be categorized as being between 0% and 12.5% of the wall thickness, between 12.5% and 25% of the wall thickness, between 25% and 40% of the wall thickness, or greater than 40% of the wall thickness. The investigating team member took the depth of the anomaly to be the highest value in the range.

It is also seen in Figure 5 that several values of field-measured depth are out of line with the tool-called depth. This may have to do with inaccuracies in the field depth measurements as will be discussed.

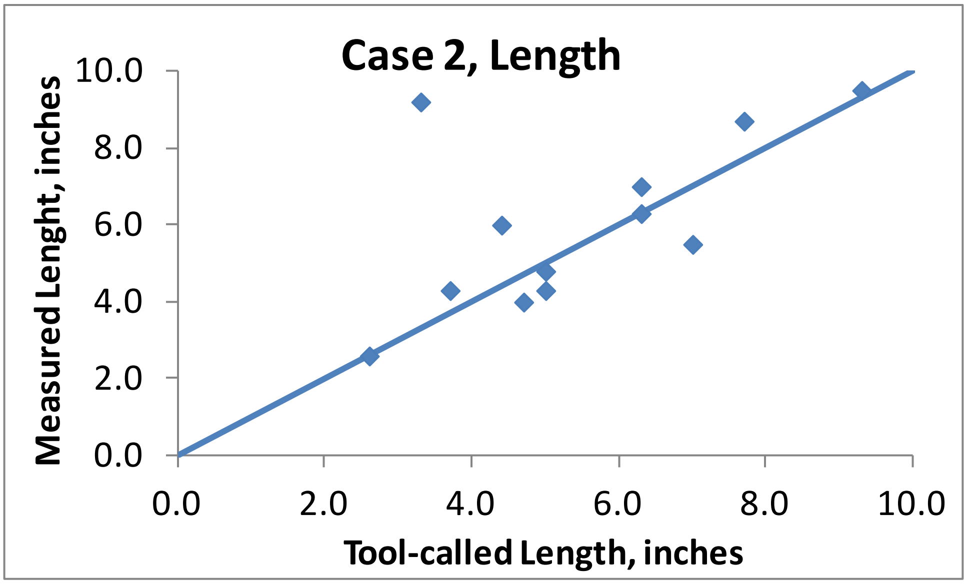

Figure 6. Comparisons between Field-determined Anomaly Length and ILI Anomaly Length, Case 2

Except in one case, the ILI lengths were in reasonable agreement with the field-measured lengths as shown in Figure 6. In the single case where the agreement was not so good, a lack-of-fusion anomaly was measured to be 9.2 inches in length upon field examination whereas the ILI-indicated length was 3.3 inches.

A comparison between failure stresses of the anomalies calculated on the basis of ILI dimensions and those calculated on the basis of field-measured dimensions is presented in Figure 7. Failure stress levels for these anomalies were calculated using the Modified Ln-Sec Equation Elliptical C-Equivalent model with a full-size-equivalent Charpy upper shelf energy of 20 ft-lb. As can be seen in Figure 7, the failure stress levels based on field-measured dimensions are well down into the operating stress range suggesting that they are likely not correct (i.e., no in-service failures have occurred and the actual operating stress of the pipeline is over 66% of SMYS near the pump stations).

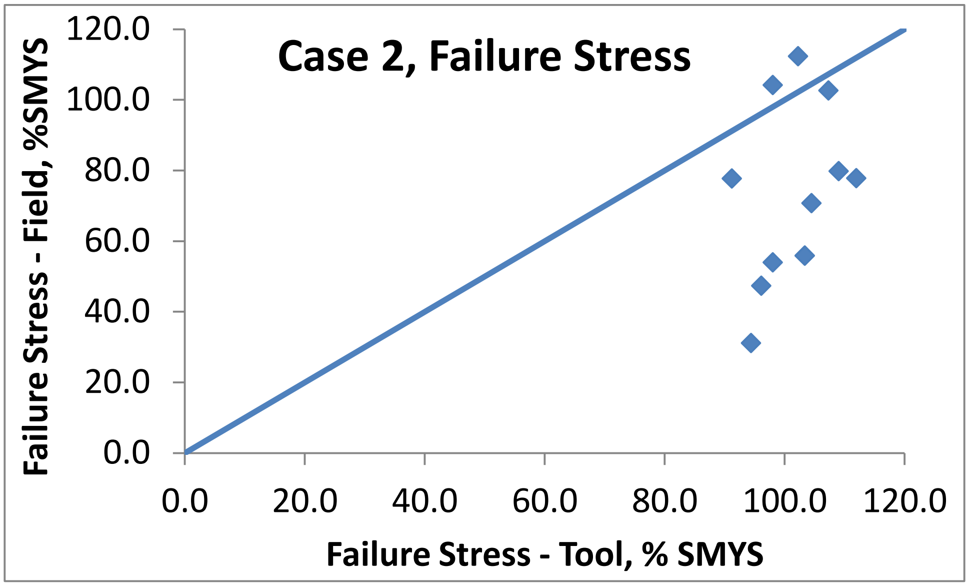

Figure 7. Comparisons between Predicted Failure Stresses Based on Field-Measured Anomaly Dimensions and Those Based on ILI Dimensions, Case 2

As in Case 1, some of the calculated failure stress levels and the field depth measurements on which they depend are suspect. In fact, another NDE vendor was brought in for four of the field examinations to repeat the work of the first vendor at those locations. The differences in depths measured by the two vendors were:

Table 6. Comparisons of d/t values measured by two different vendors

Dig Number	Vendor Number 1 d/t, %	Vendor Number 2 d/t, %
1	39	32
9	60	22
10	21	19
11	16	28

Comparisons between ILI Findings and Subsequent Service History

As noted previously, at the time this report was being prepared (5 years after the ILI crack-tool inspection), no in-service seam leaks or ruptures have occurred. Note that the actual maximum operating stress for this pipeline is about 66% of SMYS.

Comparisons between ILI Findings and Hydrostatic Test Results

The 1966 hydrostatic test was conducted too long ago to allow any meaningful comparison between the test results and the results of the 2007 ILI tool run.

Comparisons between ILI Findings and Burst Test Results

No samples of pipe containing ILI anomalies were available for the purposes of hydrostatic testing.

Comparisons between ILI Findings and Metallurgical Examinations

No samples of pipe containing ILI anomalies were available for the purposes of metallurgical examination.

Conclusions Regarding the Case 2 ILI Crack-Tool Run

Twelve comparisons between ILI anomalies and field measurements confirm that anomalies were found by the tool. The comparisons of ILI versus field-measured anomaly depths indicate very poor correlation. Unfortunately, without the benefit of a burst test or a metallurgical examination, one cannot ascertain whether or not the ILI or the field measurements or both are inaccurate. The overall conclusion is that the Case 2 ILI tool run results cannot be regarded as having proved the seam integrity of the segment to be adequate.

The Case 2 example shows that trying to evaluate the quality of inspection for a given ILI run cannot always be done merely through field NDE. In this example, there is just as much reason to doubt the accuracy of the field NDE as there is to doubt the accuracy of the ILI inspection results, so the tool results were not adequately validated. Hence, the operator really cannot have confidence that the seam integrity has been validated even though the failure stress levels of all detected anomalies were calculated, and their remaining lives were calculated.

Case 3

Pipeline Attributes and Inspection Parameters

Case 3 involves a 12.75-inch-OD liquid pipeline comprised of 0.219-inch and 0.250-inch wall, X52 low-frequency ERW pipe manufactured by Page Hersey, installed in 1961. This 54-mile segment was inspected by means of an ultrasonic crack-detection tool in 2008. The maximum operating stress level of the pipeline corresponds to 67% of SMYS (for the 0.219-inch wall pipe). This segment had experienced three in-service failures; one in 1964 (unknown cause), one in 1965 (bad normalizing heat treatment), and one in1987 (seam defect). In the 2008 ILI crack-tool run, 2,738 seam anomalies[3] (average of 51 per mile) were reported, and 275 of these were subjected to examination in the field. The field examinations consisted of visual inspection and magnetic particle inspection to characterize the type and length of the anomalies. Grinding and/or ultrasonic inspection were used to measure the depth of the anomalies. In the case of the internal anomalies, ultrasonic inspection was used to characterize the length of the anomalies as well. Since the inspection, there have been no seam failure incidents on the pipeline.

The breakdown of the 2,738 anomalies indicated by ILI by type of anomaly was: Weld Anomaly (1,471), Notch-Like (727), Crack-Like (497), and Crack Field (43). The breakdown of the 275 anomalies subjected to field examination by type of anomaly was: Weld Anomaly (163), Notch-Like (35), Crack-Like (73), and Crack Field (4). The rationale for choosing anomalies to examine appeared to have been based both on the lowest predicted failure stresses and the type of anomaly. All field-examined anomalies were repaired by means of grinding or Type B sleeves. As described later, 44 ILI features were removed from the pipe for either burst testing or metallurgical examination.

Comparisons between ILI Dimensions and Field-Measured Dimensions

The Case 3 data set includes anomalies that were investigated in the field and anomalies that were sent to the laboratory for investigation. Thus, comparisons based on both field measurements and lab measurements are provided in the following paragraphs.

Based on the field data, it appears that one lack of fusion anomaly had dimensions above the minimum detection thresholds for length and depth but was not reported by ILI. Field crews reported a measured length of 290 mm (11.4 in.) and maximum depth of 1.96 mm (0.077 in.) for this anomaly. The stated thresholds for this tool are 1.2 inches for length and 0.04 inch for depth. It should be noted that eight anomalies characterized as "lack of fusion" by field crews were sent for metallurgical examination and found to correspond with hook cracks, as discussed later in this section.

All but six of the 163 reported weld anomalies were found in the field. Approximately 83% (135) of those that were found turned out to be lack of fusion anomalies (as characterized by field personnel). Another 14% (23) of the anomalies were found to be seam over-trim or seam under-trim.

All of the 35 reported notch-like features were found in the field. Approximately 60% (21) of these were found to be lack of fusion anomalies (as characterized by field personnel). Another

[3] This includes all features with a reported "relative location" of "in the weld" and "adjacent to the weld". It also includes features classified as "weld anomalies" with a reported "relative location" of "in the base material" or "not decidable".

29% (10) of the anomalies were found to be seam over-trim or seam under-trim. The remaining 4 anomalies were found to be a gouge, an inclusion, a mill grind, and a stringer.

Similarly, all of the 73 reported crack-like features were found in the field. Approximately 47% (34) were found to be lack of fusion anomalies (as characterized by field personnel). Another 26% (19) were found to be contact marks. Approximately 18% (13) corresponded with seam over-trim or seam under-trim, while 7% (5) correspond to gouges. There was one feather burn and one anomaly described as crack-like.

The four reported crack field anomalies were all found to correspond with mill grinds.

In terms of classification, 71% of the lack of fusion anomalies (as characterized by field personnel) were classified by the ILI vendor as weld anomalies, while 18% were classified as crack-like and 11% were classified as notch-like. Seam over-trim or under-trim anomalies were classified as weld anomalies half of the time, crack-like 28% of the time, and notch-like 22% of the time. Lack of fusion and seam over/under-trim anomalies accounted for 86% of the reported seam weld features.

Table 7. Comparison between Tool-Called and Field-Measured Parameters for Case 3 contains field-measured and ILI-reported anomaly depths and lengths for the correlated features, while Table 8. Comparison between ILI and Lab-Measured Parameters for Case 3 Anomalies Examined in the Lab presents similar data for those features examined in the lab. For all eight features examined in the lab (shown in Table 8), field crews characterized the anomalies as lack of fusion. Based on the laboratory examination, the anomalies should have been classified as hook cracks.

Table 7. Comparison between Tool-Called and Field-Measured Parameters for Case 3

Type of Anomaly		Length, inches		Depth, % Wall Thickness		Wall Thickness, inch		Location (External or Internal)	
ILI	Field	ILI	Field	ILI	Field	ILI	Field	ILI	Field
Notch-Like	Seam Over-trim	12.5	2.2	31.7	7.6	0.248	0.260	Ext	Int
Weld Anomaly	Seam Over-trim	11.2	4.8	15.9	6.1	0.248	0.260	Int	Int
Weld Anomaly	Lack of Fusion	10.5	1.3	39.7	28.4	0.248	0.264	Int	Int
Crack-Like	Seam Over-trim	19.0	21.0	31.7	4.8	0.248	0.254	Int	Int
Crack-Like	Seam Over-trim	5.1	7.6	23.8	6.3	0.248	0.257	Int	Int
Crack-Like	Lack of Fusion	5.6	5.7	66.0	7.3	0.209	0.254	Ext	Ext
Weld Anomaly	Lack of Fusion	9.8	16.9	47.2	16.8	0.209	0.258	Int	Int
Crack-Like	Seam Over-trim	29.3	34.1	34.5	6.6	0.228	0.228	Int	Int

Type of Anomaly		Length, inches		Depth, % Wall Thickness		Wall Thickness, inch		Location (External or Internal)	
ILI	Field	ILI	Field	ILI	Field	ILI	Field	ILI	Field
Weld Anomaly	Lack of Fusion	5.0	5.5	47.2	22.8	0.209	0.205	Ext	Ext
Notch-Like	Seam Over-trim	12.3	14.1	18.9	3.3	0.209	0.229	Int	Int
Crack-Like	Contact Marks	3.0	3.1	47.2	5.3	0.209	0.215	Ext	Ext
Crack-Like	Contact Marks	3.0	2.9	18.9	3.1	0.209	0.215	Ext	Ext
Crack-Like	Contact Marks	3.6	3.8	28.3	4.8	0.209	0.215	Ext	Ext
Crack-Like	Lack of Fusion	7.9	11.9	37.7	21.8	0.209	0.220	Ext	Ext
Crack-Like	Lack of Fusion	2.4	11.9	28.3	24.8	0.209	0.220	Ext	Ext
Crack-Like	Lack of Fusion	2.0	0.8	9.4	9.0	0.209	0.197	Ext	Ext
Crack-Like	Seam Over-trim	7.5	10.0	37.7	10.3	0.209	0.191	Int	Int
Crack-Like	Lack of Fusion	13.5	13.1	37.7	19.4	0.209	0.201	Ext	Ext
Weld Anomaly	Lack of Fusion	10.8	11.9	37.7	14.4	0.209	0.219	Int	Int
Weld Anomaly	Lack of Fusion	7.4	7.5	37.7	14.4	0.209	0.219	Int	Int
Weld Anomaly	Lack of Fusion	1.3	6.1	9.4	5.4	0.209	0.219	Int	Int
Crack-Like	Lack of Fusion	8.1	0.9	37.7	3.6	0.209	0.219	Int	Int
Notch-Like	Gouge	2.8	47.2	9.4	7.4	0.209	0.224	Int	Ext
Crack-Like	Gouge	32.4	47.2	32.1	7.4	0.209	0.224	Int	Ext
Crack-Like	Seam Under-trim	6.1	31.7	15.1	8.2	0.209	0.202	Ext	Ext
Weld Anomaly	Lack of Fusion	5.0	7.7	37.7	15.8	0.209	0.219	Int	Ext
Crack-Like	Lack of Fusion	5.1	6.3	47.2	18.0	0.209	0.219	Int	Int
Crack-Like	Lack of Fusion	3.1	1.8	28.3	11.3	0.209	0.217	Ext	Ext
Crack-Like	Lack of Fusion	2.1	1.6	18.9	10.7	0.209	0.214	Ext	Ext
Crack-Like	Lack of Fusion	3.7	1.8	47.2	11.3	0.209	0.217	Ext	Ext
Weld Anomaly	Lack of Fusion	4.6	5.5	47.2	27.0	0.209	0.219	Int	Int
Weld Anomaly	Lack of Fusion	3.6	4.5	37.7	17.3	0.209	0.205	Int	Ext
Weld Anomaly	Seam Under-trim	10.2	10.9	47.2	19.8	0.209	0.022	Ext	Int
Weld Anomaly	Lack of Fusion	5.1	5.1	37.7	18.9	0.209	0.209	Int	Int
Crack-Like	Lack of Fusion	6.7	8.2	56.6	19.2	0.209	0.207	Ext	Ext
Crack-Like	Lack of Fusion	6.8	7.5	56.6	17.1	0.209	0.217	Ext	Ext
Crack-Like	Lack of Fusion	7.0	9.9	50.9	29.8	0.209	0.217	Ext	Ext
Weld Anomaly	Lack of Fusion	2.8	3.1	9.4	13.7	0.209	0.201	Ext	Ext
Weld Anomaly	Lack of Fusion	18.2	15.1	50.9	18.8	0.209	0.202	Ext	Ext
Weld Anomaly	Lack of Fusion	1.3	3.9	9.4	13.5	0.209	0.205	Ext	Ext
Weld Anomaly	Lack of Fusion	2.2	1.3	9.4	17.6	0.209	0.203	Ext	Ext
Weld Anomaly	Seam Over-trim	4.7	8.3	37.7	7.7	0.209	0.205	Ext	Int
Weld Anomaly	Lack of Fusion	7.2	12.6	37.7	27.6	0.209	0.214	Ext	Ext
Notch-Like	Lack of Fusion	24.0	25.6	37.7	13.3	0.209	0.207	Int	Int
Weld Anomaly	Lack of Fusion	1.9	3.8	47.2	21.6	0.209	0.201	Ext	Ext

Type of Anomaly		Length, inches		Depth, % Wall Thickness		Wall Thickness, inch		Location (External or Internal)	
ILI	Field	ILI	Field	ILI	Field	ILI	Field	ILI	Field
Crack-Like	Lack of Fusion	9.7	10.6	37.7	12.7	0.209	0.220	Ext	Ext
Crack-Like	Lack of Fusion	3.6	4.7	9.4	11.6	0.209	0.220	Ext	Ext
Crack-Like	Lack of Fusion	3.0	3.8	47.2	11.4	0.209	0.201	Ext	Ext
Weld Anomaly	Lack of Fusion	1.5	2.2	18.9	12.3	0.209	0.209	Ext	Ext
Weld Anomaly	Lack of Fusion	2.2	2.8	37.7	18.3	0.209	0.207	Ext	Ext
Weld Anomaly	Lack of Fusion	1.3	1.9	9.4	5.6	0.209	0.213	Ext	Ext
Weld Anomaly	Lack of Fusion	5.0	4.7	47.2	24.2	0.209	0.209	Ext	Mid
Weld Anomaly	Lack of Fusion	3.5	3.3	28.3	21.2	0.209	0.214	Ext	Ext
Crack-Like	Lack of Fusion	8.5	10.2	34.5	30.6	0.228	0.209	Ext	Ext
Weld Anomaly	Lack of Fusion	1.7	2.8	17.2	17.7	0.228	0.209	Ext	Ext
Weld Anomaly	Lack of Fusion	4.9	5.9	66.0	22.8	0.209	0.213	Ext	Ext
Weld Anomaly	Lack of Fusion	4.1	4.1	37.7	17.5	0.209	0.209	Ext	Ext
Weld Anomaly	Lack of Fusion	8.6	9.1	34.5	28.1	0.228	0.209	Ext	Ext
Notch-Like	Lack of Fusion	2.7	2.2	8.6	9.4	0.228	0.209	Ext	Mid
Weld Anomaly	Seam Over-trim	9.4	10.6	47.2	11.2	0.209	0.187	Ext	Ext
Weld Anomaly	Lack of Fusion	9.3	10.4	34.5	38.0	0.228	0.205	Ext	Ext
Weld Anomaly	Lack of Fusion	13.4	15.2	37.7	19.3	0.209	0.196	Ext	Ext
Weld Anomaly	Lack of Fusion	6.3	6.9	43.1	18.2	0.228	0.217	Ext	Ext
Notch-Like	Lack of Fusion	3.0	4.9	9.4	4.6	0.209	0.212	Int	Int
Weld Anomaly	Seam Over-trim	7.6	8.3	43.4	9.3	0.209	0.212	Int	Int
Weld Anomaly	Seam Over-trim	1.0	1.0	9.4	5.3	0.209	0.225	Int	Int
Weld Anomaly	Lack of Fusion	5.4	5.6	34.5	17.0	0.228	0.224	Ext	Ext
Weld Anomaly	Lack of Fusion	6.2	3.1	46.6	29.5	0.228	0.213	Int	Int
Crack-Like	Lack of Fusion	7.4	9.1	34.5	45.3	0.228	0.214	Ext	Mid
Weld Anomaly	Seam Over-trim	4.9	5.9	28.3	6.0	0.209	0.197	Int	Int
Weld Anomaly	Lack of Fusion	6.9	6.7	37.7	16.0	0.209	0.197	Int	Int
Weld Anomaly	Lack of Fusion	6.2	5.3	36.2	28.8	0.228	0.205	Int	Int
Notch-Like	Lack of Fusion	3.6	3.7	8.6	19.2	0.228	0.205	Ext	Ext
Notch-Like	Seam Over-trim	10.7	15.7	17.2	8.3	0.228	0.236	Ext	Int
Weld Anomaly	Lack of Fusion	5.0	0.8	8.6	8.7	0.228	0.208	Ext	Ext
Weld Anomaly	Lack of Fusion	2.4	3.9	8.6	7.7	0.228	0.214	Int	Ext
Weld Anomaly	Lack of Fusion	7.7	9.3	56.9	40.7	0.228	0.213	Ext	Ext
Weld Anomaly	Lack of Fusion	2.5	2.7	69.8	19.5	0.209	0.202	Int	Int
Weld Anomaly	Lack of Fusion	5.9	5.0	37.7	22.2	0.209	0.213	Ext	Ext
Weld Anomaly	Lack of Fusion	3.4	1.4	18.9	22.2	0.209	0.213	Ext	Ext
Notch-Like	Lack of Fusion	4.3	6.3	9.4	9.3	0.209	0.213	Int	Int
Notch-Like	Lack of Fusion	4.3	4.5	9.4	11.8	0.209	0.201	Ext	Mid

Type of Anomaly		Length, inches		Depth, % Wall Thickness		Wall Thickness, inch		Location (External or Internal)	
ILI	Field	ILI	Field	ILI	Field	ILI	Field	ILI	Field
Notch-Like	Seam Over-trim	2.9	6.3	9.4	9.8	0.209	0.201	Int	Int
Notch-Like	Seam Over-trim	3.1	5.1	9.4	9.8	0.209	0.201	Int	Int
Weld Anomaly	Lack of Fusion	5.2	4.9	37.7	9.3	0.209	0.212	Ext	Ext
Crack-Like	Lack of Fusion	6.0	9.6	18.9	27.8	0.209	0.213	Ext	Mid
Notch-Like	Lack of Fusion	1.9	3.1	9.4	9.3	0.209	0.211	Ext	Ext
Weld Anomaly	Lack of Fusion	2.5	2.8	28.3	16.4	0.209	0.211	Ext	Ext
Weld Anomaly	Lack of Fusion	3.9	4.0	37.7	18.9	0.209	0.213	Ext	Ext
Weld Anomaly	Seam Over-trim	2.4	8.3	34.5	8.8	0.228	0.222	Int	Int
Notch-Like	Lack of Fusion	1.4	16.5	8.6	41.7	0.228	0.209	Ext	Mid
Crack-Like	Lack of Fusion	9.2	16.5	43.1	41.7	0.228	0.209	Ext	Par
Crack-Like	Seam Over-trim	16.1	16.3	34.5	6.1	0.228	0.194	Int	Int
Weld Anomaly	Lack of Fusion	1.2	2.6	34.5	9.2	0.228	0.215	Int	Int
Weld Anomaly	Lack of Fusion	2.0	3.0	67.2	37.5	0.228	0.215	Ext	Ext
Weld Anomaly	Lack of Fusion	2.6	2.6	34.5	9.1	0.228	0.217	Int	Int
Weld Anomaly	Lack of Fusion	4.3	4.7	17.2	9.1	0.228	0.217	Ext	Mid
Weld Anomaly	Lack of Fusion	1.2	1.4	17.2	8.8	0.228	0.224	Int	Int
Weld Anomaly	Lack of Fusion	2.4	2.8	25.9	16.8	0.228	0.215	Ext	Ext
Weld Anomaly	Lack of Fusion	12.0	7.5	46.6	18.2	0.228	0.217	Int	Int
Notch-Like	Lack of Fusion	4.3	12.4	5.2	28.2	0.228	0.218	Ext	Ext
Weld Anomaly	Seam Over-trim	2.8	2.8	37.7	13.2	0.209	0.209	Int	Int
Notch-Like	Lack of Fusion	2.0	2.3	9.4	9.4	0.209	0.209	Ext	Ext
Weld Anomaly	Lack of Fusion	4.3	4.3	43.1	18.7	0.228	0.211	Int	Int
Weld Anomaly	Lack of Fusion	4.7	4.7	8.6	17.5	0.228	0.217	Ext	Ext
Weld Anomaly	Lack of Fusion	3.3	3.5	43.1	32.7	0.228	0.217	Ext	Ext
Weld Anomaly	Lack of Fusion	2.5	2.4	8.6	16.4	0.228	0.217	Ext	Ext
Crack-Like	Lack of Fusion	4.3	4.2	47.2	25.0	0.209	0.221	Int	Int
Weld Anomaly	Lack of Fusion	3.4	4.4	47.2	19.2	0.209	0.209	Int	Ext
Crack-Like	Seam Over-trim	15.7	15.4	37.7	5.6	0.209	0.211	Int	Int
Crack-Like	Lack of Fusion	2.0	2.2	28.3	9.3	0.209	0.211	Int	Int
Crack-Like	Seam Over-trim	1.2	2.1	37.7	9.5	0.209	0.207	Int	Int
Crack-Like	Seam Over-trim	3.6	4.7	18.9	4.8	0.209	0.205	Int	Int
Crack-Like	Seam Over-trim	4.8	5.2	9.4	9.4	0.209	0.209	Int	Int
Notch-Like	Mill Grind	9.4	20.1	18.9	5.7	0.209	0.209	Ext	Ext
Weld Anomaly	Seam Over-trim	6.7	40.9	28.3	5.5	0.209	0.215	Int	Int
Weld Anomaly	Seam Over-trim	7.9	40.9	37.7	5.5	0.209	0.215	Int	Int
Weld Anomaly	Lack of Fusion	5.9	0.6	28.3	9.2	0.209	0.215	Int	Int
Crack-Like	Lack of Fusion	1.3	10.0	37.7	19.6	0.209	0.205	Ext	Ext

Type of Anomaly		Length, inches		Depth, % Wall Thickness		Wall Thickness, inch		Location (External or Internal)	
ILI	Field	ILI	Field	ILI	Field	ILI	Field	ILI	Field
Weld Anomaly	Lack of Fusion	3.8	1.8	28.3	17.0	0.209	0.199	Ext	Ext
Weld Anomaly	Lack of Fusion	1.8	3.1	28.3	15.1	0.209	0.209	Ext	Ext
Weld Anomaly	Lack of Fusion	1.1	0.7	9.4	10.1	0.209	0.207	Ext	Ext
Crack-Like	Seam Over-trim	5.7	15.2	34.5	7.4	0.228	0.213	Int	Int
Weld Anomaly	Lack of Fusion	2.0	4.9	43.1	27.9	0.228	0.209	Int	Ext
Weld Anomaly	Lack of Fusion	6.6	7.5	37.7	18.1	0.209	0.217	Int	Int
Weld Anomaly	Seam Over-trim	3.7	19.3	37.7	11.3	0.209	0.210	Int	Int
Crack Field	Mill Grind	9.9	6.2	9.4	14.4	0.209	0.186	Ext	Ext
Crack Field	Mill Grind	6.7	6.2	9.4	14.4	0.209	0.186	Ext	Ext
Crack Field	Mill Grind	4.8	6.2	9.4	14.4	0.209	0.186	Ext	Ext
Weld Anomaly	Lack of Fusion	1.5	1.5	20.0	13.7	0.197	0.205	Ext	Mid
Weld Anomaly	Lack of Fusion	1.2	3.3	20.0	13.4	0.197	0.203	Ext	Ext
Weld Anomaly	Lack of Fusion	5.2	2.7	50.0	28.9	0.197	0.199	Ext	Ext
Weld Anomaly	Lack of Fusion	3.4	5.9	9.4	10.0	0.209	0.197	Ext	Ext
Weld Anomaly	Lack of Fusion	3.3	5.7	47.2	6.4	0.209	0.185	Ext	Ext
Weld Anomaly	Lack of Fusion	1.2	1.4	37.7	20.0	0.209	0.187	Ext	Ext
Weld Anomaly	Lack of Fusion	6.9	8.3	52.8	20.0	0.209	0.197	Ext	Ext
Weld Anomaly	Lack of Fusion	6.1	7.1	37.7	13.5	0.209	0.205	Ext	Ext
Weld Anomaly	Lack of Fusion	5.3	5.9	28.3	7.9	0.209	0.198	Ext	Ext
Weld Anomaly	Lack of Fusion	1.2	2.8	9.4	9.9	0.209	0.199	Int	Int
Weld Anomaly	Lack of Fusion	0.0	3.7	9.4	39.6	0.209	0.199		Mid
Crack-Like	Lack of Fusion	1.1	1.5	9.4	15.0	0.209	0.197	Ext	Ext
Weld Anomaly	Lack of Fusion	4.2	4.4	47.2	45.1	0.209	0.201	Int	Int
Crack-Like	Lack of Fusion	1.3	1.4	47.2	13.7	0.209	0.213	Ext	Ext
Crack-Like	Lack of Fusion	2.7	2.5	71.7	35.0	0.209	0.217	Ext	Ext
Weld Anomaly	Lack of Fusion	5.9	10.0	18.9	22.1	0.209	0.205	Ext	Mid
Weld Anomaly	Seam Over-trim	3.9	17.5	37.7	5.8	0.209	0.205	Int	Int
Crack-Like	Seam Over-trim	3.8	17.5	28.3	5.8	0.209	0.205	Int	Int
Weld Anomaly	Seam Over-trim	3.5	17.5	18.9	5.8	0.209	0.205	Int	Int
Crack Field	Mill Grind	5.4	9.6	18.9	5.1	0.209	0.209	Ext	Ext
Weld Anomaly	Seam Under-trim	8.1	8.3	60.4	9.4	0.209	0.209	Int	Int
Crack-Like	Lack of Fusion	10.6	0.8	25.9	9.4	0.228	0.209	Ext	Mid
Crack-Like	Lap	3.1	3.1	18.9	9.0	0.209	0.219	Ext	Mid
Weld Anomaly	Lack of Fusion	6.0	8.3	28.3	31.5	0.209	0.201	Ext	Ext
Weld Anomaly	Lack of Fusion	3.1	4.1	28.3	17.4	0.209	0.199	Ext	Ext
Weld Anomaly	Seam Over-trim	4.6	15.0	37.7	9.6	0.209	0.205	Ext	Int
Weld Anomaly	Lack of Fusion	3.1	4.3	37.7	24.7	0.209	0.204	Ext	Ext

Type of Anomaly		Length, inches		Depth, % Wall Thickness		Wall Thickness, inch		Location (External or Internal)	
ILI	Field	ILI	Field	ILI	Field	ILI	Field	ILI	Field
Notch-Like	Lack of Fusion	5.3	5.6	9.4	32.7	0.209	0.200	Ext	Mid
Weld Anomaly	Lack of Fusion	4.4	4.8	47.2	19.1	0.209	0.204	Int	Ext
Weld Anomaly	Lack of Fusion	3.1	4.3	9.4	26.6	0.209	0.204	Ext	Ext
Weld Anomaly	Lack of Fusion	2.0	3.6	18.9	19.1	0.209	0.198	Ext	Ext
Weld Anomaly	Lack of Fusion	5.8	8.7	28.3	28.5	0.209	0.194	Ext	Ext
Crack-Like	Crack-Like	4.2	0.4	47.2	9.5	0.209	0.207	Int	Int
Notch-Like	Lack of Fusion	6.1	9.2	9.4	9.0	0.209	0.218	Int	Int
Weld Anomaly	Lack of Fusion	3.3	4.4	47.2	18.3	0.209	0.196	Ext	Ext
Weld Anomaly	Lack of Fusion	1.4	3.0	28.3	18.5	0.209	0.196	Ext	Ext
Weld Anomaly	Lack of Fusion	1.7	1.7	47.2	28.5	0.209	0.207	Int	Int
Weld Anomaly	Lack of Fusion	4.4	4.4	47.2	28.5	0.209	0.207	Int	Int
Weld Anomaly	Lack of Fusion	1.6	14.0	8.6	32.2	0.228	0.193	Ext	Mid
Weld Anomaly	Lack of Fusion	9.7	14.0	17.2	32.2	0.228	0.193	Ext	Mid
Weld Anomaly	Lack of Fusion	5.9	7.1	34.5	18.2	0.228	0.217	Int	Int
Weld Anomaly	Lack of Fusion	3.9	5.7	34.5	30.7	0.228	0.200	Int	Mid
Weld Anomaly	Lack of Fusion	5.6	6.3	17.2	13.2	0.228	0.209	Ext	Ext
Crack-Like	Feather Burns	21.6	2.2	34.5	11.3	0.228	0.209	Ext	Ext
Weld Anomaly	Seam Over-trim	10.1	1.0	8.6	10.7	0.228	0.220	Ext	Int
Weld Anomaly	Seam Under-trim	6.5	1.1	34.5	7.0	0.228	0.224	Int	Int
Notch-Like	Lack of Fusion	1.2	1.4	8.6	14.4	0.228	0.213	Ext	Ext
Notch-Like	Seam Over-trim	7.1	7.1	8.6	13.2	0.228	0.209	Int	Int
Crack-Like	Seam Over-trim	22.2	22.4	25.9	17.0	0.228	0.209	Int	Int
Weld Anomaly	Lack of Fusion	2.6	3.5	18.9	12.2	0.209	0.204	Ext	Ext
Weld Anomaly	Seam Over-trim	6.3	6.5	37.7	8.9	0.209	0.220	Int	Int
Weld Anomaly	Lack of Fusion	1.5	2.8	9.4	25.4	0.209	0.197	Ext	Ext
Notch-Like	Lack of Fusion	3.5	0.6	9.4	10.0	0.209	0.197	Ext	Mid
Weld Anomaly	Lack of Fusion	3.2	4.5	28.3	18.5	0.209	0.213	Int	Int
Weld Anomaly	Seam Over-trim	1.8	2.8	9.4	5.6	0.209	0.213	Ext	Int
Weld Anomaly	Lack of Fusion	2.1	2.2	9.4	18.5	0.209	0.213	Ext	Mid
Weld Anomaly	Lack of Fusion	6.3	7.3	56.6	40.2	0.209	0.213	Ext	Ext
Weld Anomaly	Lack of Fusion	4.2	5.3	28.3	18.5	0.209	0.213	Ext	Int
Weld Anomaly	Lack of Fusion	3.0	4.3	18.9	22.2	0.209	0.213	Ext	Ext
Weld Anomaly	Lack of Fusion	5.2	6.7	18.9	22.8	0.209	0.213	Ext	Ext
Weld Anomaly	Lack of Fusion	5.5	6.5	37.7	18.9	0.209	0.209	Ext	Ext
Weld Anomaly	Lack of Fusion	5.0	4.5	37.7	22.1	0.209	0.209	Ext	Ext
Weld Anomaly	Lack of Fusion	3.3	5.1	37.7	11.5	0.209	0.209	Int	Ext
Notch-Like	Lack of Fusion	2.9	3.9	9.4	27.8	0.209	0.213	Ext	Mid

Type of Anomaly		Length, inches		Depth, % Wall Thickness		Wall Thickness, inch		Location (External or Internal)	
ILI	Field	ILI	Field	ILI	Field	ILI	Field	ILI	Field
Weld Anomaly	Seam Over-trim	1.9	19.7	9.4	17.5	0.209	0.224	Int	Int
Notch-Like	Lack of Fusion	16.0	19.5	34.0	24.5	0.209	0.209	Int	Int
Weld Anomaly	Lack of Fusion	5.8	10.4	9.4	9.4	0.209	0.209	Int	Int
Weld Anomaly	Seam Over-trim	10.6	12.4	34.5	9.4	0.228	0.210	Int	Int
Notch-Like	Seam Over-trim	6.8	8.5	18.9	7.5	0.209	0.220	Int	Int
Weld Anomaly	Lack of Fusion	1.8	1.6	75.5	63.3	0.209	0.215	Ext	Int
Weld Anomaly	Lack of Fusion	2.4	2.6	9.4	20.0	0.209	0.197	Ext	Int
Weld Anomaly	Lack of Fusion	2.6	1.8	18.9	20.1	0.209	0.209	Ext	Ext
Weld Anomaly	Lack of Fusion	2.2	2.4	47.2	18.3	0.209	0.207	Ext	Ext
Weld Anomaly	Lack of Fusion	5.1	5.7	28.3	29.6	0.209	0.210	Int	Int
Weld Anomaly	Lack of Fusion	5.6	5.7	71.7	18.9	0.209	0.209	Int	Int
Weld Anomaly	Lack of Fusion	6.3	7.3	37.7	21.1	0.209	0.211	Ext	Ext
Weld Anomaly	Lack of Fusion	3.6	5.1	9.4	18.8	0.209	0.210	Int	Int
Weld Anomaly	Lack of Fusion	2.8	2.8	28.3	19.2	0.209	0.205	Int	Int
Weld Anomaly	Lack of Fusion	5.2	6.9	18.9	20.5	0.209	0.209	Ext	Ext
Crack-Like	Lack of Fusion	1.9	2.0	9.4	17.9	0.209	0.220	Ext	Int
Crack-Like	Lack of Fusion	15.4	16.1	43.4	17.5	0.209	0.220	Ext	Ext
Crack-Like	Gouge	2.6	6.3	37.7	10.3	0.209	0.228	Ext	Ext
Crack-Like	Gouge	2.3	3.7	37.7	10.5	0.209	0.228	Ext	Ext
Crack-Like	Gouge	5.6	12.6	37.7	13.4	0.209	0.228	Ext	Ext
Crack-Like	Gouge	3.8	5.1	9.4	6.0	0.209	0.228	Ext	Ext
Notch-Like	Seam Over-trim	3.2	5.5	17.2	5.3	0.228	0.224	Int	Int
Notch-Like	Seam Over-trim	22.7	20.1	17.2	7.1	0.228	0.220	Int	Int
Weld Anomaly	Lack of Fusion	7.4	9.8	48.3	41.1	0.228	0.220	Ext	Ext
Weld Anomaly	Lack of Fusion	7.1	12.6	25.9	13.0	0.228	0.213	Int	Int
Notch-Like	Stringer	3.0	3.9	17.2	7.4	0.228	0.224	Ext	Ext
Notch-Like	Inclusion	3.0	21.3	8.6	18.2	0.228	0.217	Ext	Int
Weld Anomaly	Lack of Fusion	9.4	10.4	25.9	14.8	0.228	0.213	Ext	Int
Weld Anomaly	Lack of Fusion	5.7	7.1	34.5	14.8	0.228	0.213	Ext	Ext
Crack-Like	Contact Marks	4.4	13.0	17.2	11.1	0.228	0.213	Ext	Ext
Crack-Like	Contact Marks	5.7	6.2	17.2	7.7	0.228	0.209	Ext	Ext
Crack-Like	Contact Marks	3.8	4.4	17.2	5.2	0.228	0.206	Ext	Ext
Crack-Like	Contact Marks	3.1	3.7	17.2	6.2	0.228	0.204	Ext	Ext
Crack-Like	Contact Marks	17.4	1.8	17.2	6.2	0.228	0.203	Ext	Ext
Crack-Like	Contact Marks	6.2	6.0	17.2	5.5	0.228	0.202	Ext	Ext
Crack-Like	Contact Marks	5.5	5.4	25.9	7.4	0.228	0.198	Ext	Ext
Crack-Like	Contact Marks	5.8	6.6	25.9	7.9	0.228	0.204	Ext	Ext

Type of Anomaly		Length, inches		Depth, % Wall Thickness		Wall Thickness, inch		Location (External or Internal)	
ILI	**Field**	**ILI**	**Field**	**ILI**	**Field**	**ILI**	**Field**	**ILI**	**Field**
Crack-Like	Contact Marks	16.4	17.6	25.9	5.1	0.228	0.209	Ext	Ext
Crack-Like	Contact Marks	6.5	7.6	8.6	7.8	0.228	0.206	Ext	Ext
Crack-Like	Contact Marks	6.0	7.1	8.6	5.9	0.228	0.206	Ext	Ext
Crack-Like	Contact Marks	4.0	7.3	25.9	5.9	0.228	0.207	Ext	Ext
Crack-Like	Contact Marks	3.9	5.5	8.6	7.6	0.228	0.207	Ext	Ext
Crack-Like	Contact Marks	17.5	21.0	25.9	8.1	0.228	0.209	Ext	Ext
Crack-Like	Contact Marks	19.4	24.5	25.9	4.2	0.228	0.204	Ext	Ext
Crack-Like	Contact Marks	2.4	7.4	8.6	7.5	0.228	0.210	Ext	Ext
Crack-Like	Lack of Fusion	6.5	6.6	34.5	9.2	0.228	0.215	Ext	Int
Weld Anomaly	Lack of Fusion	10.8	9.9	25.9	25.7	0.228	0.215	Ext	Int
Crack-Like	Lack of Fusion	11.3	13.4	41.5	18.1	0.209	0.213	Ext	Ext
Weld Anomaly	Seam Over-trim	7.0	6.9	18.9	7.1	0.209	0.220	Ext	Int
Weld Anomaly	Lack of Fusion	5.1	7.5	37.7	31.5	0.209	0.213	Ext	Ext
Weld Anomaly	Lack of Fusion	4.6	4.7	50.9	15.7	0.209	0.209	Ext	Ext
Crack-Like	Lack of Fusion	3.5	2.6	18.9	13.5	0.209	0.213	Ext	Ext
Weld Anomaly	Lack of Fusion	3.9	3.9	56.6	11.6	0.209	0.217	Int	Ext
Weld Anomaly	Lack of Fusion	2.1	2.2	9.4	17.9	0.209	0.220	Int	Int
Weld Anomaly	Lack of Fusion	9.3	18.1	43.4	45.9	0.209	0.202	Ext	Ext
Notch-Like	Lack of Fusion	1.4	0.6	9.4	9.4	0.209	-	Ext	Ext
Notch-Like	Lack of Fusion	3.8	5.9	9.4	9.4	0.209	-	Ext	Ext
Crack-Like	Lack of Fusion	12.8	15.8	18.9	13.2	0.209	-	Ext	Ext
Weld Anomaly	Lack of Fusion	2.0	3.3	18.9	13.2	0.209	-	Int	Int
Weld Anomaly	Lack of Fusion	2.7	2.7	9.4	9.4	0.209	-	Ext	Mid
Weld Anomaly	Lack of Fusion	4.3	12.8	28.3	9.4	0.209	-	Ext	Ext
Crack-Like	Lack of Fusion	11.7	1.3	9.4	15.1	0.209	-	Ext	Mid
Weld Anomaly	Not Found	4.3	0.0	28.3	-	0.209	-	Ext	-
Weld Anomaly	Lack of Fusion	1.9	1.8	25.9	15.5	0.228	-	Int	Ext
Weld Anomaly	Lack of Fusion	2.4	10.7	28.3	18.9	0.209	-	Int	Int
Weld Anomaly	Lack of Fusion	6.7	2.7	17.2	10.3	0.228	-	Ext	Int
Weld Anomaly	Lack of Fusion	1.4	1.8	8.6	8.6	0.228	-	Int	Int
Notch-Like	Lack of Fusion	2.6	2.8	25.9	8.6	0.228	-	Int	Int
Notch-Like	Under-trim	21.1	25.6	34.5	17.2	0.228	-	Int	Int
Notch-Like	Lack of Fusion	7.5	8.1	8.6	12.1	0.228	-	Int	Int
Weld Anomaly	Lack of Fusion	1.8	1.5	8.6	17.2	0.228	-	Int	Int
Notch-Like	Lack of Fusion	11.7	12.3	17.2	8.6	0.228	-	Int	Int
Weld Anomaly	Lack of Fusion	3.2	3.4	37.7	35.8	0.209	-	Int	Int
Weld Anomaly	Lack of Fusion	5.4	6.9	37.7	34.0	0.209	-	Ext	Ext

Type of Anomaly		Length, inches		Depth, % Wall Thickness		Wall Thickness, inch		Location (External or Internal)	
ILI	**Field**	**ILI**	**Field**	**ILI**	**Field**	**ILI**	**Field**	**ILI**	**Field**
Weld Anomaly	Not Found	7.4	0.0	18.9	-	0.209	-	Ext	-
Weld Anomaly	Not Found	6.1	0.0	18.9	-	0.209	-	Ext	-
Weld Anomaly	Lack of Fusion	2.0	4.4	9.4	-	0.209	-	Ext	Mid
Weld Anomaly	Not Found	6.1	0.0	18.9	-	0.209	-	Ext	-
Weld Anomaly	Not Found	4.0	0.0	9.4	-	0.209	-	Ext	-
Weld Anomaly	Lack of Fusion	5.2	6.0	28.3	9.4	0.209	-	Ext	Ext
Weld Anomaly	Lack of Fusion	2.4	3.5	9.4	9.4	0.209	-	Ext	Ext
Weld Anomaly	Lack of Fusion	2.0	2.4	18.9	17.0	0.209	-	Ext	Ext
Weld Anomaly	Not Found	4.3	0.0	28.3	-	0.209	-	Ext	-

Table 8. Comparison between ILI and Lab-Measured Parameters for Case 3 Anomalies Examined in the Lab

Type of Anomaly		Length, inches		Depth, % Wall Thickness		Wall Thickness, in.		Location (External or Internal)	
ILI	Observed	ILI	Measured	ILI	Measured	ILI	Measured	ILI	Measured
Weld Anomaly	Hook Crack	12.17	17.64	43.4	30.4	0.209	0.209	Ext	Ext
Weld Anomaly	Hook Crack	8.61	9.70	62.3	24.5	0.209	0.209	Ext	Ext
Weld Anomaly	Hook Crack	7.87	7.76	28.3	40.6	0.209	0.209	Ext	Ext
Crack-Like	Hook Crack	7.48	4.56	37.7	40.6	0.209	0.209	Ext	Ext
Notch-Like	Hook Crack	4.49	3.32	34.5	23.1	0.228	0.228	Ext	Ext
Notch-Like	Hook Crack	18.66	18.42	25.9	29.1	0.228	0.228	Ext	Ext
Weld Anomaly	Hook Crack	10.43	10.15	37.7	17.2	0.209	0.209	Ext	Ext
Weld Anomaly	Hook Crack	3.31	2.35	47.2	22.6	0.209	0.209	Ext	Ext

Note: For all eight features examined in the lab, field crews erroneously characterized the anomalies as lack of fusion. Based on the laboratory examination, the anomalies should have been classified as hook cracks.

Comparisons between ILI crack-tool parameters and field NDE parameters are presented in Figure 8 through Figure 11. The first of these, Figure 8, compares the ILI depths to those determined in the field.

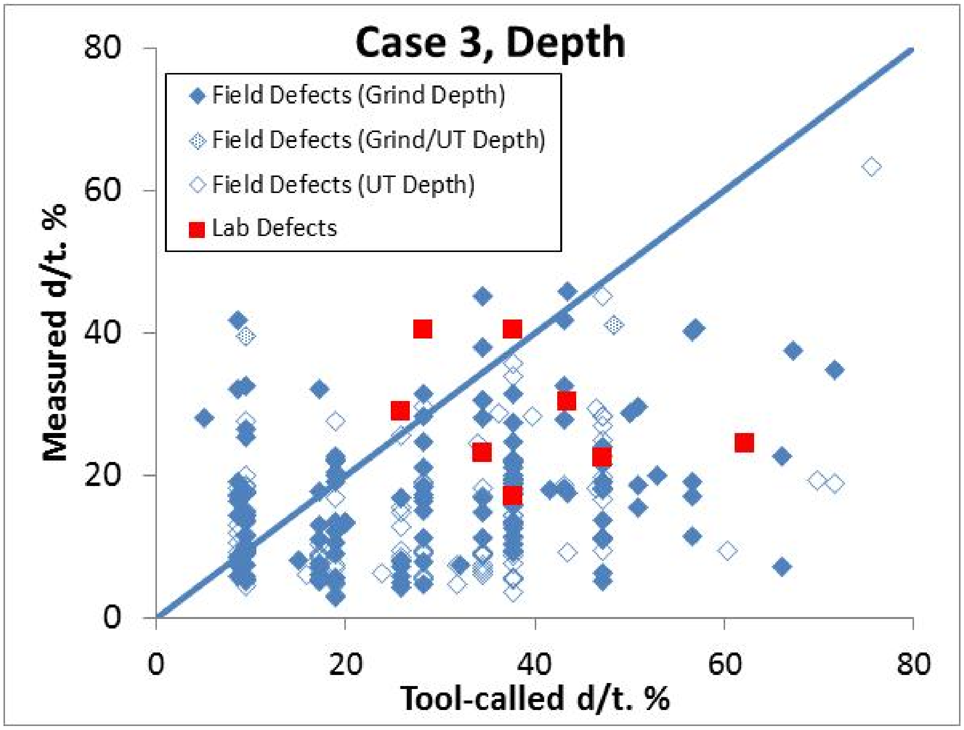

Figure 8. Comparisons between Field-determined Anomaly Depth and ILI Anomaly Depth, Case 3

As seen in Figure 8, for the majority of the anomalies (77%), the depths reported by ILI were deeper than the depths determined by field NDE. In fact, the ILI depths of 42% of features exceeded the depths determined by field NDE by a factor of 2 or more. It is also clear that a number of features reported by ILI with a shallow depth were indicated by field NDE to be deeper (i.e., features with a reported depth of approximately 10% WT were indicated to have depths as much as 42% WT). One interesting observation is that relatively deep anomalies (between 40% and 45% WT) were indicated by field NDE for most depth ranges reported by the ILI. Further, the distribution of field NDE indications is similar to that of the grind measurements, possibly an indication that the field NDE measurements were reasonably accurate (although a separate grind or lab vs. ultrasonic depth correlation would be required in order to be conclusive).

For those anomalies (corresponding with hook cracks) sent to the lab for examination (red symbols in Figure 8), approximately 63% were reported by the ILI as deeper than they actually were. The general sizing performance is similar to that for those anomalies that were examined in the field.

The comparisons between lengths determined by the tool with lengths determined by field NDE are shown in Figure 9.

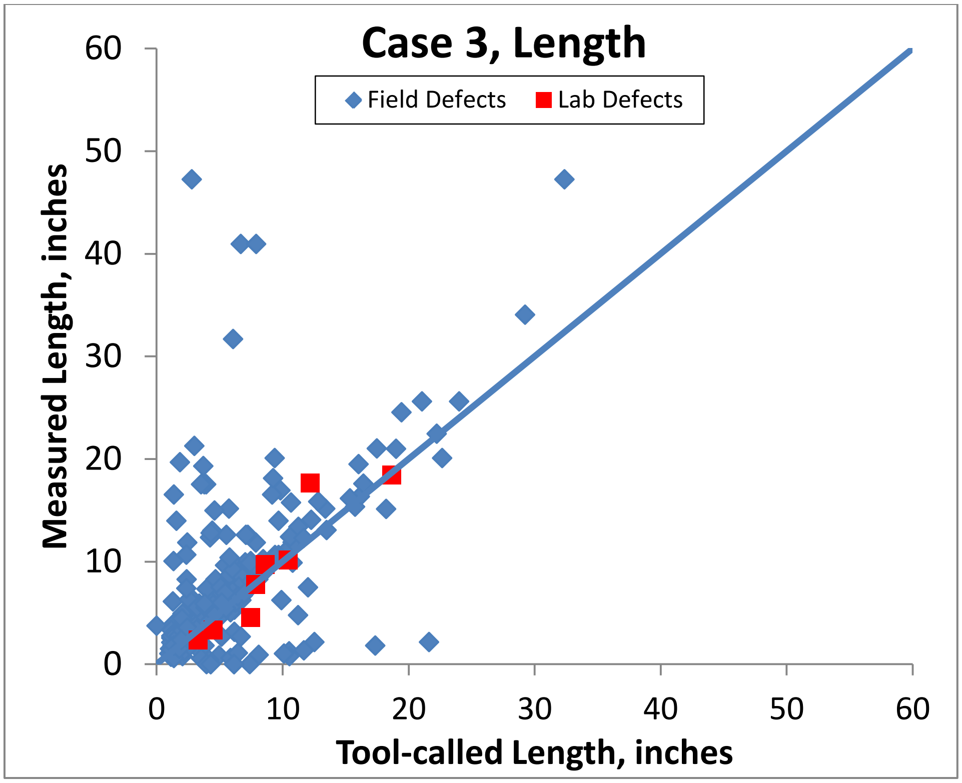

Figure 9. Comparisons between Field-determined Anomaly Length and ILI Anomaly Length, Case 3

For field-examined anomalies (blue symbols in Figure 9), only 23% were reported by the ILI as being longer than they actually were. Of those whose length was under-reported, a handful of anomalies (corresponding to three trim and one gouge anomalies) had actual lengths that were considerably longer than what the tool reported (between 5 and 17 times longer). The trending suggests that most lengths are under-reported, which could be attributable to the tool's inability to detect shallow parts of the cracks.

For those anomalies (corresponding with hook cracks) sent to the lab for examination (red symbols in Figure 9), seven out of the eight anomalies had actual measured lengths within 3 mm of the tool-reported value and the eighth anomaly was within 5.5 mm. The ILI lengths agreed well with the lab-measured lengths.

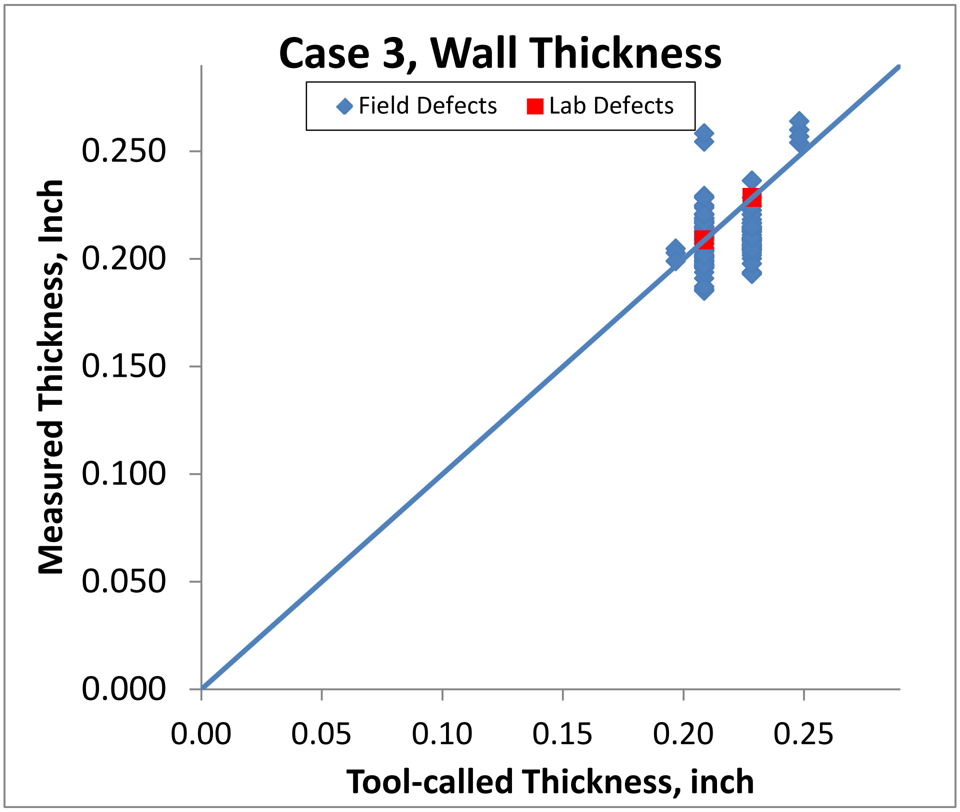

Figure 10. Comparisons between Field-determined Wall Thickness and ILI Wall Thickness, Case 3

Figure 10 shows a comparison of the pipe wall thickness measurements from the field with the ILI wall thickness values. On the basis of the data associated with the field examinations (blue symbols in Figure 10), the field-measured wall thickness values were within 15% of the ILI-reported value. The largest deviation was 22%, with no apparent explanation. As for the data associated with the lab examinations (red symbols in Figure 10), the lab-measured values matched the ILI-reported values.

A comparison between failure stresses of the anomalies calculated on the basis of ILI dimensions and those calculated on the basis of field-measured dimensions is presented in Figure 11. Failure stress levels for these anomalies were calculated using the CorLAS™ fracture mechanics model with a full-size-equivalent Charpy upper shelf energy of 7 ft-lb (based on Charpy v-notch test results for the weld seam of this material. The notches were centered on the bondline). Figure 11 shows that the ILI-based failure stresses were all conservative (data above the 1:1 line) except for the smaller flaws, where the failure stresses were well above 100% of SMYS.

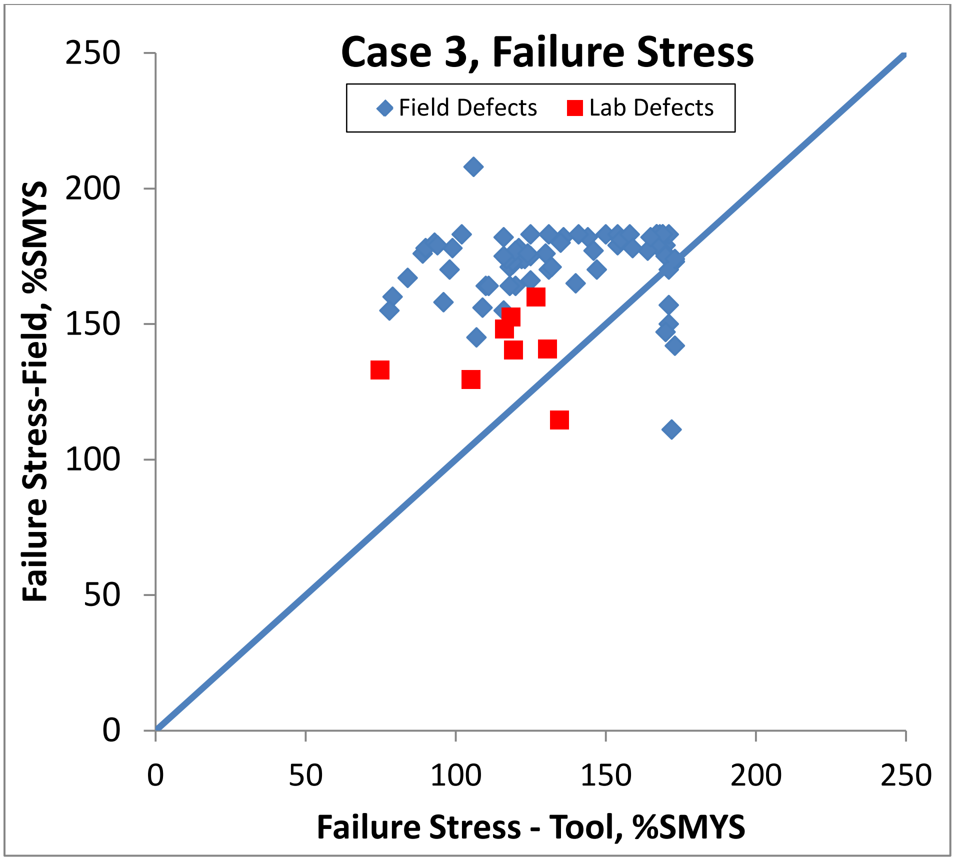

Figure 11. Comparisons between Predicted Failure Stresses Based on Field-Measured Anomaly Dimensions and Those Based on ILI Dimensions, Case 3

Comparisons between ILI Findings and Subsequent Service History

As noted previously, at the time this report was being prepared (4 years after the ILI crack-tool inspection), no in-service seam leaks or ruptures have occurred since the 2008 ultrasonic crack-tool inspection.

Comparisons between ILI Findings and Hydrostatic Test Results

The seam integrity of this segment was last assessed by means of a hydrostatic test in 1987, with part of the segment being tested again in 2002. One failure occurred during the test in 1987 (due to a seam defect), at a stress level of 82% SMYS. During the 2002 hydrostatic test, three seam failures occurred at stress levels between 91% SMYS and 95% SMYS. However, the ages of the tests tend to render any comparison between the test results and the results of the 2008 ILI tool run unproductive.

Comparisons between ILI Findings and Burst Test Results

Two pipe sections, which contained 17 ILI-reported seam anomalies (including 13 Weld Anomalies and 4 Notch-Like features), were subjected to burst testing. One test section failed at a pressure 54% higher than the predicted burst pressure based on the ILI-reported feature dimensions (a failure pressure corresponding to 116% SMYS). Coincidently, the other test section also failed at a pressure 54% higher than the predicted burst pressure based on the ILI-reported feature dimensions (a failure pressure corresponding to 127% SMYS). These results indicate that, at least for the tested pipe sections, predicted burst stresses based on tool-reported feature dimensions are generally conservative.

Comparisons between ILI Findings and Metallurgical Examinations

Eight features were sent for metallurgical examination (which included 5 Weld Anomalies, 2 Notch-Like and 1 Crack-Like features), where hook cracks were identified as the defect type. The sizing comparisons were presented in preceding figures.

Conclusions Regarding the Case 3 ILI Crack-Tool Run

The Case 3 ultrasonic-crack-tool inspection exhibited a high probability of detection and small propensity for false calls. Only one anomaly was found by field examination that should have been detected but was not. Only six ILI anomalies out of 275 examined in the field appeared to be false calls where no anomaly could be found upon examination. While most of the lack of fusion anomalies (as characterized by field personnel) were classified as weld anomalies by the ILI, many ILI features said to be notch-like and crack-like were also indicated to be lack of fusion anomalies by the field NDE personnel. As noted, all eight anomalies sent for metallurgical analysis corresponded with hook cracks and not lack of fusion. These results suggest that the other anomalies characterized as lack of fusion by field personnel could actually be hook cracks instead. Seam over-trim and under-trim anomalies tend to be classified as weld anomalies most often, but can also be classified as crack-like and notch-like.

With respect to depth sizing, the ILI depths tended to exceed those measured by Field NDE, by a factor of 2 or more in about one third of the cases. However, features reported as shallow were considerably undersized. The ILI lengths showed a better correlation with actual flaw lengths as compared with depth sizing. Lab data confirmed that the field measurements were reasonably accurate, illustrating that the ILI depths more often than not exceeded the actual depths of the anomalies.

Based on an analysis of the data, including the results of the burst testing and metallurgical analysis, the investigating team concludes that the ILI undersized defects that had high predicted burst stresses, but oversized those where the predicted burst stresses were low. This factor provides considerable confidence that "reported" anomalies would tend to be less injurious than the ILI-reported dimensions would suggest. In this sense, it is reasonable to conclude that the seam integrity of the Case 3 pipeline was confirmed. However, it should not be forgotten that the tool missed an 11.4-inch-long, 0.077-inch-deep anomaly that exceeded the length and depth detection thresholds of 1.2-inch in length and 0.04-inch in depth.

Case 4

Pipeline Attributes and Inspection Parameters

Case 4 involves a liquid pipeline 64 miles long comprised of 12.75-inch-OD, 0.250-inch (X56) or 0.375-inch wall (X52), high-frequency-welded (HF) ERW pipe manufactured by Stelco. The pipe was installed in 1986 and was inspected in 2008 by means of an ultrasonic crack-detection tool. The maximum operating stress of the pipeline corresponds to 55% of SMYS (for 0.250-inch wall pipe). This segment has not experienced any in-service failures. As a result of the 2008 ILI crack-tool run, 387 seam anomalies (average of 6 per mile) were reported and 16 of these were subjected to examination in the field. The field examinations consisted of visual inspection and magnetic particle inspection to characterize the types and lengths of the anomalies. Grinding or ultrasonic inspection was used to measure the depths of the anomalies. In the case of internal anomalies, ultrasonic inspection was used to characterize the lengths of the anomalies as well. None of the anomalies was removed for either burst testing or metallurgical examination. No seam failures have occurred since the last inspection.

The breakdown of the 387 anomalies reported by ILI by type of anomaly was: Weld Anomaly (55), Notch-Like (277), Crack-Like (55), and Crack Field (0). The breakdown of the 16 anomalies subjected to field examination by type of anomaly was: Weld Anomaly (3), Notch-Like (3), and Crack-Like (10). The rationale for choosing anomalies to examine appeared to have been based both on the lowest predicted failure stresses and the type of anomaly. All field-examined anomalies were repaired by means of grinding or Type B sleeves.

Comparisons between ILI Dimensions and Field-Measured Dimensions

Anomalies from the Case 4 data set were investigated in the field; none was sent for laboratory examination. Based on the field data, it appears that one seam under-trim anomaly that met the length and depth detection threshold for the tool was not reported by the tool. Field crews reported a measured length of 670 mm (26.4 inches) and maximum depth of 1.43 mm (0.056 inch) for this anomaly.

All three of the reported weld anomalies were found in the field. Two of those were indicated by field NDE to be lack of fusion anomalies. The third was found to be seam over-trim. All three of the reported notch-like anomalies were found in the field, corresponding with lack of fusion anomalies as described by the field NDE. Similarly, all 10 of the reported crack-like features were found in the field. Four of them were indicated to be lack of fusion anomalies. Half corresponded with seam over-trim anomalies. One anomaly was indicated to be a stringer. There were no reported crack field anomalies in the Case 4 pipe.

In terms of classification, 44% of the field-classified lack of fusion anomalies were ILI-classified as crack-like, while 33% were ILI-classified as notch-like and 22% were ILI-classified as weld anomalies. Seam over-trim anomalies indicated in the field were ILI-classified as crack-like anomalies 83% of the time and one was ILI-classified as a weld anomaly. Lack of fusion anomalies accounted for 56% of the reported seam weld features, while seam over-trim anomalies accounted for 38%. The lone stringer accounted for 6% of the weld features.

Table 9 contains field-measured and ILI-reported anomaly depths and lengths for the correlated features.

Table 9. Comparison between ILI-Called and Field-Measured Parameters for Case 4

Type of Anomaly		Length, inches		Depth, % Wall Thickness		Wall Thickness, inch		Location (External or Internal)	
ILI	Field	ILI	Field	ILI	Field	ILI	Field	ILI	Field
Crack-Like	Seam Over-Trim	6.0	8.0	37.7	8.0	0.209	0.220	Int	Int
Crack-Like	Lack of Fusion	3.9	4.2	18.9	7.2	0.209	0.208	Ext	Ext
Crack-Like	Lack of Fusion	3.5	6.5	18.9	5.3	0.209	0.209	Ext	Ext
Crack-Like	Seam Over-Trim	15.6	16.8	37.7	11.4	0.209	0.220	Int	Int
Crack-Like	Seam Over-Trim	6.9	7.3	28.3	9.6	0.209	0.206	Int	Int
Crack-Like	Seam Over-Trim	11.6	16.5	37.7	9.6	0.209	0.205	Int	Int
Weld Anomaly	Seam Over-Trim	7.6	16.9	47.2	9.4	0.209	0.210	Int	Int
Weld Anomaly	Lack of Fusion	5.1	5.3	47.2	15.6	0.209	0.213	Ext	Ext
Weld Anomaly	Lack of Fusion	2.5	4.9	37.7	14.3	0.209	0.209	Int	Ext
Crack-Like	Seam Over-Trim	21.2	23.8	40.0	7.7	0.197	0.206	Int	Int
Crack-Like	Stringer	4.5	16.2	39.7	3.7	0.248	0.285	Ext	Ext
Crack-Like	Lack of Fusion	3.5	3.6	23.8	33.3	0.248	0.284	Int	Int
Notch-Like	Lack of Fusion	2.5	2.5	23.8	33.6	0.248	0.296	Int	Int
Notch-Like	Lack of Fusion	1.9	1.8	15.9	30.9	0.248	0.296	Int	Int
Crack-Like	Lack of Fusion	2.4	2.5	39.7	32.6	0.248	0.292	Ext	Int
Notch-Like	Lack of Fusion	3.2	2.9	15.9	30.6	0.248	0.296	Int	Int

Comparisons of ILI-reported depths of anomalies with those determined by field NDE are shown in Figure 12.

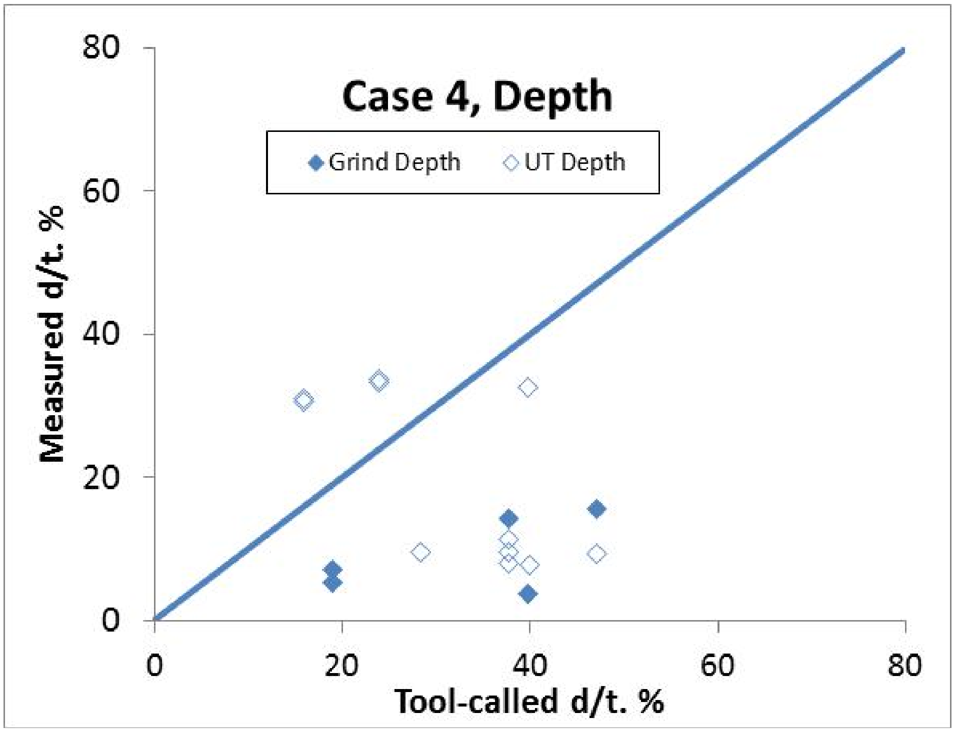

Figure 12. Comparisons between Field-determined Anomaly Depth and ILI Anomaly Depth, Case 4

As shown in Figure 12, the majority of depths (75%) reported by the ILI exceed those measured by field NDE. In fact, 69% of ILI depths exceeded those determined by field NDE by a factor of 2 or more. Thus, the tool appears to have overcalled the depths if the field NDE depths are to be believed accurate. In contrast, one feature reported with a shallow depth was actually found to be twice the reported depth. Although the Case 4 data set is smaller than the Case 3 data set, one can make the same observation that relatively deep anomalies (approximately 30% WT) were found for several depth ranges reported by the ILI tool. Further, it is difficult to say whether the distribution of field NDE indications is similar to that of the grind measurements based on the data provided. A separate grind vs. field-NDE depth correlation would be required in order to evaluate the accuracy of the ultrasonic measurements.

Comparisons of ILI-reported lengths of anomalies with those determined by field NDE are shown in Figure 13.

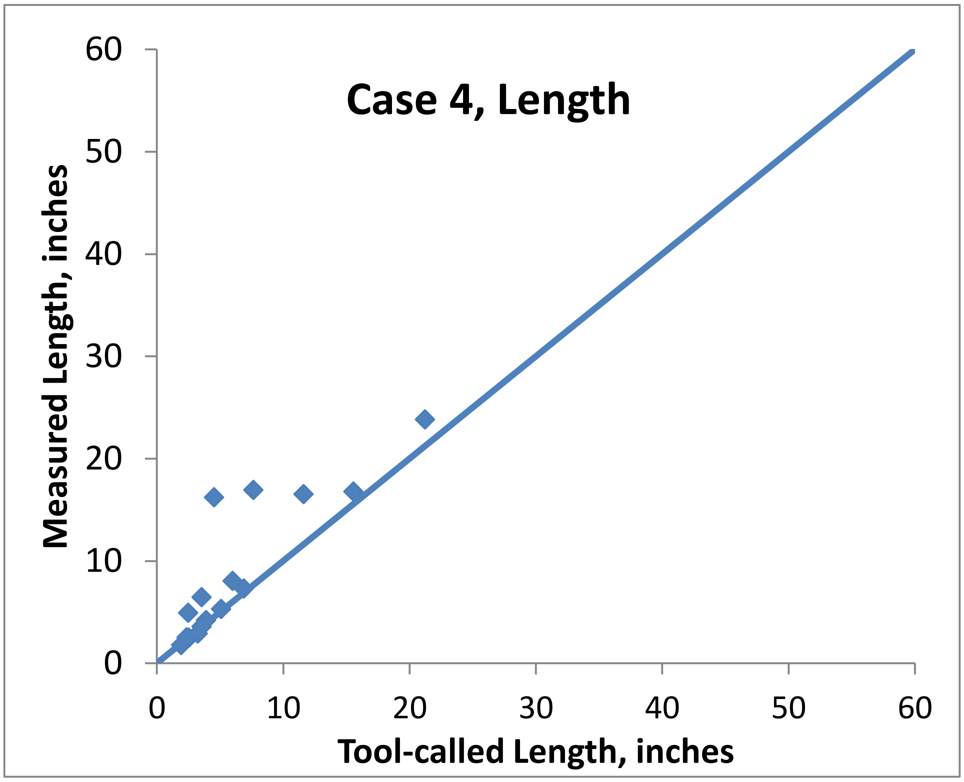

Figure 13. Comparisons between Field-determined Anomaly Length and ILI Anomaly Length, Case 4

Figure 13 shows that most (81%) of the anomalies were measured to be longer than what the ILI reported. Further, most data are aligned within a reasonable scatter band. Again, the trending suggests that most lengths are under-reported, which can be attributable to the tool's inability to detect shallow parts of the cracks.

Comparisons of ILI-reported wall thicknesses with those determined by field NDE for the nominal 0.250-inch-thick pipe are shown in Figure 14.

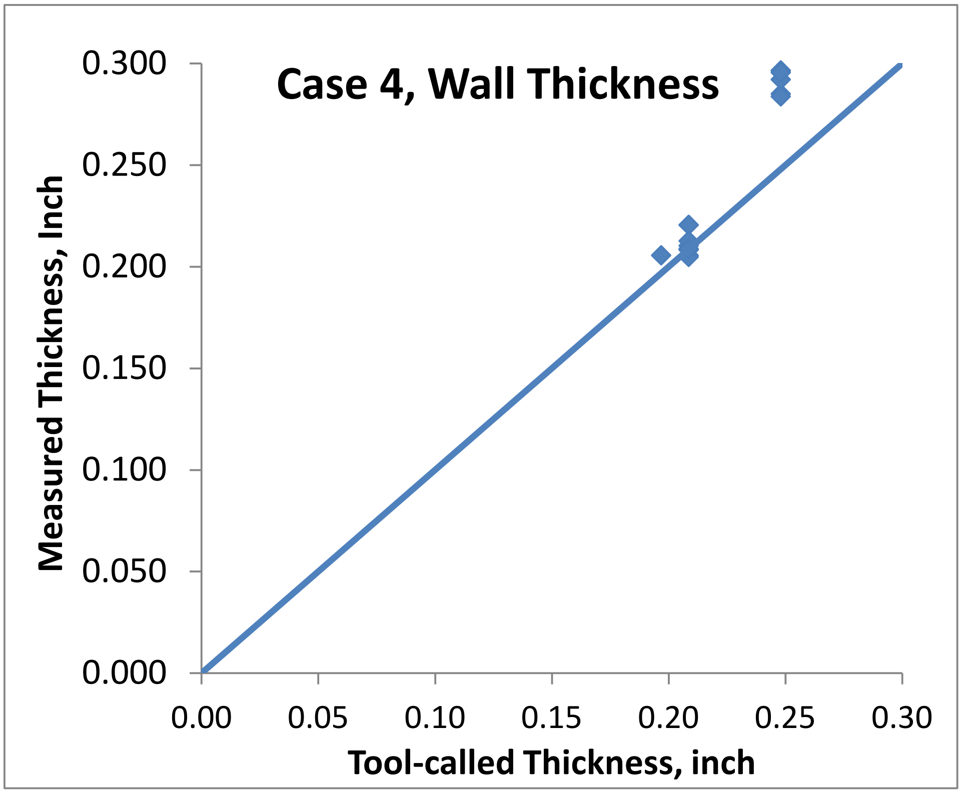

Figure 14. Comparisons between Field-determined Wall Thickness and ILI Wall Thickness, Case 4

The data shown in Figure 14 indicate that approximately half of the wall thicknesses measured by field NDE fluctuated within 5% of the ILI-reported values, while the other half appeared to be about 19% higher than the ILI-reported values. Thus, the tool appeared to under-call the wall thickness in half of the cases.

Figure 15 shows a comparison between failure stresses of the anomalies calculated on the basis of ILI dimensions and those calculated on the basis of field-measured dimensions. Failure stress levels for these anomalies were calculated using the CorLAS™ fracture mechanics model with a full-size-equivalent Charpy upper shelf energy of 7 ft-lb (based on Charpy v-notch test results for a similar material). As can be seen in Figure 15, the failure stress levels based on field-measured dimensions are above 150% SMYS. The plot shows a slight tendency for the ILI-based failure stress to be lower than the field and laboratory-based failure stress. This is the result of most anomalies being reported as being deeper than the field NDE indicated. These results indicate the predicted failure stresses based on ILI dimensions tended to be less than those predicted on the basis of dimensions determined by field NDE.

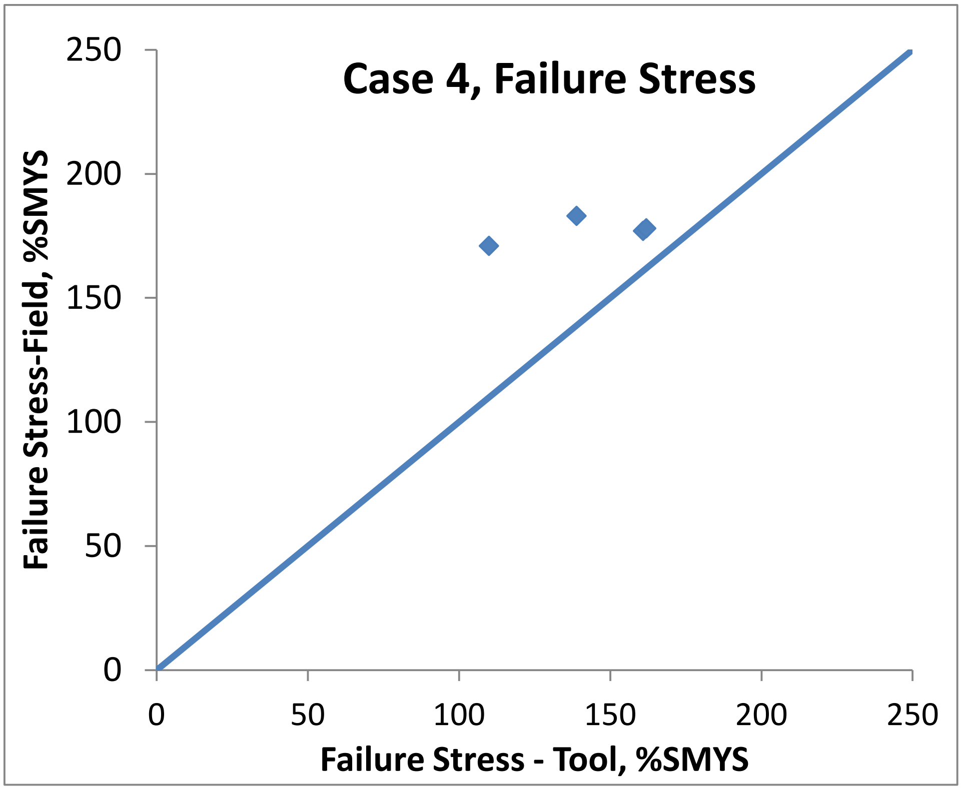

Figure 15. Comparisons between Predicted Failure Stresses Based on Field-Measured Anomaly Dimensions and Those Based on ILI Dimensions, Case 4

Comparisons between ILI Findings and Subsequent Service History

This segment has not experienced any in-service failures either before or after the ultrasonic crack-tool inspection.

Comparisons between ILI Findings and Hydrostatic Test Results

Except for 62 km of pipe that was replaced with new pipe in 1988 (subject to a post-construction hydrostatic test), the seam integrity of this segment was last assessed by means of hydrostatic tests in 1987 (although a small portion of the pipe was also tested in 2002). No failures occurred during either test, although the stress levels achieved during the tests were not provided to the investigating team. Regardless, both tests were conducted too long ago to allow any meaningful comparison between the test results and the results of the 2008 ILI tool run.

Comparisons between ILI Findings and Burst Test Results

No samples of pipe containing ILI anomalies were available for the purposes of hydrostatic testing.

Comparisons between ILI Findings and Metallurgical Examinations

No samples of pipe containing ILI anomalies were available for the purposes of metallurgical examination.

Conclusions Regarding the Case 4 ILI Crack-Tool Run

With respect to depth sizing, the ILI tended to report depths that exceed those determined by Field NDE, by a factor of 2 or more in about one third of cases. However, features reported as shallow can be considerably undersized. The ILI-reported lengths showed a better correlation with field-measured flaw lengths as compared with depth sizing.

Without the benefit of a burst test or a metallurgical examination, it is difficult to ascertain which set of measurements (ILI or the field measurements or both) are inaccurate. The overall conclusion is that the Case 4 ILI tool run results cannot be regarded as having proved the seam integrity of the segment to be adequate. Moreover the fact that an anomaly was missed that should have been reported prevents one from having total confidence in the tool.

As previously stated, trying to evaluate the quality of inspection for a given ILI run cannot always be done merely through field NDE. In this example, the accuracy of the field NDE is just as questionable as the accuracy of the ILI inspection results, so the ILI results were not adequately validated. Because of this and because of the "missed" anomaly, validation of the seam integrity cannot be assured.

Case 5

Pipeline Attributes and Inspection Parameters

Case 5 involves a 40-mile liquid pipeline segment consisting of 12.75-inch-OD, 0.219-inch and 0.250-inch wall, X52 low-frequency ERW pipe manufactured by Alberta Phoenix and installed in 1961. The pipeline segment was inspected by means of an ultrasonic crack-detection tool in 2008. The maximum operating stress of the pipeline corresponds to 67% of SMYS (for 0.219-inch wall pipe). As a result of the 2008 ILI crack-tool run, 1,668 seam anomalies (average of 42 per mile) were reported and 29 of these were subjected to examination in the field. The field examinations consisted of visual inspection and magnetic particle inspection to characterize the type and length of the anomaly. Grinding or ultrasonic inspection was used to measure the depth of the anomaly. In the case of an internal anomaly, ultrasonic inspection was used to characterize the length of the anomaly as well. No seam weld failures have occurred since the inspection.

The breakdown of the 1,668 anomalies indicated by the ILI by type of anomaly was: Weld Anomaly (619), Notch-Like (859), Crack-Like (179), and Crack Field (11). The breakdown of the 29 anomalies subjected to field examination by type of anomaly was: Weld Anomaly (14), Notch-Like (7), and Crack-Like (8). None of the Crack Field anomalies were examined in the field. The rationale for choosing anomalies to examine appeared to have been based both on the lowest predicted failure stresses and the type of anomaly. All field-examined anomalies were repaired by means of grinding or Type B sleeves.

Comparisons between ILI Dimensions and Field-Measured Dimensions

The Case 5 data set includes anomalies that were investigated in the field; none was sent to the laboratory for investigation. Based on the field data, it appears that no significant unreported anomalies (having dimensions above the minimum detection threshold) were observed.

All 14 of the reported weld anomalies were found in the field. Approximately 57% (8) were found to be lack of fusion anomalies. The remaining 43% (6) were found to be seam over-trim or seam under-trim. All 7 of the reported notch-like features were found in the field. Approximately 71% (5) were found to be seam over-trim or seam under-trim. One was found to be a lack of fusion anomaly and one was found to be SCC. Similarly, all of the 8 reported crack-like features were found in the field. Half of them were found to be lack of fusion anomalies and the other half corresponded with seam over-trim or seam under-trim.

In terms of classification, 62% of the field NDE classified lack of fusion anomalies were classified by the ILI vendor as weld anomalies, while 31% were ILI-classified as crack-like and one was ILI-classified as notch-like. Seam over-trim or under-trim anomalies were ILI-classified as weld anomalies 40% of the time, notch-like 33% of the time, and crack-like 27% of the time. Seam over/under-trim anomalies accounted for 52% of the reported seam weld features and lack of fusion anomalies accounted for 45% of the reported seam weld features.

Table 10 contains field-measured and ILI-reported anomaly depths and lengths for the correlated features.

Table 10. Comparison between ILI and Field-Measured Parameters for Case 5

Type of Anomaly		Length, inches		Depth, % Wall Thickness		Wall Thickness, inch		Location (External or Internal)	
ILI	Field	ILI	Field	ILI	Field	ILI	Field	ILI	Field
Notch-Like	Seam Over-Trim	17.9	15.4	37.7	7.0	0.209	0.224	Int	Int
Weld Anomaly	Lack of Fusion	4.0	5.1	47.2	9.2	0.209	0.214	Ext	Ext
Crack-Like	Lack of Fusion	9.7	10.8	37.7	32.7	0.209	0.217	Int	Int
Weld Anomaly	Seam Under-Trim	7.9	8.0	50.0	10.8	0.197	0.204	Int	Int
Weld Anomaly	Seam Under-Trim	4.2	6.8	20.0	7.4	0.197	0.213	Int	Int
Weld Anomaly	Seam Under-Trim	4.6	7.5	20.0	9.4	0.197	0.209	Int	Int
Notch-Like	Seam Under-Trim	31.0	19.8	20.0	9.2	0.197	0.214	Int	Int
Notch-Like	Seam Over-Trim	21.7	23.4	40.0	9.6	0.197	0.206	Int	Int
Weld Anomaly	Seam Under-Trim	4.6	5.1	28.3	3.8	0.206	0.207	Int	Int
Weld Anomaly	Seam Under-Trim	2.5	3.0	9.4	3.8	0.209	0.207	Int	Int
Weld Anomaly	Seam Over-Trim	6.2	7.5	37.7	7.8	0.209	0.202	Int	Int
Crack-Like	Seam Over-Trim	12.8	15.1	28.3	20.8	0.209	0.189	Int	Int
Crack-Like	Seam Over-Trim	22.1	17.0	9.4	20.4	0.209	0.193	Ext	Int
Crack-Like	Seam Over-Trim	18.5	19.3	40.0	0.0	0.197	0.219	Int	Int
Notch-Like	Lack of Fusion	1.3	2.2	25.9	26.9	0.228	0.232	Ext	Ext
Crack-Like	Lack of Fusion	4.8	6.5	39.7	17.4	0.228	0.226	Ext	Ext
Weld Anomaly	Lack of Fusion	5.7	0.9	47.2	33.5	0.209	0.219	Int	Int
Weld Anomaly	Lack of Fusion	6.6	5.8	47.2	21.4	0.209	0.220	Int	Int
Weld Anomaly	Lack of Fusion	3.6	3.9	47.2	38.6	0.209	0.224	Int	Int
Crack-Like	Lack of Fusion	3.1	3.1	18.9	17.7	0.209	0.224	Ext	Ext
Crack-Like	Lack of Fusion	5.5	5.9	18.9	10.5	0.209	0.224	Ext	Ext
Weld Anomaly	Lack of Fusion	5.2	5.8	28.3	15.8	0.209	0.224	Int	Int
Weld Anomaly	Lack of Fusion	3.3	3.8	47.2	21.1	0.209	0.224	Int	Int
Weld Anomaly	Lack of Fusion	6.0	6.6	52.8	46.7	0.209	0.224	Ext	Ext
Weld Anomaly	Lack of Fusion	2.5	3.7	18.9	16.7	0.209	0.224	Ext	Ext
Notch-Like	Seam Over-Trim	3.7	19.7	9.4	3.5	0.209	0.224	Int	Int
Crack-Like	Seam Over-Trim	6.7	19.7	47.2	7.0	0.209	0.224	Int	Int
Notch-Like	SCC	3.6	0.8	9.4	5.3	0.209	0.224	Ext	Ext
Notch-Like	Seam Over-Trim	25.3	25.0	9.4	10.5	0.209	0.224	Int	Int

The comparisons of anomaly depths as indicated by the ILI with those determined by field NDE are presented in Figure 16.

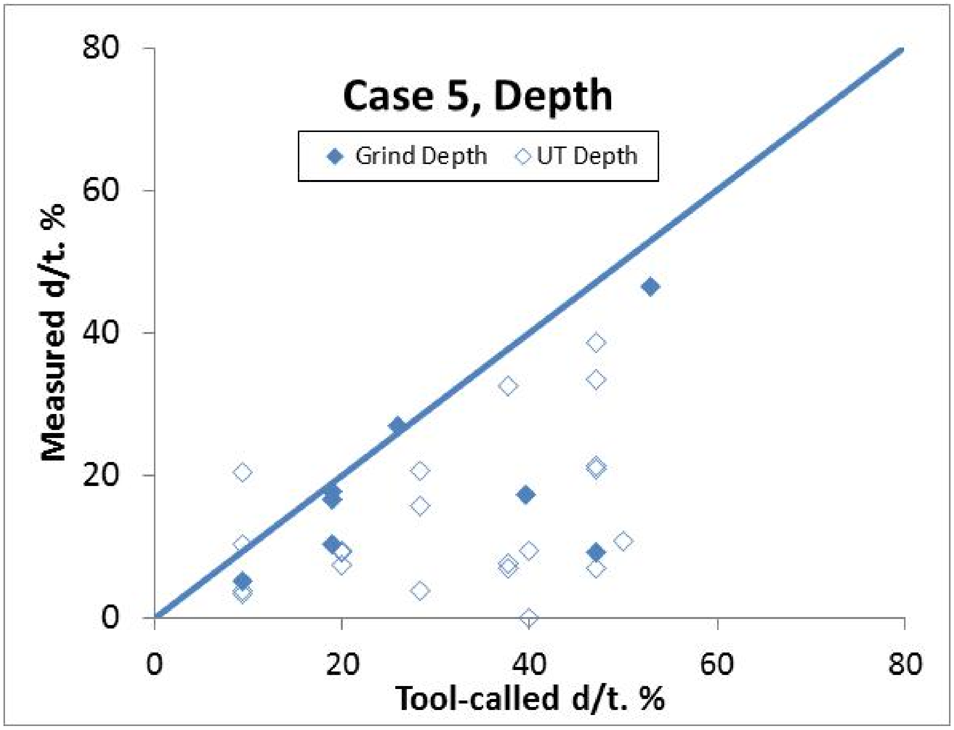

Figure 16. Comparisons between Field-determined Anomaly Depth and ILI Anomaly Depth, Case 5

As shown in Figure 16, the majority of features (90%) were reported by the ILI as being deeper than indicated by the field NDE. In fact, 55% of features were over-sized by a factor of 2 or more. In contrast, one feature reported with a shallow depth was found by field NDE to be twice as deep. Unlike the Case 3 and Case 4 data, the Case 5 data show that the upper bound field-measured depth increases with increasing tool-reported depths. Further, the distribution of field-NDE ultrasonic measurements is similar to that of the grind measurements, possibly an indication that the field-NDE measurements were reasonably accurate (although a separate grind vs. field-NDE depth correlation would be required in order to be conclusive).

The comparisons of anomaly lengths indicated by ILI with those determined by field NDE are presented in Figure 17.

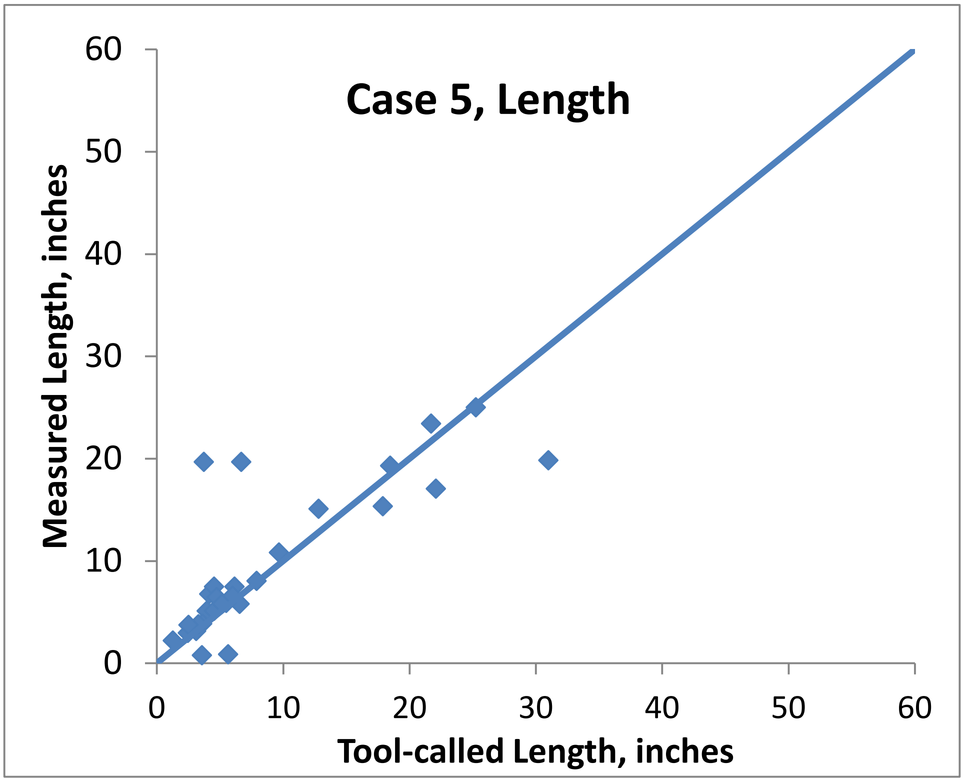

Figure 17. Comparisons between Field-determined Anomaly Length and ILI Anomaly Length, Case 5

Figure 17 is a plot of the field versus ILI-reported anomaly lengths, which indicates most data are aligned within a reasonable scatter band. Only 24% were reported by the ILI as being longer than they appeared to be on the basis of field NDE. Of those whose length was under-reported, two anomalies (corresponding to under/over-trim anomalies) had field-measured lengths that were considerably longer than what the ILI reported (between 3 and 5 times longer). The trend suggests reasonable length accuracy, but under-reported values can be attributable to the tool's inability to detect shallow parts of the cracks.

The comparisons of wall thickness as indicated by ILI with those determined by field NDE are presented in Figure 18.

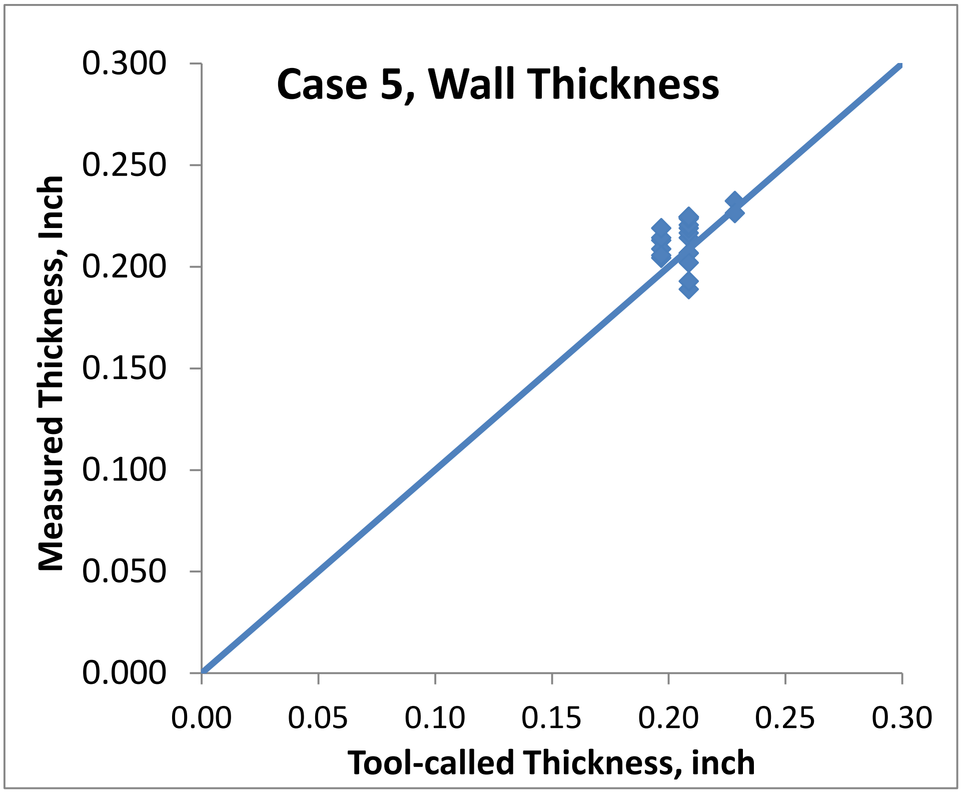

Figure 18. Comparisons between Field-determined Wall Thickness and ILI Wall Thickness, Case 5

Based on a review of the ILI-reported and field measured wall thickness values (shown in Figure 18), all the field-measured wall thickness values fluctuated within 10% of the ILI-reported values.

Figure 19 shows a comparison between failure stresses of the anomalies calculated on the basis of ILI dimensions and those calculated on the basis of field-measured dimensions. Failure stress levels for these anomalies were calculated using the CorLAS™ fracture mechanics model with a full-size-equivalent Charpy upper shelf energy of 7 ft-lb (based on Charpy v-notch test results for a similar material). As can be seen in Figure 19, the failure stress levels based on field-measured dimensions are above 150% SMYS. The plot shows a tendency for the ILI-based failure stress to be lower than the field-based failure stress. This is the result of most anomalies being reported as being deeper than indicated by the field NDE.

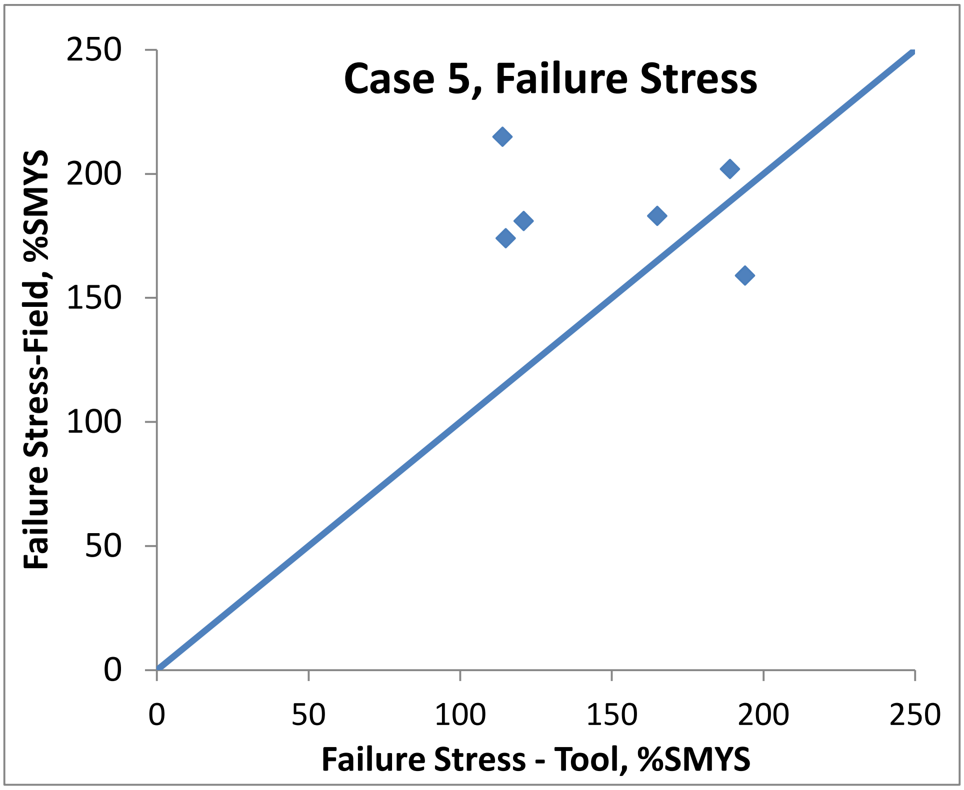

Figure 19. Comparisons between Predicted Failure Stresses Based on Field-Measured Anomaly Dimensions and Those Based on ILI Dimensions, Case 5

Comparisons between ILI Findings and Subsequent Service History

This segment has not experienced any in-service failures either before or after the 2008 ultrasonic crack-tool inspection.

Comparisons between ILI Findings and Hydrostatic Test Results

The seam integrity of this segment was last assessed by means of hydrostatic tests in 1987 (although a small portion of Case 5 pipe was also tested in 2002). One failure occurred during the test in 1987 (due to a seam defect), although the achieved stress level could not be confirmed by the investigation team. No failures occurred during the test in 2002. Both tests were conducted too long ago to allow any meaningful comparison between the test results and the results of the 2008 ILI tool run.

Comparisons between ILI Findings and Burst Test Results

None of the anomalies was removed for burst testing.

Comparisons between ILI Findings and Metallurgical Examinations

None of the anomalies was removed for metallurgical examination.

Conclusions Regarding the Case 5 ILI Crack-Tool Run

On the basis of the 29 field examinations the Case 5 ultrasonic crack-tool inspection appears not to have missed any defect or made any false calls. However, this is a relatively small sample (much less than a mile of pipe out of 40 miles for determining the absence of missed defect and 29 out of 1,668 anomalies for determining the absence of false calls). While most of the lack of fusion anomalies classified by field NDE were classified as weld anomalies by the ILI (which is consistent with Case 3 observations but inconsistent with Case 4 observations), there is a chance that features classified as crack-like and notch-like anomalies also correspond to lack of fusion anomalies. Similarly, seam over-trim and under-trim anomalies tended to be classified as weld anomalies most often (consistent with Case 3 observations but inconsistent with Case 4 observations), but some were classified as notch-like or crack-like anomalies.

With respect to depth sizing, the ILI depths tended to exceed those determined by Field NDE, by a factor of 2 or more in more than half of the cases. However, features reported as shallow can be considerably undersized. The tool-reported lengths showed a better correlation with field-measured flaw lengths as compared with depth sizing.

Without the benefit of a burst test or a metallurgical examination, one cannot ascertain whether it was the ILI or the field measurements or both that are inaccurate. The overall conclusion is that the Case 5 ILI tool run results cannot be regarded as having proved the seam integrity of the segment to be adequate.

Case 6

Pipeline Attributes and Inspection Parameters

Case 6 involves a 16-mile segment of a liquid pipeline comprised of 12.75-inch-OD, 0.250-inch wall, X52 low-frequency ERW pipe manufactured by Prairie Pipe. The pipe segment was installed in 1961 and inspected in 2008 by means of an ultrasonic crack-detection tool. The maximum operating stress of the pipeline corresponds to 59% of SMYS. As a result of the 2008 ILI crack-tool run, 1,409 seam anomalies (average of 89 per mile) were reported and 21 of these were subjected to examination in the field. The field examinations consisted of visual inspection and magnetic particle inspection to characterize the type and length of the anomaly. Grinding or ultrasonic inspection was used to measure the depth of the anomaly. In the case of an internal anomaly, ultrasonic inspection was used to characterize the length of the anomaly as well. No seam failures have occurred either before or after the inspection.

The breakdown of the 1,409 anomalies indicated by ILI by type of anomaly was: Weld Anomaly (375), Notch-Like (830), Crack-Like (199), and Crack Field (5). The breakdown of the 21 anomalies subjected to field examination by type of anomaly was: Weld Anomaly (7), Notch-

Like (2), and Crack-Like (12). The rationale for choosing anomalies to examine appeared to have been based both on the lowest predicted failure stresses and the type of anomaly. All field-examined anomalies were repaired by means of grinding.

Comparisons between ILI Dimensions and Field-Measured Dimensions

The Case 6 data set includes anomalies that were investigated in the field; none were sent to the laboratory for investigation. Based on the field data, no unreported lack of fusion anomalies were found with dimensions above the minimum detection threshold. All 7 of the reported weld anomalies were found in the field. All of them were found to be seam over-trim or seam under-trim. Both (two) of the reported notch-like features were found in the field and both of them were found to be seam over-trim or seam under-trim. Similarly, all 12 of the reported crack-like features were found in the field. Approximately 67% (8) were found to be gouges. The other 33% (4) were found to be seam under-trim.

In terms of classification, all 8 of the gouges found were classified by the ILI vendor as crack-like. Nearly half (7 of the 13) seam over-trim or under-trim anomalies were classified as weld anomalies, while 4 were classified as crack-like and 2 were classified as notch-like. Seam over-trim or under-trim anomalies accounted for 62% of the reported seam weld features.

Table 11 contains field-measured and ILI-reported anomaly depths and lengths for the correlated features.

Table 11. Comparison between ILI and Field-Measured Parameters for Case 6

Length, inches		Depth, % Wall Thickness		Wall Thickness, inch		Location (External or Internal)	
ILI	Field	ILI	Field	ILI	Field	ILI	Field
18.0	85.8	31.7	3.3	0.248	0.250	Ext	Ext
26.7	85.8	31.7	3.9	0.248	0.250	Ext	Ext
5.7	85.8	7.9	2.8	0.248	0.250	Ext	Ext
7.5	85.5	15.9	3.9	0.248	0.250	Ext	Ext
17.2	17.7	33.3	18.4	0.236	0.256	Int	Int
15.6	15.9	41.7	12.3	0.236	0.256	Int	Int
45.6	140.6	36.7	4.0	0.236	0.254	Ext	Ext
34.5	140.6	33.3	2.3	0.236	0.257	Ext	Ext
10.5	140.6	25.0	4.0	0.236	0.257	Ext	Ext
10.4	140.6	16.7	2.3	0.236	0.252	Ext	Ext
14.0	15.0	53.3	12.3	0.236	0.256	Int	Int
13.5	15.4	31.7	20.1	0.236	0.255	Int	Int
4.1	3.9	7.9	5.7	0.248	0.276	Int	Int
16.1	17.8	31.7	10.0	0.248	0.276	Int	Int
23.7	24.4	31.7	10.0	0.248	0.276	Int	Int
3.5	6.3	7.9	9.3	0.248	0.276	Int	Int
1.7	0.6	7.9	4.4	0.248	0.268	Int	Int
14.8	14.4	42.9	5.9	0.248	0.268	Int	Int
15.7	15.9	47.6	7.4	0.248	0.268	Int	Int
4.0	6.7	15.9	5.9	0.248	0.268	Int	Int
5.9	6.3	7.9	4.4	0.248	0.268	Ext	Int

Comparisons of depths of ILI anomalies to those measured by field NDE are presented in Figure 20.

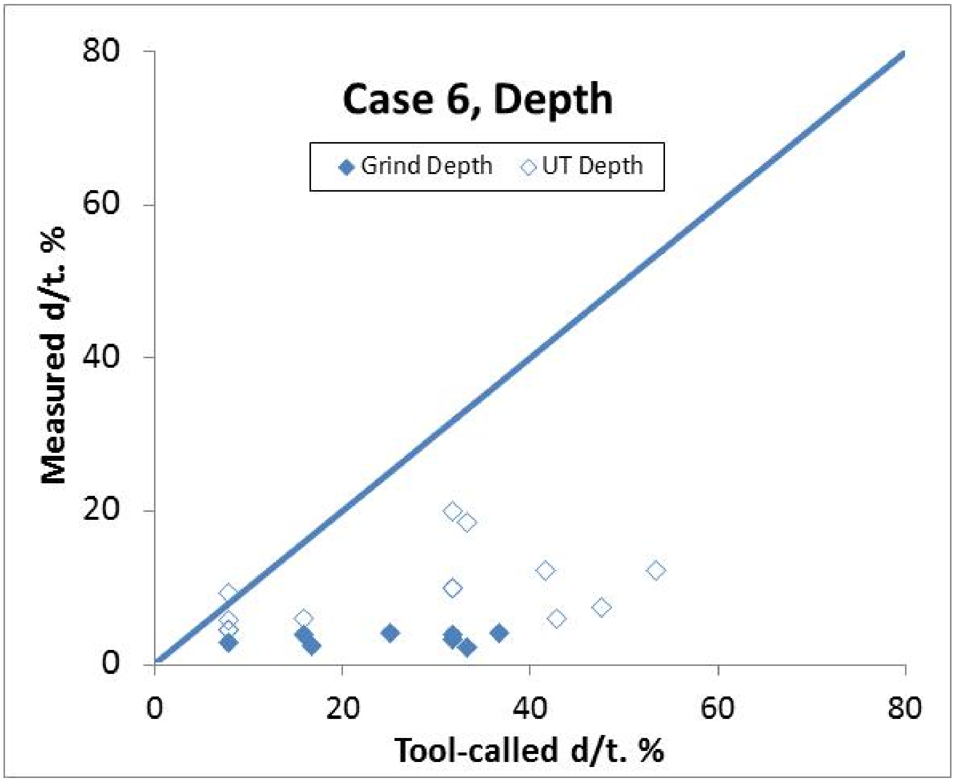

Figure 20. Comparisons between Field-determined Anomaly Depth and ILI-called Anomaly Depth, Case 6

All but one (95%) of the features were reported by the ILI as being deeper than the depths measured by field NDE. In fact, 71% of features were oversized by a factor of 2 or more. Thus, depth sizing was conservative if the field measure depths are to be believed accurate. One anomaly was reported by the ILI as being shallower than the field-measure depth by about15%. With few exceptions, the ILI-reported depths do not seem to correlate well with the field measured values. Further, it is difficult to say whether the distribution of field-NDE ultrasonic measurements is similar to that of the grind measurements based on the data provided. A separate grind vs. ultrasonic depth correlation would be required in order to evaluate the accuracy of the ultrasonic measurements.

Comparisons of lengths of ILI anomalies to those measured by field NDE are presented in Figure 21.

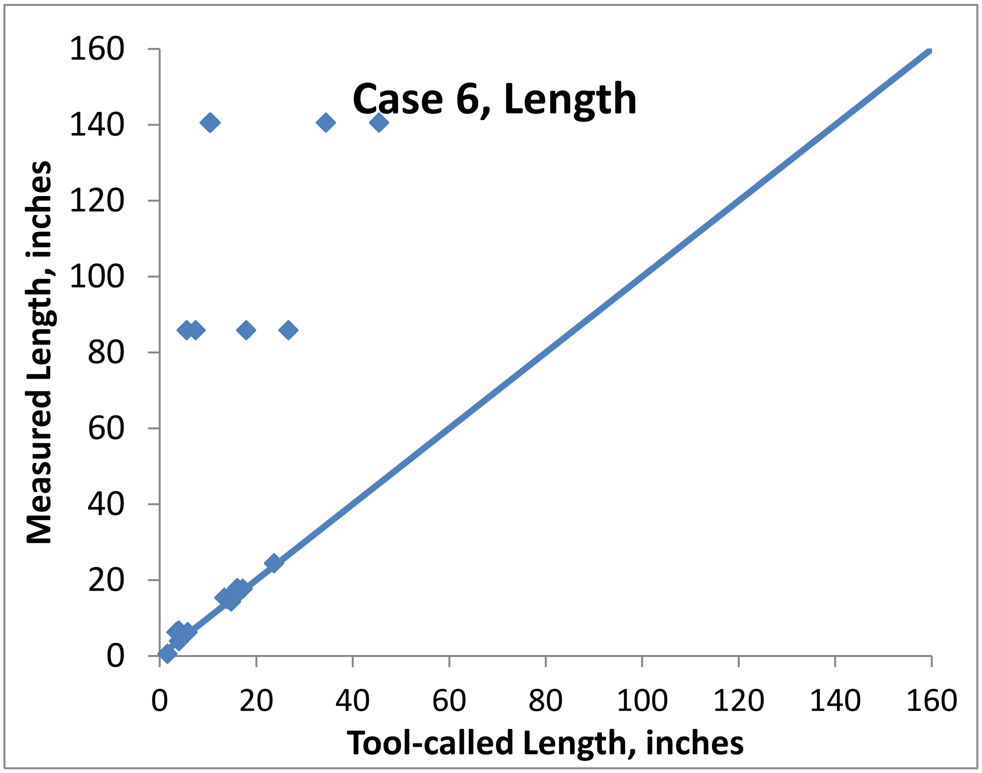

Figure 21. Comparisons between Field-determined Anomaly Length and ILI Anomaly Length, Case 6

Regarding the comparisons shown in Figure 21, only 14% were reported by the ILI as being longer than the field-measured lengths. While 62% of the data aligned within a reasonable scatter band, more than a third represented ILI-reported lengths that were smaller than the field-measure lengths by a factor of three or more. The trending suggests that the lengths of approximately one third of anomalies could be under-reported, which could be attributable to the tool's inability to detect shallow parts of the features.

Comparisons of ILI-indicated wall thicknesses to those measured by field NDE are presented in Figure 22.

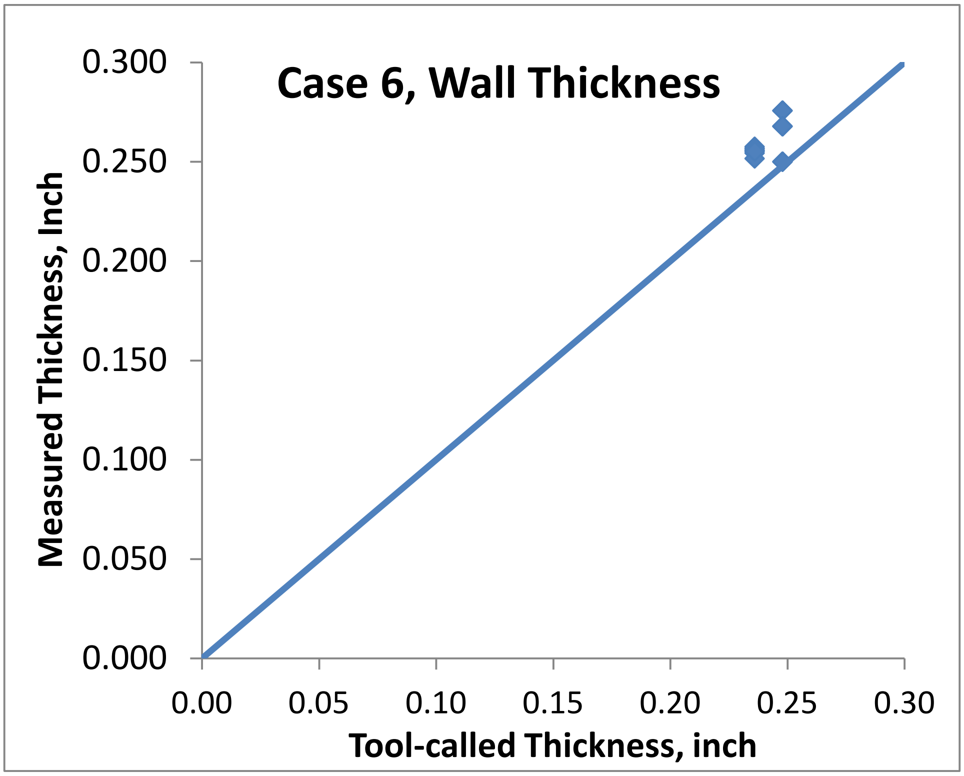

Figure 22. Comparisons between Field-determined Wall Thickness and ILI Wall Thickness, Case 6

The wall thickness comparisons for Case 6 show that the field-measured wall thickness values generally fluctuated within 11% of the ILI-reported value. This is typical of the range observed by the investigating team.

Comparisons of predicted failure stresses based on the dimensions of tool-called anomalies to those based on dimensions measured by field NDE are presented in Figure 23.

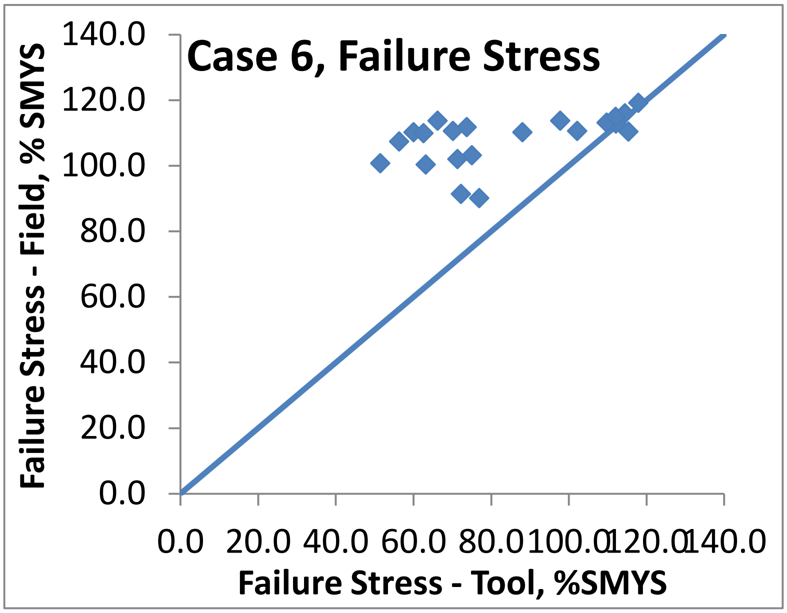

Figure 23. Comparisons between Predicted Failure Stresses Based on Field-Measured Anomaly Dimensions and Those Based on ILI Dimensions, Case 6

Figure 23 shows a comparison between failure stresses of the anomalies calculated on the basis of ILI dimensions and those calculated on the basis of field-measured dimensions. Failure stress levels for these anomalies were calculated using the Modified Ln-Sec Elliptical C-Equivalent model with a full-size-equivalent Charpy upper shelf energy of 20 ft-lb (based on Charpy v-notch test results). As can be seen in Figure 23, the failure stress levels based on field-measured dimensions are above 90% SMYS. The plot shows a tendency for the ILI-based failure stress to be lower than the field-based failure stress. This is the result of anomaly depths reported by the tool being deeper than those measured by field NDE.

Comparisons between ILI Findings and Subsequent Service History

This segment has not experienced any in-service failures.

Comparisons between ILI Findings and Hydrostatic Test Results

The seam integrity of this segment was last assessed by means of a hydrostatic test in 1987, during which no failures occurred. Details of the achieved stress levels were not made available to the investigation team, but because the test was performed so long ago, a meaningful comparison between the test results and the results of the 2008 ILI tool run cannot be performed anyway.

Comparisons between ILI Findings and Burst Test Results

None of the anomalies was removed for burst testing.

Comparisons between ILI Findings and Metallurgical Examinations

None of the anomalies was removed for metallurgical examination.

Conclusions Regarding the Case 6 ILI Crack-Tool Run

On the basis of the 21 field examinations, the Case 6 ultrasonic crack-tool inspection appears not to have missed any defect or made any false calls. However, this is a relatively small sample (much less than a mile of pipe out of 16 miles for determining the absence of missed defect and 21 out of 1,409 anomalies for determining the absence of false calls). Unlike the other cases, no lack of fusion anomalies were classified by field examinations conducted on Case 6 pipe. Seam over-trim and under-trim anomalies tend to be classified as weld anomalies most often (consistent with both Case 3 and Case 5 findings but inconsistent with Case 4 findings), but they could also be classified as crack-like or notch-like anomalies.

With respect to depth sizing, the ILI depths were greater by a factor of 2 or more than the depths measured by field NDE in more about 3/4 of the cases. The propensity for features reported as shallow to be considerably undersized is not evident with the Case 6 observations, unlike some other cases. The ILI-reported lengths tended to be significantly shorter than the lengths determined by field NDE.

Without the benefit of a burst test or a metallurgical examination, one cannot ascertain whether it was the ILI or the field measurements or both that were inaccurate. The overall conclusion is that the Case 6 ILI tool run results cannot be regarded as having proved the seam integrity of the segment to be adequate.

Case 7

Pipeline Attributes and Inspection Parameters

A 22-mile segment of a liquid pipeline comprised of 16-inch-OD, 0.250-inch-wall, X42 direct-current-welded ERW pipe manufactured by Youngstown Sheet and Tube Company installed in 1953 was inspected by means of an ultrasonic crack-detection tool. The maximum operating stress of the pipeline corresponds to 72% of SMYS; however, the normal operating stress is about 30% of SMYS. The year of inspection was 2007. This segment had experienced no in-service failures. The seam integrity of this segment was assessed by means of hydrostatic testing in 1994 and 2012. The 1994 hydrostatic test was carried out at stress levels ranging from 69% to 71% of SMYS. No test failure occurred. The 2012 hydrostatic test was carried out to a minimum stress level of 91.5 % of SMYS. Two ruptures from seam defects occurred during the 2012 test.

As a result of the 2007 ILI crack-tool run, 61 seam anomalies (average of 3 per mile) were reported and 23 of these were subjected to examination in the field. The field examinations consisted of visual inspection and magnetic particle inspection (MT) to characterize the type and length of the anomaly and ultrasonic inspection (UT) to measure the depth of the anomaly or, in the case of an internal anomaly, to characterize the length of the anomaly as well. None of the anomalies was removed after the crack-tool inspection for either burst testing or metallurgical examination. The history of the segment between the time of the 2007 inspection and the 2012 hydrostatic test involves no in-service seam failure incident.

The breakdown of the 61 anomalies indicated by the ILI by type of anomaly is: Weld Anomaly (16), Notch-Like (24), Crack-Like (16), and Crack Field (5). The breakdown of the 23 anomalies subjected to field examination by type of anomaly is: Weld Anomaly (10), Notch-Like (2), Crack-Like (9), and Crack Field (2). The rationale for choosing anomalies to examine appeared to have been based both on the lowest predicted failure stresses and the type of anomaly. Three of the field-examined anomalies were repaired by means of Type B sleeves, and one was repaired by means of a composite wrap. The remaining anomalies were judged to be non-injurious, and pipe was merely recoated.

Comparisons between ILI Dimensions and Field-Measured Dimensions

Comparisons between the ILI anomaly dimensions and those measured in the field are presented in Table 12. The first two columns in Table 12 present comparisons between the types of anomalies indicated by the ILI and the nature of the anomaly as it appeared to the field investigators. The other columns present comparisons between ILI size parameters and the size parameters that field investigators were able to measure. As seen in the table, some elements of data are missing from the field measurements for reasons that were not apparent to the investigating team (i.e., KAI, DNV, or Battelle).

Table 12. Comparison between ILI and Field-Measured Parameters for Case 7

Type of Anomaly		Length, inches		Depth, % Wall Thickness		Wall Thickness, inch	
ILI	Field	ILI	Field	ILI	Field	ILI	Field
Crack-Like	lamination	6.4				0.248	0.248
Crack-Like	lamination	12				0.248	0.25
Crack Field	Mill defect	9.3	1	25	6.0	0.236	0.258
Notch-Like	Mill defect	3.2	3	25	3.6	0.236	0.253
Weld Anomaly	Mill defect	2.1	2			0.236	0.247
Crack-Like	Mill defect	2.4	2			0.236	0.248
Weld Anomaly	Mill defect	3.8	15	25	4.8	0.236	0.251
Crack-Like	Mill defect	3	2.75	25	20.0	0.248	0.256
Crack-Like	Mill defect	6.2	4	25	15.0	0.248	0.248
Weld Anomaly	Mill defect	3.6	1.625	25	20.1	0.236	0.254
Crack-Like	Mill defect	1.9	0.5	25	13.0	0.236	0.248
Crack-Like	Mill defect	10	4.5	25	18.0	0.236	0.245
Weld Anomaly	Mill defect	2.4	1.5	40	14.0	0.248	0.248
Weld Anomaly	Mill defect	11.1	11	40	23.0	0.248	0.248
Weld Anomaly	Mill defect	1.2	1	25	17.0	0.248	0.248
Weld Anomaly	Mill defect	2.3	0.625	25	15.0	0.248	0.249
Weld Anomaly	Mill defect	6.4	4.5	25	17.0	0.248	0.251
Weld Anomaly	Mill defect	2.5	2.5	25	8.0	0.248	0.246
Crack-Like	Mill defect	10	4.5	12.5	17.0	0.248	0.251
Crack-Like	lamination	7.6				0.248	0.255
Notch-Like	Mill defect	2.8	1.1			0.248	0.25
Crack Field	OD crack	4.8	4	12.5	19.4	0.354	0.372
Weld Anomaly	Bottom Dent	4.2				0.248	0.253

The field-observed anomaly types consisted of 3 laminations, 1 OD crack, 1 bottom dent, and 19 “mill defects.” Unfortunately, the term “mill defect” does not capture the exact nature of the anomaly. In the case of anomaly No. 22, the OD crack is not associated with an ERW seam. Rather it turned out to be three cracks in the body of a piece of 0.375-inch-wall, Grade B, seamless pipe. It was not clear whether or not the laminations were associated with the ERW seams of the pipes in which they were found. The bottom dent, Anomaly No. 23, is not a seam manufacturing defect.

The comparisons between field-measured and ILI anomaly dimensions listed in Table 12 are illustrated in Figure 24, Figure 25, Figure 26, and Figure 27 for anomaly depth, anomaly length, pipe thickness, and failure stress predictions, respectively.

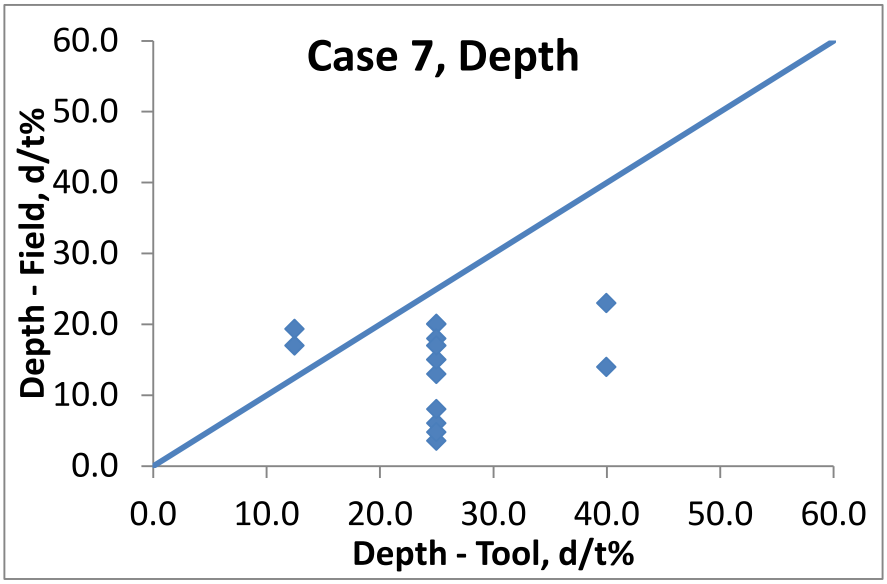

Figure 24. Comparisons between Field-determined Anomaly Depth and ILI Anomaly Depth, Case 7

It is seen in Figure 24 that the ILI dimensions are clustered at values of 12.5%, 25%, and 40%. That is because the depth-sizing capability of the tool was such that depth calls could only be categorized as being between 0% and 12.5% of the wall thickness, between 12.5% and 25% of the wall thickness, between 25% and 40% of the wall thickness, or greater than 40% of the wall thickness. In each case the investigating team member took the depth of the anomaly to be the highest value in the particular range. The depths of the laminations and that of the bottom dent were omitted from Figure 24 because they are not actually crack-like or weld defects. Except for two of the anomalies, the ILI depths were greater than those determined by non-destructive examination in the field. If the depths determined in the field non-destructive examinations can be believed to be accurate, the tool was over-estimating the depths of the anomalies in most cases.

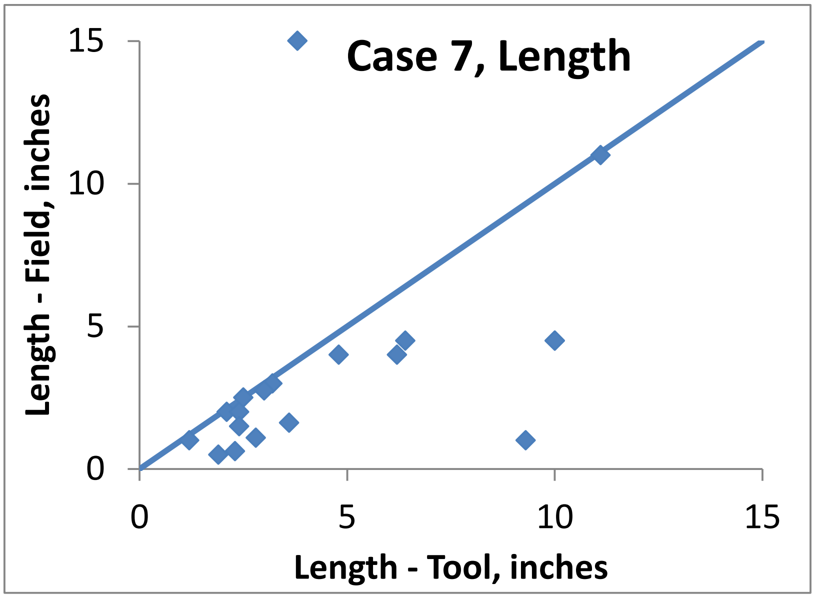

Figure 25. Comparisons between Field-determined Anomaly Length and ILI Anomaly Length, Case 7

Unlike in most of the previously-examined cases, the ILI lengths were almost always longer than the field-measured lengths as shown in Figure 25. The reason for this was not apparent to the investigating team member.

Figure 26 illustrates the degree to which the wall thicknesses indicated by the ILI aligned with those measured in the field. The alignment is very good.

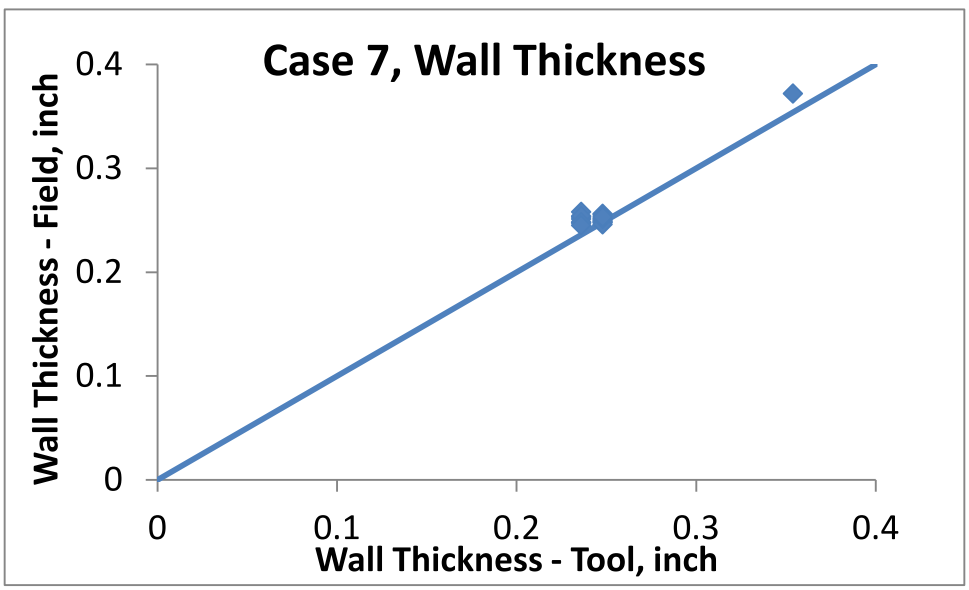

Figure 26. Comparisons between Field-determined Wall Thickness and ILI Wall Thickness, Case 7

A comparison between failure stresses of the anomalies calculated on the basis of ILI dimensions and those calculated on the basis of field-measured dimensions is presented in Figure 27. Failure stress levels for these anomalies were calculated using the Modified Ln-Sec Equation Elliptical C-Equivalent model with a full-size-equivalent Charpy upper shelf energy of 20 ft-lb. In one case (Anomaly No. 14), the calculated failure stress based on the ILI dimensions was 70.1% of SMYS. In contrast, the calculated failure stress based on the field-measured dimensions was 89.8% of SMYS. The disparity is largely the result of the large difference between the ILI depth (40% of SMYS) and the field-measured depth (23% of SMYS).

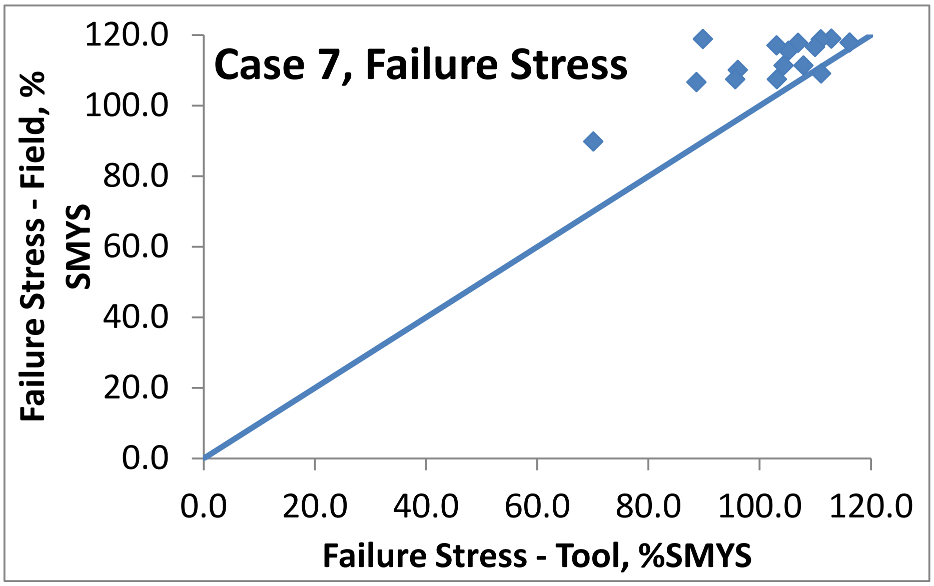

Figure 27. Comparisons between Predicted Failure Stresses Based on Field-Measured Anomaly Dimensions and Those Based on ILI Dimensions, Case 7

Comparisons between ILI Findings and Subsequent Service History

As noted previously, at the time this report was being prepared (5 years after the ILI crack-tool inspection), no in-service seam leaks or ruptures have occurred. Note that the normal operating stress of this segment is about 30% of SMYS.

Comparisons between ILI Findings and Hydrostatic Test Results

During the 2012 hydrostatic test of this segment to a stress level 91.5 % of SMYS, two ERW seam splits occurred. One of these occurred at a stress level of 86.1 % of SMYS, and the other occurred at a stress level of 93.2 % of SMYS. Both involved seam manufacturing defects that are still under investigation, but neither of these defects had been identified by the 2007 crack-tool inspection.

Comparisons between ILI Findings and Burst Test Results

No samples of pipe containing ILI seam anomalies were available for the purposes of hydrostatic testing.

Comparisons between ILI Findings and Metallurgical Examinations

No samples of pipe containing ILI anomalies were available for the purposes of metallurgical examination.

Conclusions Regarding the Case 7 ILI Crack-Tool Run

On the basis of the 23 comparisons between ILI anomalies and field observations, only 19 anomalies can be said to have been ERW seam anomalies. Of the 4 that are probably not seam anomalies, three appear to be laminations and one turned out to be a dent. Three of the 19 seam anomalies were repaired by means of Type B sleeves, but the remaining 16 seam anomalies were left in the pipeline unrepaired. The 2012 hydrostatic test to 91.5% of SMYS eliminated two seam anomalies (seam splits at 86.1% and 93.2% of SMYS), and it demonstrated that the pipeline segment is fit for service at its normal operating pressure of about 30% of SMYS.

The Case 7 example shows that trying to evaluate the quality of inspection for a given ILI run cannot always be done merely through field NDE. In this example, there is just as much reason to doubt the accuracy of the field NDE as there is to doubt the accuracy of the ILI inspection results, so the ILI results were not adequately validated. Hence, the operator really cannot have confidence that the seam integrity has been validated even though the failure stress levels of all detected anomalies were calculated, and their remaining lives were calculated. The 2012 hydrostatic test shows that two anomalies, neither of which was a current threat to pipeline integrity, were not identified in the 2007tool run. These two defects were obviously more severe than any of the 16 anomalies identified by the ILI that were not repaired or the 38 anomalies identified by the ILI that were not examined.

Case 8

Pipeline Attributes and Inspection Parameters

A 120-mile segment of an HVL pipeline comprised of 12.75-inch-OD, 0.250-inch-wall, X52 low-frequency-welded ERW pipe manufactured by Lone Star installed in 1961 was inspected by means of an ultrasonic crack-detection tool. The maximum operating pressure of the pipeline is 1,440 psig which corresponds to 71% of SMYS. The year of inspection was 2005. This segment had experienced no in-service failures prior to the 2005 inspection. The most recent seam integrity assessment of this segment prior to the 2005 inspection had been by means of hydrostatic testing in 1984. The 1984 hydrostatic test was carried out at stress levels ranging from 86.4% to 97.6% of SMYS. Sixteen seam-related test failures occurred during the 1984 test. As a result of the 2005 ILI crack-tool run, 1,353 seam anomalies (average of 11 per mile) were identified, and excavations of 42 entire joints of pipe were carried out to evaluate a sample of the anomalies found by the tool run. The field examinations consisted of visual inspection and magnetic particle inspection (MT) to characterize the type and length of the anomaly and ultrasonic inspection (UT) to measure the depth of the anomaly or, in the case of an internal anomaly, to characterize the length of the anomaly as well. Besides normal manual UT scanning, the exposed pipes were also inspected using phased-array UT equipment.

The visual examinations and manual UT scans of the exposed seams revealed 101 anomalies most of which corresponded to anomalies identified by the tool. The types of anomalies identified by the tool were: Notch-Like (20), Crack-Like (49), Crack Field (5), Lack of Fusion (1), Dent (2), and Not Decidable (17). Seven anomalies were discovered for which no ILI indication had been reported even though the lengths and depths of 6 of them exceeded the threshold detection limits of the tool (Length > 1.2 inches, Depth > 0.04 inch (see anomalies 29-35 in Table 13 below). The breakdown of the 101 anomalies subjected to field examination by type of anomaly as identified by field observation is as listed below.

Corrosion	1
Crack Like	1
Cracks	21
Hook Cracks	5
Internal Inclusion	1
Internal Lack of Fusion	6
Internal Metal Loss	3
Internal Misalignment	3
Intermittent Laminations	1
Internal Inclusions	2
Lack of Fusion	52
Lamination	1
LOF /Crack	1
Roller/Tool Mark	1
Dent	2

The manual UT scans were used only to examine the locations of anomalies found by the ILI tool. The phased-array UT scans covered the entire seam of each excavated joint. The phased-array UT scans revealed many anomalies in addition to those found by the ILI crack-tool. Most of the additional anomalies appeared to be either laminations or intermittent lack of fusion in the seam. The latter tended to be short and not particularly deep. To confirm the nature of what was found in these 42 joints of pipe, 6 complete joints were cut out to be subjected to burst testing and metallographic examination based on the initial analysis of the ILI data. A reanalysis of the data (not available to the investigating team member) resulted in the cutting out of 15 additional joints of pipe.

Comparisons between ILI Dimensions and Field-Measured Dimensions

Except for the two dents, comparisons between the ILI anomaly dimensions and those measured in the field are presented in Table 13. The dents are not discussed because they are not relevant to the seam-weld-anomaly scope of this document. The crack lengths highlighted in yellow and orange represent arrays of short, closely-spaced cracks.

Table 13. Comparison between ILI and Field-Measured Parameters for Case 8

Anomaly Number	Joint Number	Type of Anomaly		Length, inches		Depth, % Wall Thickness		Wall Thickness, inch		Location (External or Internal)	
		ILI	Field	ILI	Field	ILI	Field	ILI	Field	ILI	Field
1	Jt-149	Crack Like	Cracks	9.3	10.25	40	28.8	0.236	0.253	Ext	Ext
2	Jt-175	Crack Like	Lack of Fusion	3.6	3.875	40	24.4	0.236	0.255	Ext	Ext
3	Jt-177	Crack Like	Lack of Fusion	2	1.125	40	18.8	0.236	0.251	Ext	Ext
4	Jt-179	Crack Field	Corrosion	17.6	18.5	12.5	10	0.236	0.252	Ext	Ext
5	Jt-193	Crack Like	Lack of Fusion	2	3.75	40	29.6	0.236	0.252	Ext	Ext
6	Jt-241	Notch Like	Lack of Fusion	3.1	0.3		11.2	0.236	0.255	Ext	Ext
7		Notch Like	Lack of Fusion	1.6	2.5		9.6	0.236	0.253	ND	Ext
8		Crack Like	Hook Cracks	1.9	2.125	25	10.8	0.236	0.252	Ext	Ext
9		Crack Like	Hook Cracks	9.2	10	50	35.6	0.236	0.25	Ext	Ext
10		Crack Like	Hook Cracks	1.42	1	25	12.8	0.236	0.248	Ext	Ext
11		Crack Field	Internal Inclusions	4.7	67.8	25	23.2	0.246	0.257	Ext	Ext
12	Jt-295	Crack Like	Hook Cracks	1.8	1.75	25	18.8	0.226	0.256	Ext	Ext
13		Crack Like	Hook Cracks	3.1	3	40	24.4	0.226	0.257	Ext	Ext
14	Jt-296	Crack Like	Int. Metal Loss	1.6	8		12	0.226	0.251	Ext	Int
15		Crack Like	Lack Of Fusion	2.2	1.25	40	20	0.226	0.254	Ext	Ext
16	Jt-302	Crack Field	Cracks	6.2	6.5	25	30	0.246	0.254	Ext	Ext
17		Crack Field	Internal Inclusions	5.3	6	12.5	25.6	0.246	0.255	Ext	Ext
18		Notch-Like	Lack of Fusion	2.9	2.625		16.4	0.246	0.254	Ext	Ext
19	Jt-324	Crack Like	Cracks	70.400	26.000	40.00	36.80	0.246	0.260	Ext	Ext
20	Jt-329	Crack Like	Cracks	3.3	11.5		10.4	0.246	0.253	Ext	Ext
21		Crack Like	Cracks	43.7	34.875	25	8.8	0.246	0.251	Ext	Ext
22		Crack Like	Cracks	49.2	18	25	13.36	0.246	0.252	Ext	Ext
23		Crack Like	Cracks	88.9	4	40	30.4	0.246	0.247	Ext	Ext
24	Jt-332	Notch-Like	Cracks	2	2		41.6	0.246	0.251	Ext	Ext
25	Jt-353	Crack Like	Cracks	25.4	19.5	40	25.6	0.236	0.252	Ext	Ext
26		Crack Field	Cracks	73.5	54	25	13.2	0.236	0.252	Ext	Ext
27	Jt-675	Crack Like	Lack of Fusion	4.7	8		11.6	0.236	0.254	Ext	Ext
28	Jt-761	Crack Like	Cracks	649.9	38.5	40	20.4	0.226	0.251	Ext	Ext
29		No Call	Lack of Fusion		5.5		20.8		0.251		Ext
30		No Call	Cracks		2		10.8		0.251		Ext
31		No Call	Cracks		1.75		6.4		0.252		Ext
32		No Call	Lack of Fusion		8.125		7.2		0.253		Ext
33		No Call	Cracks		6.375		14.8		0.252		Ext
34		No Call	Cracks		1.75		7.2		0.251		Ext
35		No Call	Crack Like		1		12.4		0.253		Ext
36	Jt- 1139	Crack Like	Cracks	8.9	37.75	40	14.8	0.226	0.249	Ext	Ext
37	Jt-1318	Notch-Like	Lack of Fusion	3.6	3.5		12	0.236	0.251	ND	Ext
38	Jt-1415	Crack Like	Cracks	686.8	7.12	40	28.4	0.236	0.25	Ext	Ext
39	Jt-3640	Crack Like	Int. Misalignment	7.9	21.5		19.2	0.236	0.253	ND	Int
40	Jt-3640	Crack Like	Int. Misalignment	8.2	15.25		14	0.236	0.253	ND	Int
41	Jt-3640	Notch Like	Int. Misalignment	9.8	15		10.8	0.236	0.253	Int	Int
42	Jt-3640	Notch Like	Int. Lack of Fusion	6.3	6.5		24.4	0.236	0.254	Ext	Int
43	Jt-4077	Notch Like	Lack of Fusion	1.2	2.125	12.5	10.4	0.236	0.253	Int	Ext
44	Jt-5073	Crack Like	Cracks	7.7	9	12.5	15.2	0.226	0.257	Ext	Ext
45	Jt-5162	Notch-Like	Lack of fusion	3	2.875	12.5	15.2	0.236	0.254	Ext	Ext
46	Jt-5204	Crack Like	Lack of Fusion	3.4	3.5	40	28.8	0.236	0.255	Ext	Ext
47		Notch Like	Lack of Fusion	2	1.875		30.4	0.236	0.255	Ext	Ext
48		Crack Like	Lack of Fusion	2	2.25		40.8	0.236	0.254	Ext	Int
49		Notch Like	Lack of Fusion	1.4	1.5		33.6	0.236	0.253	Ext	Int
50		Crack Like	Lack of Fusion	10.2	11	40	41.6	0.236	0.256	Ext	Ext

Table 13. (continued). Comparison between ILI and Field-Measured Parameters for Case 8

Anomaly Number	Joint Number	Type of Anomaly		Length, inches		Depth, % Wall Thickness		Wall Thickness, inch		Location (External or Internal)	
		ILI	Field	ILI	Field	ILI	Field	ILI	Field	ILI	Field
51		Crack Like	Lack of Fusion	1.8	1.5	40	35.6	0.236	0.253	Ext	Ext
52		Crack Like	Lack of Fusion	3.4	4.75	40	39.2	0.236	0.253	Ext	Ext
53		Notch Like	Lack of Fusion	1.6	2.25		33.2	0.236	0.251	Ext	MW
54		Notch Like	Lack of Fusion	1.6	1.625		42.8	0.236	0.254	Ext	Ext
55	Jt-6262	Crack-Like	Lack of Fusion	2.9	2.75	25	21.6	0.236	0.258	Ext	Int
56	Jt-6265	Crack-Like	Lack of Fusion	8.8	8.5	40	32.8	0.236	0.254	Ext	Ext
57		Notch-Like	Lack of Fusion	1.6	1.5		19.2	0.236	0.256	Ext	Ext
58	Jt-6266	Crack-Like	Lamination	2.4	5	40	19.2	0.236	0.253	Ext	Int
59		Notch-Like	Lack of Fusion	1.8	2		26.8	0.236	0.246	Ext	Ext
60		Crack-Like	Lack of Fusion	8.1	8.125		22.8	0.236	0.248	Ext	MW
61	Jt-6418	Crack-Like	Cracks	52.4	54	40	36.8	0.236	0.253	Ext	Ext
62	Jt-6468	Crack-Like	Cracks	2.8	5	40	36.4	0.236	0.254	Ext	Ext
63		Notch-Like	Cracks	1.6	2.5		25.2	0.236	0.254	Ext	Ext
64		Crack-Like	Lack of fusion	3.3	3.125	50	25.6	0.236	0.252	Ext	Ext
65		Crack-Like	Int Inclusion	7.1	8.5	25	5.6	0.236	0.254	Int	MW
66	Jt-6511	Crack-Like	Lack of fusion	2.2	2.25	25	22.4	0.236	0.253	Ext	Ext
67		Notch-Like	Int Lack of fusion	2.4	2.5		25.6	0.236	0.253	Ext	Mw
68		Crack-Like	Int Lack of fusion	4.1	4	40	38.4	0.236	0.255	Ext	Mw
69		Crack-Like	Lack of fusion	1.2	1.125		18.4	0.236	0.253	Ext	Ext
70		Crack-Like	Int Lack of fusion	2.2	4		20.8	0.236	0.252	Ext	Mw
71	Jt-6903	Crack-Like	Lack of Fusion	66.7	67	40	36	0.246	0.264	Ext	Ext
72		Crack-Like	Int.Lack of fusion	44.4	43.5	40	37.6	0.246	0.253	Ext	MW
73		Crack-Like	Int Lack of Fusion	4.1	75	40	40.8	0.246	0.255	Ext	MW
74		Crack-Like	Lack of fusion		18.5	25	30.4	0.246	0.253	Ext	Ext
75	Jt-7423	Crack-Like	Lack of Fusion	3.5	3.125	40	24.8	0.236	0.252	Ext	Ext
76		Crack-Like	LOF /Crack	10.1	9.75		25.6	0.236	0.253	Ext	Ext
77		Crack-Like	Lack of Fusion	2.8	4.25	50	32.4	0.236	0.254	Ext	Ext
78	Jt-8429	Notch-Like	Roller/Tool Mark	12.4	12.375		10.4	0.236	0.258	Int	Ext
79		Notch-Like	Lack of Fusion	2.7	0.375		22.4	0.236	0.256	Ext	Ext
80		Notch-Like	Lack of Fusion	1.7	2		18.4	0.236	0.257	Ext	Int
81	Jt-8596	Crack-Like	Lack of Fusion	1.4	1.625		12	0.246	0.258	Ext	MW
82		Not-Decidable	Lack of Fusion	37.5	38		21.2	0.246	0.256	Ext	MW
83	Jt-9015	Not Decidable	Int. Metal Loss	11.4	15		6.4	0.236	0.256	Ext	Ext
84	Jt-10737	Not Decidable	Lack of Fusion	4.9	5.5		17.2	0.246	0.251	Ext	Int/Ext/MW
85		Not Decidable	Lack of Fusion	46.7	49		47.2	0.246	0.252	Ext	Int/Ext/MW
86		Not Decidable	Lack of Fusion	4.1	4.25		25.6	0.246	0.254	Ext	Int/Ext/MW
87		Not Decidable	Lack of Fusion	3.2	3.5		36	0.246	0.256	Ext	Int/Ext/MW
88		Not Decidable	Lack of Fusion	10.2	11		25.2	0.246	0.253	Ext	Int/Ext/MW
89		Not Decidable	Lack of Fusion	2.9	4		30	0.246	0.256	Ext	Int/Ext/MW
90		Not Decidable	Lack of Fusion	6.4	6.75		38	0.246	0.257	Ext	Int/Ext/MW
91		Not Decidable	Lack of Fusion	1.4	1.75		32.8	0.246	0.255	Ext	Int/Ext/MW
92		Lack of Fusion	Intermittent Laminations	7.875	22.075		60	0.246	0.257	nt/Ext/MW	MW
93		Not Decidable	Lack of Fusion	2	2.5		36	0.246	0.257	Ext	Int/Ext/MW
94		Not Decidable	Lack of Fusion	14.8	14.75		20	0.246	0.254	Ext	Int/Ext/MW
95		Not Decidable	Lack of Fusion	16.2	18		34.4	0.246	0.257	Ext	Int/Ext/MW
96		Not Decidable	Lack of Fusion	37.8	41		32.8	0.246	0.258	Ext	Int/Ext/MW
97		Not Decidable	Lack of Fusion	48.8	49		44.8	0.246	0.257	Ext	Int/Ext/MW
98		Not Decidable	Lack of Fusion	36.7	68		37.2	0.246	0.255	Ext	Ext
99	Jt-11896	Not Decidable	Int. Metal Loss	32	37.25		11.6	0.236	0.259	Ext	Ext

The six joints of pipe removed for hydrostatic burst testing were:

- Jt 324,
- Jt 332,
- Jt 5204,
- Jt 6418,
- Jt 6903, and
- Jt 10737

The comparisons between field-measured (manual UT) and ILI anomaly dimensions listed in Table 13 are illustrated in Figure 28, Figure 29, Figure 30, and Figure 31 for anomaly depth, anomaly length, wall thickness, and predicted failure stress, respectively.

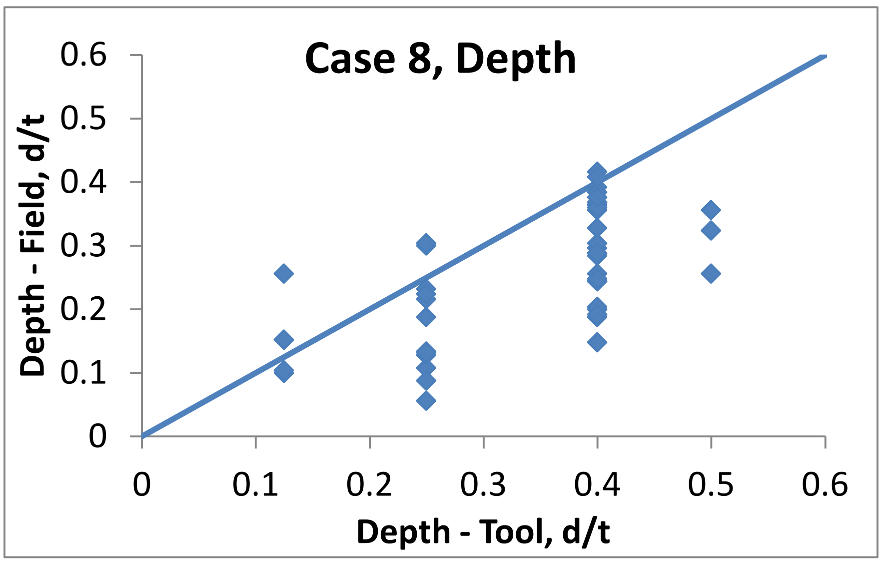

Figure 28. Comparisons between Field-determined Anomaly Depth and ILI Anomaly Depth, Case 8

It is seen in Figure 28 that the ILI dimensions are clustered at values of 12.5%, 25%, 40% and 50%. That is because the depth-sizing capability of the tool was such that depth calls could only be categorized as being between 0% and 12.5% of the wall thickness, between 12.5% and 25% of the wall thickness, between 25% and 40% of the wall thickness, or greater than 40% of the wall thickness. In each case the investigating team member took the depth of the anomaly to be the highest value in the particular range and values exceeding 40% to be 50%. Except for four of the anomalies, the ILI depths were greater than those determined by non-destructive examination in the field. If the depths determined in the field non-destructive examinations can be believed to be accurate, the tool was over-estimating the depths of the anomalies in most cases.

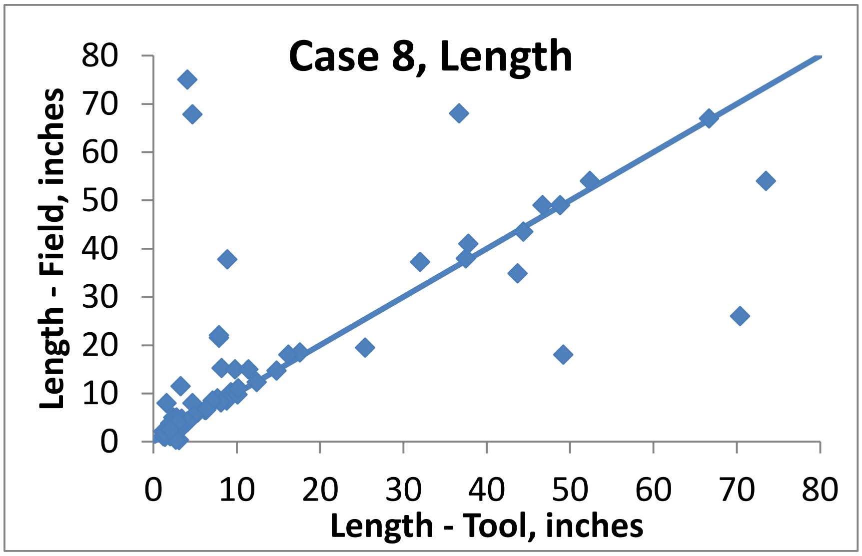

Figure 29. Comparisons between Field-determined Anomaly Length and ILI Anomaly Length, Case 8

As seen in Figure 29, many of the ILI lengths line up with the field-measured lengths, but in a few cases the lengths do not agree well. One reason for this could be that most of the anomalies were short but closely spaced such that the manner in which the lengths were interpreted by the ILI could have differed from the manner in which the lengths were interpreted by the UT technician in the field.

Figure 30 illustrates the degree to which the wall thicknesses indicated by the ILI aligned with those measured in the field. The ILI thicknesses tended to be less than the field-measured thicknesses, although not more than 12 % (much less in most cases). The ILI thicknesses were stratified as 0.226, 0.236, or 0.246 inch.

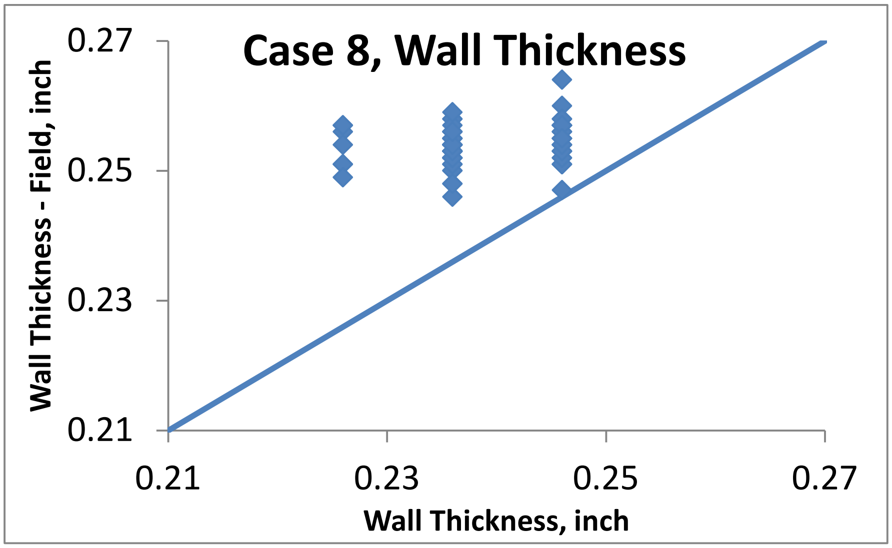

Figure 30. Comparisons between Field-determined Wall Thickness and ILI Wall Thickness, Case 8

A comparison between failure stresses of the anomalies calculated on the basis of ILI dimensions and those calculated on the basis of field-measured dimensions is presented in Figure 31. Failure stress levels for these anomalies were calculated using the Modified Ln-Sec Equation Elliptical C-Equivalent model with a full-size-equivalent Charpy upper shelf energy of 20 ft-lb. In many cases the predicted failure stresses based on ILI anomaly dimensions are below those predicted on the basis of the field-measured anomaly dimensions. Most likely that is because the ILI anomaly depths in many cases exceeded the field-measured anomaly depths. It is noted that the comparisons in Figure 31 are limited to the cases where the ILI depths and lengths were available. As one can see by scanning Table 13, there were numerous cases where an ILI depth and/or length were not given.

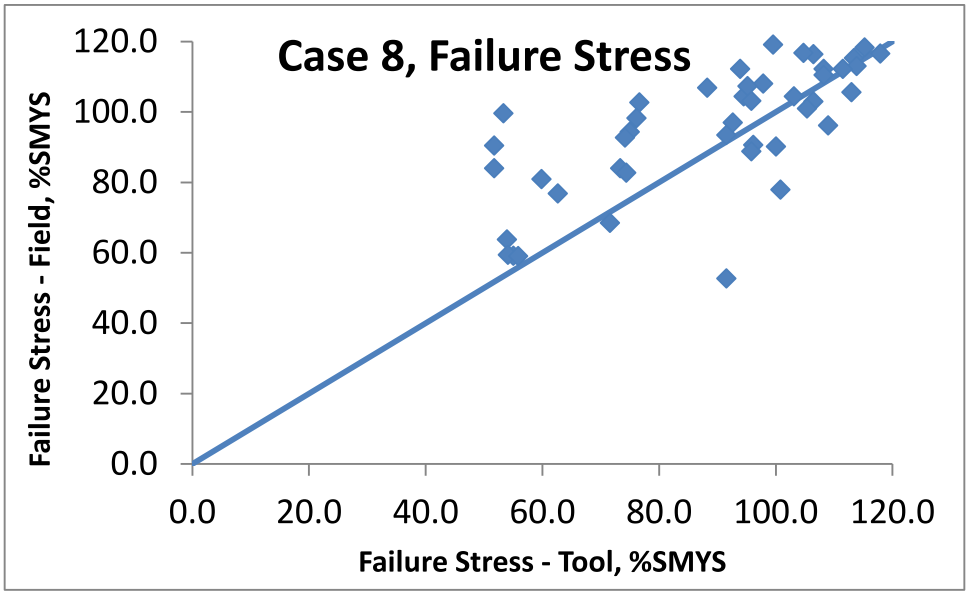

Figure 31. Comparisons between Predicted Failure Stresses Based on Field-Measured Anomaly Dimensions and Those Based on ILI Dimensions, Case 8

In 2006, the vendor was asked to re-examine the ILI crack-tool data using a more stringent screening criterion. As a result, the total of anomalies called grew to 14,721. Fifteen additional joints of pipe were removed from the pipeline for burst testing and metallurgical examination. The results of these tests are described below.

Comparisons between ILI Tool Findings and Burst Test Results

Twenty-one joints of pipe containing ILI seam anomalies were subjected to hydrostatic testing by Laboratory A. The results of the burst tests are summarized in Table 14 where the locations of the fracture origins are compared to the locations of the ILI indications to evaluate whether or not the ILI had identified the defect that caused the failure.

Table 14. Results of Burst Tests of Pipe Joints Removed from the Pipeline Described in Case 8 (12.75-inch-OD, 0.250-inch-wall, X52)
Page 1

Joint Number	Failure Stress, %SMYS	Defect That Failed in the Burst Test	Anomaly Indicated by the ILI	ILI Found Anomaly
6105	141	ID hook crack, 3 inches long, 49% through the wall at 25'-5" from USGW	None at 25'-5" from USGW 1.4-inch-long anomaly at 27'-2" from USGW	No
2797	141	Origin not apparent, but one long hook crack was found centered at 12'-4" from USGW	An anomaly was indicated at 12'-4" from USGW	Yes
324	156	OD hook crack, 3 inches long, 37% through the wall at 22'-6" from USGW	2.5-inch-long anomaly at 22'-6" from USGW	Yes
6903	123	Origin not apparent, but cold welds were present at 2' from USGW	A group of anomalies extending from about 1' to 10' from USGW	Yes
6106	157	OD hook crack, 0.5-inch-long, 55% through the wall at 5'-10" from USGW	Anomaly reported at 4'-6" from USGW	Maybe
2796	132	OD hook crack, 2.0-inch-long, 32% through the wall at 50' from USGW	No indications within the entire 4'-8" fracture	No
6102	132	Origin uncertain, possibly shallow hook crack at 44'-2" from USGW	Shallow anomaly located at 44'-2" from USGW	Yes

Table 14. Results of Burst Tests of Pipe Joints Removed from the Pipeline Described in Case 8 (12.75-inch-OD, 0.250-inch-wall, X52)
Page 2

2753	110	Layers of hook cracks, 8-inch-long at 32’-5” from USGW	Indication at 32’-5” from USGW	Yes
4013	137	ID hook cracks centered at 44’-8” and 45’-10” from USGW	Indication at 45’-6” from USGW	Yes
6418	148	OD and ID hook cracks with combined depth of 60% through the wall at 4’-3” from USGW	No indications within the entire 4’-8” fracture	No
10737	110	Origin not apparent, but layer hook cracks were located at 5’-9” from USGW	Indication at 5’-9” from USGW	Yes
7757	136	Layered hook cracks at 42’-5” from USGW	Status of indications on this joint not mentioned	Unknown
3897	136	Hook crack 22% through the wall at 8’-5” from USGW	Status of indications on this joint not mentioned	Unknown
5204	101	Long hook crack, 50% through the wall centered at 7’-6” from USGW	Crack-like feature 3.4-inch-long, 40% through the wall at 8’-11” from USGW	Maybe
3645	130	Long hook crack, 28% through the wall centered at 31’-8” from USGW	Indication at 31’-6” from USGW	Yes

Table 14. Results of Burst Tests of Pipe Joints Removed from the Pipeline Described in Case 8 (12.75-inch-OD, 0.250-inch-wall, X52)
Page 3

332	159	Chevrons point to brittle region centered at 13'-10" from USGW	No indications within the entire 10'-9" fracture	No
6005	142	Long OD Hook crack, 34% though the wall centered at 53'-5" from USGW	Nearest indication was at 50'-10" from USGW but no flaw found on fracture surface at that location.	No
7634	152	Long OD Hook crack, 48% though the wall centered at 0'-8" from USGW	Status of indications on this joint not mentioned	Unknown
2405	150	Origin thought to be a hook crack at 51' from USGW	Indication reported at 49'-3" from USGW. A hook crack coincided with this location but not the one thought to be the origin	Maybe
386	136	Long OD Hook crack, 35% though the wall centered at 34'-10 from USGW	No indications within the entire 7'-3" fracture	No
8769	140	Several small cold welds	No indications within the entire 4'-7" fracture	No

The burst test stress levels ranged from 101 % of SMYS to 159% of SMYS, so none of the pipe joints selected for burst testing was a threat to the integrity of the pipeline at its maximum operating pressure. The Laboratory A report indicates that no evidence of fatigue crack growth was found on any of the fracture surfaces created by the burst tests. In cases where a distinct originating defect was present, it was possible to assess whether or not the origin defect coincided with an ILI anomaly. It is noted that Laboratory A experts declined to identify the exact origin of failure in every one of the tests.

The last column of Table 14 states whether the ILI did or did not identify the origin defect.

It is seen that the origin of the failure coincided with an ultrasonic crack-detection tool indication in eight cases (a "Yes"). Three cases were considered a "Maybe." The origin did not coincide with an ultrasonic crack-detection tool indication in seven cases (a "No"). In three cases ("Unknown") the Laboratory A report did not mention the location of the tool call for the particular joint. Each joint of pipe was selected because of having at least one ultrasonic crack-detection tool indication, but it seems clear that the most severe ultrasonic crack-detection tool indication in a joint of pipe does not necessarily coincide with the actual most-severe defect.

Comparisons between ILI Findings and Metallurgical Examinations

Laboratory A experts conducted metallurgical examinations of the origins in the burst tests described in Table 14. They were able to identify most of the originating defects by type based on these examinations, and the results of their examinations are shown in Columns 3 and 4 of Table 14.

Comparisons between ILI Findings and Subsequent Service History

Unfortunately, in 2007, 2 years after the ILI crack-tool had been run and all repairs deemed necessary had been made, an in-service seam failure occurred within the inspected segment at a hoop stress level of about 70% of SMYS. This failure was investigated by the National Transportation Safety Board (NTSB). The NTSB concluded that the probable cause "was a failure of a weld that caused the pipe to fracture along the longitudinal seam weld, a portion of the upstream girth weld, and portions of the adjacent pipe joints." No specific point of origin of the failure is called out by the NTSB's investigators, so their report does not implicate a specific seam anomaly as being the cause of failure. However, the report did identify "island-like features" located along the fracture surfaces of the ERW seam, and it noted that these features were J-shaped in cross section implying that they were hook cracks.

Other experts not connected with the NTSB who had seen the fracture surfaces tended to focus on one of the island-like features in particular as the probable origin of the failure. This particular feature is a hook crack with a length of 2.4 inches and a depth of 27% of the wall thickness. While it is difficult to reconcile the size of this defect with the failure stress level of 70% of SMYS on the basis of a ductile fracture initiation model such as the Modified Ln-Sec Equation, it is reasonable to believe that such a defect could have precipitated the failure if the surrounding material behaved in a brittle manner in response to stress on the defect. One thing is clear, however, and that is that this particular defect should have been identified by the ultrasonic crack-detection ILI and it was not. The ILI was said to capable of detecting a defect with a length exceeding 1.2 inches and a depth exceeding 0.04 inch (16% of the wall thickness of this pipe) with 85% confidence. Even a post-accident examination of the raw data by the ILI vendor failed to reveal an anomaly corresponding to this hook crack.

Comparisons between ILI Findings and Hydrostatic Test Results

Shortly after the in-service failure in 2007, the operator of the pipeline conducted a hydrostatic test of the 12-mile portion of the pipeline that contained the location of the in-service failure. During that test one seam rupture occurred at a hoop stress level of 93.9% of SMYS. No distinct origin of this rupture was obvious, though a few short hook cracks with depths of no more than 20% of the wall thickness were visible on the fracture surface. Upon checking with the ILI vendor, it was found that the ILI had identified an anomaly corresponding to the location of this test failure origin.

In 2008 the entire 120-mile segment was subjected to hydrostatic testing to stress levels ranging from 90.5 % of SMYS to 98.0 % of SMYS. Four ERW seam ruptures and one ERW seam leak occurred during the tests. The failures were examined at the facilities of Laboratory A. A summary of the test breaks and leak is presented in Table 17.

Table 15. Summary of Test Failures in 2008

Test Failure Identification	Pressure at Failure, psig	Hoop Stress at Failure, % SMYS	Mode of Failure	Cause	Joint Number
1A-1	1875	91.9	Rupture	Stitching	2968
1A-2	1934	94.8	Rupture	Hook crack	2843
1A-3	1934	94.8	Rupture	Hook crack	2681
2AB-1	1941	95.2	Leak	Cold weld	6000
2AA-1	1990	97.6	Rupture	Hook crack	8493

Upon review of the ILI data, the following facts were determined.

- No ILI indications were listed for either Joint 2681 or Joint 2843
- An 8.4-inch-long anomaly was indicated at a location within 3 feet of the origin of rupture of Joint 2968. No depth estimation was made for this anomaly. The origin of rupture was a 12-inch-long feature which was called “stitching” in the Laboratory A report. The Laboratory A metallographic section of the defect shows a defect that some might say was a hook crack located very close to the bondline.
- A 3.1-inch-long anomaly with a depth in the range of 12.5 to 25% of the wall thickness was indicated at the exact location of the origin of rupture of Joint 8493. The origin was designated a “hook crack” in the Laboratory A report. The photographs of the fracture and the metallographic section confirm the presence of numerous hook cracks corresponding to what some might call a “woody” fracture.

- Although ILI indications were made in Joint 6000, none was located anywhere close to the origin of the fracture.

Conclusions Regarding the Case 8 ILI Crack-Tool-Run

The Case 8 ILI crack-tool run can be evaluated as follows. First, it is clear that the ILI located ERW seam features as verified both by field examinations, by some of the burst tests conducted on pipes removed from the pipeline, and by examinations of origins of hydrostatic test ruptures. It is equally clear that the ILI failed to identify some of the anomalies that failed in the burst tests and in the hydrostatic test. More importantly, the ILI failed to identify a defect that caused a service failure at the maximum operating pressure 2 years after the tool run. Also, as in previous cases examined in this document, the Case 8 example reveals that field NDE measurements of anomalies indicated by ILI are not necessarily any more reliable than the measurements implied by the ILI. This seems to be true whether manual UT or phased-array UT or both are used. Hence, the operator really cannot have confidence that the seam integrity has been validated by this tool run.

Case 9

Pipeline Attributes and Inspection Parameters

A 120-mile segment of an HVL pipeline comprised of 12.75-inch-OD, 0.250-inch-wall, X52 low-frequency-welded ERW pipe manufactured by Lone Star installed in 1961 was inspected by means of a circumferential magnetic flux leakage (CMFL) tool. The maximum operating pressure of the pipeline is 1,440 psig which corresponds to 71% of SMYS. The year of inspection was 2008. This segment is the same as that covered in Case 8 except that the Case 9 inspection was carried out after the 2007 in-service failure using a different tool technology.

It should be noted that as the result of electronics problems, the first run of the tool failed to produce data. Second and third runs were made during each of which sensor loss occurred. Both runs were used to evaluate the pipeline. As a result of the 2008 CMFL tool runs, 548 seam anomalies (average of 4.6 per mile) were identified of which 1 was judged to be a Type A anomaly (having all of the characteristics of a crack-like anomaly), 19 were judged to be Type B anomalies (having some of the characteristics of a crack-like anomaly), and 528 were classified as metal loss in the seam as the result of the manufacturing process (e.g., excessive trim, mismatched edges).

Twenty-eight entire joints of pipe that contained 46 anomalies called by the CMFL tool were removed from the pipeline for detailed examination and burst testing. The examinations consisted of visual inspection and the use of phased-array UT to characterize the type and length of each anomaly and to determine the depth of the anomaly. The visual examinations and phased-array UT scans of the seams revealed 373 anomalies of which 41corresponded to anomalies identified by the ILI. At five locations corresponding to ILI indications, no anomaly was found. The characteristics of the 46 locations indicated by ILI that were subjected to detailed examination are presented in Table 18. Note that the last column in the table labeled "Most Injurious Anomaly not indicated by ILI" gives the predicted failure stress levels of the most severe anomalies found by phased-array UT scanning that were not reported by the ILI vendor. Some of these have predicted failure stress levels less than those of the anomalies reported by the ILI vendor on the same piece of pipe.

Table 16. Characteristics of Anomalies Identified by the ILI

Pipe Number	Type of Anomaly Indicated by ILI	As Found Upon Visual Examination	Depth to Thickness Ratio		Length, inches		Predicted Failure Stress,%SMYS		
			ILI	Field NDE	ILI	Field NDE	ILI	Field NDE	Most Injurious, not indicated by ILI*
1	Type B	external corrosion	0.170	0.110	1.38	1.00	116.9	118.4	118.8
2	Manufacturing	metal gain, thickness variations	0.200		6.93	38.40	99.1		93.3
3	Type B	lack of fusion	0.130	0.192	0.91	1.25	118.4	116.9	78.6
4	Type B	external metal loss.	0.200	0.100	1.42	2.00	116.2	116.9	115.4
5	Type B	gouge	0.170	0.130	0.98	4.00	117.9	111.3	116.6
5	Manufacturing	thickness variations	0.140		7.44		104.2		116.6
6	Type B	gouge	0.130	0.140	0.51	1.00	119.0	118.2	103.9
7	Manufacturing	lack of fusion	0.150	0.188	5.71	3.00	106.1	118.5	117.0
7	Manufacturing	nearest anomaly is a dent	0.220		7.01		97.0		117.0
8	Type B	OD lack of fusion	0.200	0.160	2.32	4.00	112.9	109.4	95.4
8	Type B	lack of fusion	0.200	0.320	1.18	4.00	117.0	98.5	95.4
9	Type B	ID Crack	0.140	0.720	0.59	0.75	118.8	110.0	107.2
10	Manufacturing	mismatched edges	0.230	0.080	4.53	4.50	103.0	113.6	
11	Type B	gouge	0.180	0.170	0.75	0.30	118.4	119.1	93.0
12	Type B	OD lack of fusion	0.110	0.120	3.58	8.50	113.4	105.1	51.7
13	Manufacturing	wall thickness variations	0.130		6.26		106.9		51.7
13	Manufacturing	lack of fusion	0.200	0.150	5.63	6.00	102.1	105.6	51.7
13	Manufacturing	mill related	0.130	0.230	7.72	7.50	104.8	95.0	51.7
13	Manufacturing	mill related	0.160		6.22	48.00	104.3	76.2	51.7
13	Manufacturing	lack of fusion	0.170	0.060	6.58	2.50	102.7	117.3	51.7
14	Type B	crack	0.110	0.360	0.91	17.00	118.5	69.0	69.0
15	Manufacturing	OD lack of fusion	0.140	0.240	5.98	1.75	106.5	114.0	107.5
15	Manufacturing	lack of fusion or crack	0.270	0.120	6.22	6.50	94.2	107.5	107.5
16	Manufacturing	feature not found.	0.110		3.19		114.2		85.4
16	Manufacturing	OD lack of fusion	0.170	0.420	12.8	0.40	95.6	118.4	85.4
16	Manufacturing	feature not found.	0.130		9.05		103.4		85.4
17	Manufacturing	OD lack of fusion	0.220	0.240	5.98	1.75	99.4	114.0	84.1
18	Manufacturing	OD lack of fusion	0.180	0.152	5.04	20.00	105.2	95.0	86.0
18	Manufacturing	OD lack of fusion	0.200	0.296	9.96	6.50	94.4	91.0	86.0
19	Manufacturing	laminar tear	0.130	0.210	2.17	4.50	115.7	104.5	115.8
19	Manufacturing	mismatched edges	0.260	0.125	7.01	8.00	93.1	105.0	115.8
20	Manufacturing	mismatched edges	0.230	0.140	9.45	10.25	91.7	101.1	104.6
21	Manufacturing	No indications found. Excess metal	0.130		8.19		104.3		
21	Manufacturing	No indications found. Excess metal	0.190		3.58		108.9		
21	Manufacturing	No indications found. Excess metal	0.290		10.55		83.4		
21	Manufacturing	No indications found. Excess metal	0.120		2.52		115.2		
21	Manufacturing	No indications found. Excess metal	0.160		2.87		112.7		
22	Manufacturing	No indications found. Excess metal	0.210		9.41		94.0		
22	Manufacturing	No indications found. Excess metal	0.160		6.22		104.3		
22	Manufacturing	No indications found. Excess metal	0.220		9.49		92.8		
23	Manufacturing	feature not found.	0.230		10.43		90.4		73.0
24	Type B	OD Crack	0.140	0.500	1.02	1.00	118.1	112.9	86.7
25	Manufacturing	feature not found.	0.210		9.37		94.0		108.3
26	Type A	gouge	0.210	0.260	0.59	0.88	118.6	117.4	110.3
27	Manufacturing	wall thickness variations	0.170		5.04	18.00	106.0	119.2	116.8
28	Manufacturing	feature not found.	0.130		2.56		114.7		115.2

** "Most Injurious Anomaly not indicated by ILI" gives the predicted failure stress levels of the most severe anomalies found by phased-array UT scanning that were not reported by the ILI vendor. Some of these have predicted failure stress levels less than those of the anomalies reported by the ILI vendor on the same piece of pipe.*

The types of anomalies found included lack of fusion (cold welds), mismatched plate edges, mill-related anomalies (such as trim irregularities, roller marks, etc.), cracks, corrosion, dents, gouges, excess metal, thickness variations, and one laminar tear. In five locations, no anomaly was found to correspond to the ILI indications. Comparisons between ILI depths and depths measured by NDE are shown in Figure 32. Comparisons between ILI lengths and NDE lengths measured are shown in Figure 33.

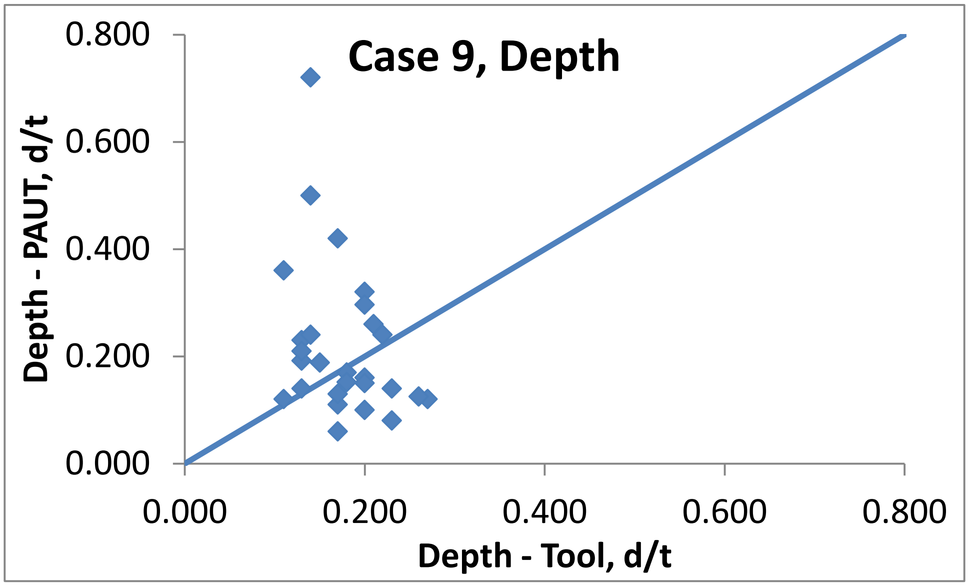

Figure 32. Comparisons of Depths as Indicated by the ILI and Those Found by Phased-Array UT

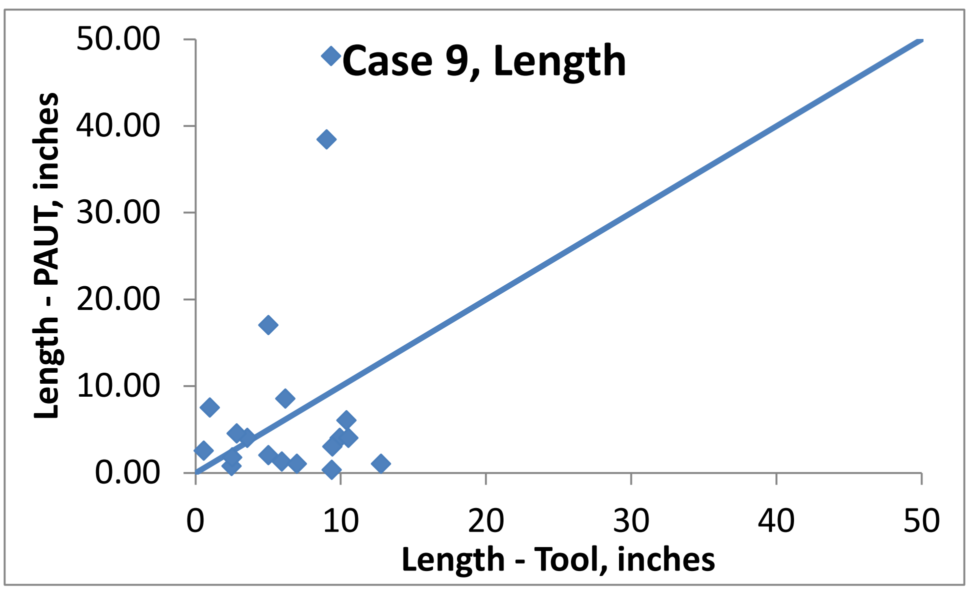

Figure 33. Comparisons of Lengths as Indicated by ILI and Those Found by Phased-Array UT

There is no consistent relationship between the ILI dimensions and those measured by means of phased-array UT.

A summary of the 332 anomalies that were found on the pipes examined but were not indicated by the ILI is presented in Table 19.

Table 17. Summary of Anomalies Found by Direct Scanning with Phased-Array UT that Were Not Indicated by the ILI

Pipe Number	Number of Anomalies Found	Description	Most Injurious Anomaly		
			d/t ratio	Length, inches	Predicted Failure Stress, %SMYS
1	2	OD and ID cracks	0.200	0.50	118.8
2	19	lack of fusion and cracks	0.328	5.00	93.3
3	45	lack of fusion, cracks,and corrosion	0.276	18.75	78.6
4	5	lack of fusion and cracks	0.224	1.50	115.4
5	3	lack of fusion and mill related	0.600	0.50	116.6
6	6	lack of fusion and mill related	0.344	2.75	103.9
7	7	lack of fusion and a dent	0.252	1.00	117.0
8	34	lack of fusion	0.360	4.00	95.4
9	20	lack of fusion	0.208	3.75	107.2
11	12	lack of fusion and cracks	0.176	16.25	93.0
12	32	lack of fusion and cracks	0.276	9.50	86.5
13	21	lack of fusion, cracks, and mill related	0.500	18.00	51.7
14	8	lack of fusion and cracks	0.360	17.00	69.0
15	9	lack of fusion and cracks	0.120	6.50	107.5
16	3	lack of fusion and mismatch	0.560	3.00	85.4
17	20	lack of fusion and cracks	0.352	7.00	84.1
18	30	lack of fusion, cracks, and mill related	0.268	10.50	86.0
19	5	lack of fusion	0.348	1.00	115.8
20	3	lack of fusion	0.120	9.00	104.6
23	6	lack of fusion and mismatch	0.460	7.00	73.0
24	12	lack of fusion and excess metal	0.240	13.00	86.7
25	4	lack of fusion	0.320	2.25	108.3
26	23	lack of fusion, cracks, and gouges	0.200	3.00	110.3
27	1	crack	0.104	2.00	116.8
28	2	lack of fusion	0.195	1.75	115.2

It should be noted that the CMFL tool vendors do not claim to be able to detect and size tight cracks. This CMFL tool is said to be able to characterize narrow axial defects that have a width of more than 0.008 inch, so it is not surprising that the ILI did not identify the cracks and lack of fusion anomalies listed in Table 19.

Burst tests were conducted on 12 of the 28 full joints of pipe removed for examination at Laboratory A. The results of the burst tests are presented in Table 20.

Table 18. Results of Burst Tests Conducted by Laboratory A (USGW means upstream girth weld)

Laboratory A Test Number	Pipe Number	Burst Stress, %SMYS	Cause of Failure	Distance of Origin from USGW, ft	Distance of Tool Call from USGW, ft	Was There a Match?
1	3	133.1	Hook crack	51.66	56.84	no
2	8	102.7	Hook crack	42.00	36.95	no
3	9	133.9	Hook crack	4.3	50.43	no
4	6	139.3	Hook crack	26.1	37.45	no
5	16	138.0	Hook crack	23.66	32.35	no
6	13	148.8	Hook crack	15.33	24.83	no
7	24	108.6	Cold weld	29.1	28.15	maybe
8	18	127.0	Hook crack	21.75	36.21	no
9	26	139.8	Cold	31.8	41.8	no
10	17	142.9	Hook crack	20.5	14.32	no
11	5	142.7	Hook crack	14.9	9.79	no
12	2	137.3	Stitching	26.4	15.87	no

A few of Laboratory A's burst test origins coincided with anomalies that were found by the phased-array UT scans. Those are as shown in Table 21.

Table 19. Anomalies Found by Phased-Array UT that Coincided with Origins of Burst Tests in Table 18

Pipe Number	Burst Stress, %SMYS	Length of Anomaly, inches	Depth of Anomaly, % of Wall	Predicted Failure Stress of Anomaly, % SMYS
3	133.1	1.25	0.192	116.9
8	102.7	1.00	0.240	117.2
9	133.9	2.00	0.300	110.7
13	148.8	3.00	0.176	111.5
17	142.9	1.75	0.196	115.9

Portions of 9 of the 28 full joints of pipe removed for examination were subjected to fatigue testing and burst testing at Laboratory B. Only one of these samples (Sample 8) contained an anomaly identified by the CMFL ILI. The 10-foot-long samples were selected as parts of full joints of pipe based on the findings of the phased-array UT scans of the seams, so these tests were more of verification of the capabilities of the phased-array UT scans than of the capabilities of the CMFL ILI. The samples were first subjected to 31,200 cycles of pressure ranging from 300 psig to 1,400 psig to simulate 20 years of service. None of the samples failed during the pressure-cycle tests. Each of the samples was then internally pressurized until it burst. The results of the burst tests are presented in Table 22. Neither the odometer locations of the origin of each failure nor descriptions of defects that caused each failure were available, so there is no way to know whether or not the origins coincided with anomalies found by the UT scans. The table does show the characteristics of the anomalies found by UT that were located within the sample. Note that the anomaly in Sample 8 had been identified by the CMFL ILI as being 7 inches in length and 26% through the wall. Its predicted failure stress based on these ILI dimensions was 93.1 % of SMYS.

Table 20. Burst Tests Conducted at Laboratory B

Sample Number	Actual Failure Stress, %SMYS	Characteristics of Anomalies Found by Phased-Array UT		
		Length, inches	d/t	Predicted Failure Stress, %SMYS
1	118	None present in sample		
2	119	6	0.228	98.7
		2.5	0.100	116.0
3	137	4.75	0.208	103.9
		1.25	0.124	117.8
4	153	2.75	0.112	115.0
5	138	5.5	0.120	109.0
		4.5	0.148	108.9
6	133	0.75	0.212	118.2
7	153	0.5	0.084	119.1
		0.75	0.212	118.2
8	121	8	0.130	105.0
9	155	3	0.144	113.0
		2	0.168	115.0

The fact that the predicted failure stress levels for the UT anomalies are consistently lower than the actual failure stresses is a function of how "flow stress" is defined in the Modified Ln-Sec Equation. Because it is defined as SMYS+10,000 psi, the maximum value of failure stress predicted for an X52 material will be 119.2 % of SMYS corresponding to a defect-free pipe. Also, the actual yield strengths of the materials tended to exceed SMYS (tests conducted by

Laboratory A showed yield strengths consistently above 60,000 psi). Therefore, the comparisons of actual failure stresses in the burst tests to predicted failure stresses should not be expected to follow a 1-to-1 relationship. A comparison of the predicted failure stresses to actual failure stresses is shown in Figure 34. The correlation coefficient "R^2" is only 0.29. An R^2 of 1 is a perfect correlation; an R^2 of zero is no correlation. The value of 0.29 represents a very poor correlation. So, there is really not much one can conclude from these comparisons about the capabilities of the phased-array UT technology as applied in this case.

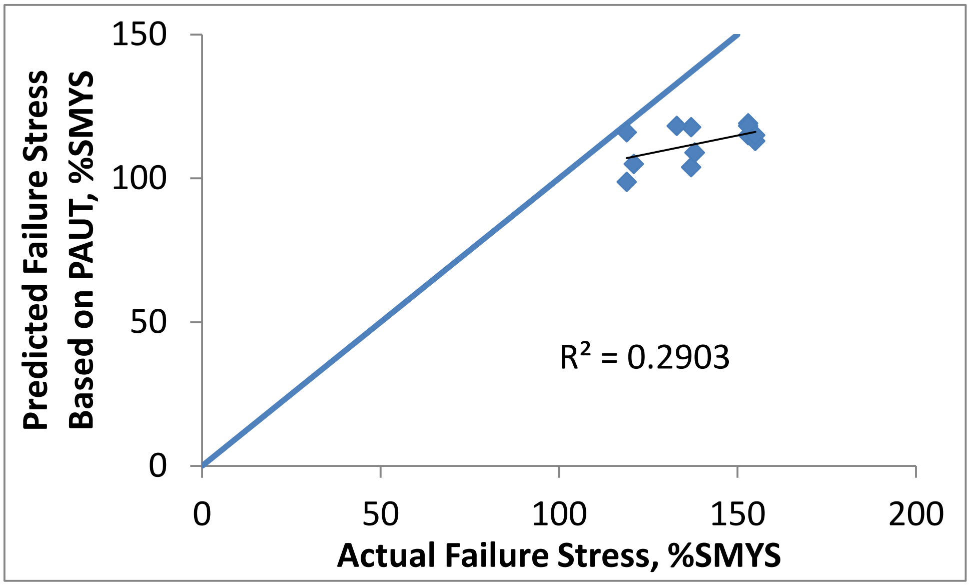

Figure 34. Comparisons of Predicted Failure Stress Levels Based on Anomaly Dimensions Determined by Phased-Array UT with Actual Failure Stress Levels Observed in Burst Tests

Comparisons between ILI Findings and Hydrostatic Test Results

A few months after the CMFL tool run in 2008, the entire 120-mile segment was subjected to hydrostatic testing to stress levels ranging from 90.5 % of SMYS to 98.0 % of SMYS. Four ERW seam ruptures and one ERW seam leak occurred during the tests. The failures were examined at the facilities of Laboratory A. It is recalled that the Case 8 ILI results were also compared to the results of the 2008 hydrostatic test. A summary of the test breaks and leak is presented in Table 23. These are the same test failure results that were presented in Table 17 under Case 8.

Table 21. Summary of Test Failures in 2008

Test Failure Identification	Pressure at Failure, psig	Hoop Stress at Failure, % SMYS	Mode of Failure	Cause	Joint Number
1A-1	1875	91.9	Rupture	Stitching	2968
1A-2	1934	94.8	Rupture	Hook crack	2843
1A-3	1934	94.8	Rupture	Hook crack	2681
2AB-1	1941	95.2	Leak	Cold weld	6000
2AA-1	1990	97.6	Rupture	Hook crack	8493

None of these defects had been identified by the CMFL ILI.

Conclusions Regarding the Case 9 CMFL Tool-Run

The Case 9 CMFL-tool run can be evaluated as follows. The ILI located some types of ERW seam features such as missing metal, extra metal, and mismatched edges at the seam. However, the ILI did not identify any of the five defects that caused failures in the 2008 hydrostatic test to hoop stress levels ranging from 90.5% of SMYS to 98% of SMYS. Moreover, the types and sizes of anomalies identified by the CMFL ILI did not correlate well with those found by scans of the ERW seams of selected joints using phased-array UT equipment. A CMFL-ILI anomaly may possibly have coincided with the origin of one of the burst tests conducted on pipes removed from the pipeline based on CMFL-ILI findings, but in 17 of 18 burst tests, the origins of failure did not coincide with CMFL-ILI anomalies. As has been noted, the CMFL tool vendors do not claim to be able to detect and size tight cracks. This CMFL tool is said to be able to detect and characterize narrow axial defects that have a width of more than 0.008 inch, so it is not surprising that the ILI did not identify the cracks and lack of fusion anomalies.

It is fair to conclude that the CMFL tool technology as employed in this case was not capable of delivering an adequate ERW seam integrity assessment.

Case 10

Pipeline Attributes and Inspection Parameters

Case 10 pertains to burst tests conducted on pipe samples removed after an integrity assessment of a 16-inch-OD, 0.250-inch-wall, X52 natural gas pipeline with a low-frequency-welded ERW seam. The pipe in this 64-mile segment was manufactured by Lone Star and A.O. Smith and the date of manufacturing of the pipe was 1956.

The assessment was made using a magnetic flux leakage tool with a circumferentially-oriented field (CMFL). The tool was run in 2007. The types of anomalies were classified as “A” meaning that the anomaly had all of the characteristics of a crack-like feature, “B” meaning that the anomaly had some of the characteristics of a crack-like feature, or “C” meaning an anomaly associated with metal loss in the seam such as excess trim.

Comparisons between ILI Dimensions and Metallurgical Dimensions

A summary of the burst test results along with the ILI dimensions of the anomalies as measured after the burst tests is presented in Table 24.

Table 22. Results of Burst Tests of Pipes Containing Anomalies Identified by Means of a CMFL ILI

Joint Number	Type of Anomaly	ILI Depth, % of wt	Actual Depth, % of wt	ILI Length, inches	Actual Length, inches	Predicted Failure Stress Based on ILI Dimensions, % SMYS	Predicted Failure Stress Based on Measured Dimensions, % SMYS	Actual Failure Stress, % SMYS
1300	B	28%	95%	1.81	1.75	113.5	36.0	83.7
3910	A	32%	55%	2.48	3.00	108.5	89.5	100.9
4550	A	26%	7%	2.01	2.00	113.5	119.2	128.4
420	C	16%	24%	3.00	4.00	113.1	105.4	123.0
1820	B	24%	70%	1.89	2.00	114.2	88.2	97.8
6770	C	16%	8%	3.58	5.00	111.4	118.7	112.4
6780	B	22%	20%	1.60	1.50	115.8	117.6	113.0
7640	B	34%	85%	0.67	0.60	118.0	108.8	120.5
7670	C	10%	3%	11.00	10.00	105.8	119.0	118.3

Comparisons of actual depths to ILI depths are shown in Figure 35. As can be seen in the figure, the tool depths for shallow defects were pretty close to the actual depths, but the tool significantly under-estimated the depths of the deeper anomalies.

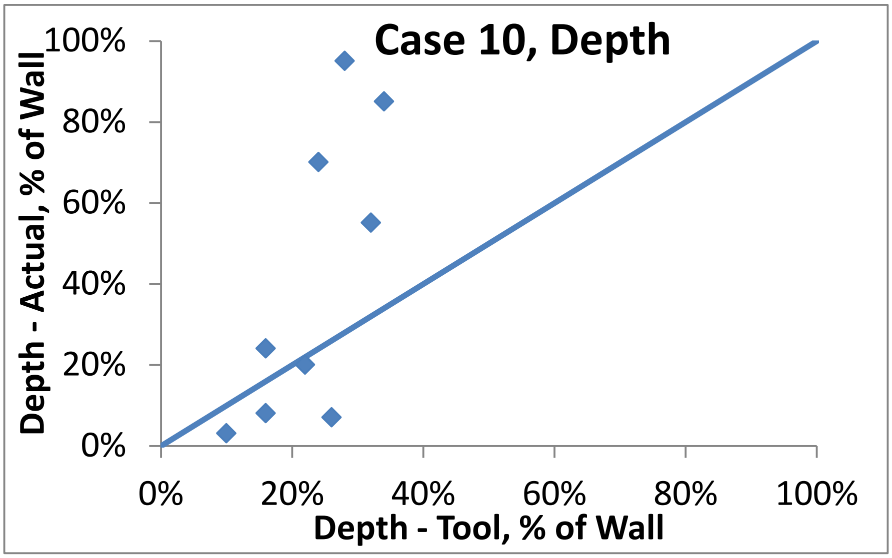

Figure 35. Actual Anomaly Depths Compared to Those Indicated by the CMFL ILI

Comparisons of actual lengths to ILI lengths are shown in Figure 36. It is seen that the ILI lengths were in reasonable agreement with the actual lengths.

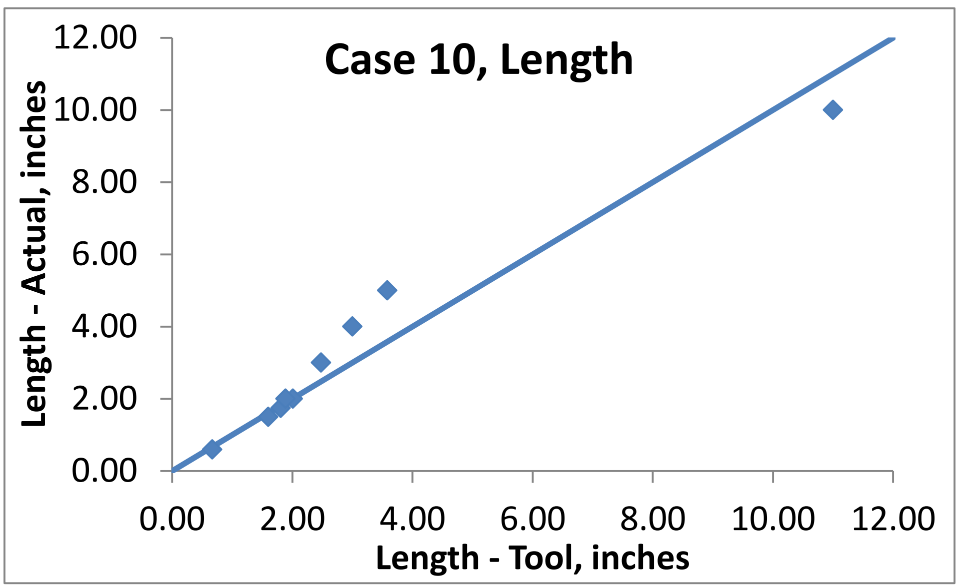

Figure 36. Actual Anomaly Lengths Compared to Those Indicated by the CMFL ILI

Comparisons of actual failure stresses to those predicted on the basis of ILI dimensions using the Modified Ln-Sec Elliptical C-Equivalent model with 20 ft lb of Charpy energy assumed are shown in Figure 37. One of the predictions based on the ILI dimensions (Joint 1300) significantly over-estimated the actual failure stress. This is a result of the fact that the ILI significantly under-estimated the depth of the anomaly.

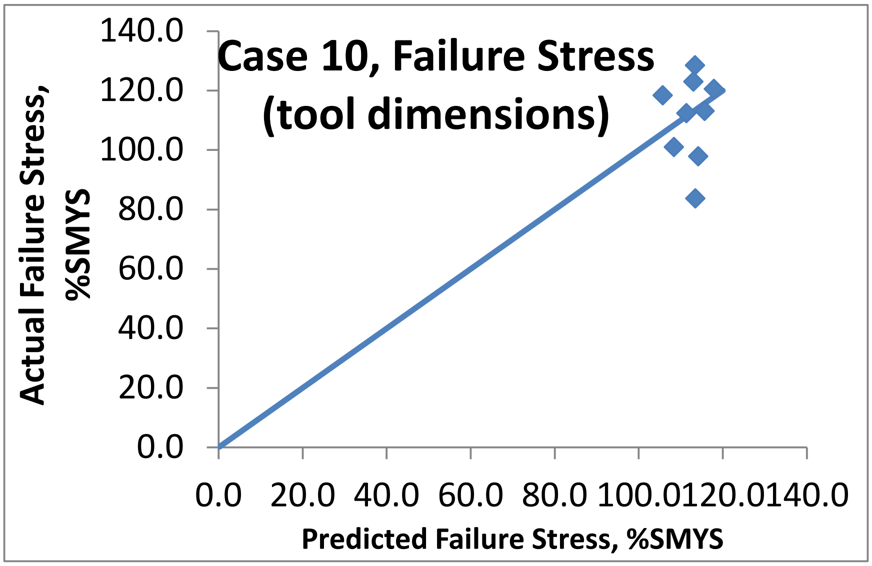

Figure 37. Actual Anomaly Failure Stresses Compared to Those Calculated on the Basis of Dimensions Indicated by the CMFL ILI

Comparisons of actual failure stresses to those predicted on the basis of actually measured dimensions using the Modified Ln-Sec Elliptical C-Equivalent with 20 ft lb of Charpy energy assumed are shown in Figure 38. The model provided reasonable predictions of the failure stress in most cases but significantly under-estimated the burst strength in one case (Joint 1300).

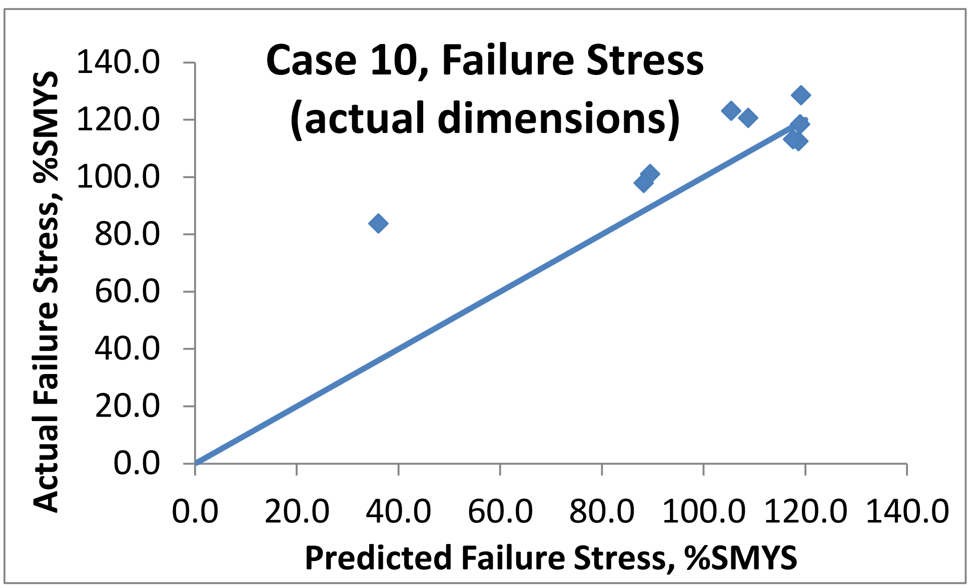

Figure 38. Actual Anomaly Failure Stresses Compared to Those Calculated on the Basis of the Actual Dimensions of the Anomaly

The deepest anomaly exposed by the burst tests and the one which also exhibited the lowest failure stress level (84% of SMYS) is shown in Figure 39. This anomaly was a cold weld in Joint 1300 that penetrated 95% of the wall thickness at the point of deepest penetration. The

Modified Ln-Sec Elliptical C-Equivalent model underestimated the failure stress by a significant amount. It predicted a failure stress of 36% of SMYS.

Figure 39. Appearance of the Anomaly in Joint 1300

Conclusions Regarding the Case 10 CMFL Tool-Run

The above comparisons indicate that the CMFL ILI used in this pipeline was capable of identifying some types of ERW seam anomalies. The ILI seemed to do a pretty good job of characterizing the lengths of the defects that it identified. In terms of depth, the ILI tended to significantly under-estimate the depths of the deeper anomalies. Consequently, one cannot have a great deal of confidence in the failure stress levels predicted on the basis of ILI anomaly dimensions. Note that the details of the CMFL findings were not reviewed. Therefore, an overall assessment of the performance of the ILI in this case was not possible.

Case 11

Pipeline Attributes and Inspection Parameters

Case 11 involve the results of an assessment of a natural gas pipeline using an Electromagnetic Acoustic Transducer (EMAT) tool. The pipeline was comprised of 16-inch-OD, 0.250-inch-wall, X52 low-frequency-welded ERW pipe. The manufacturer of the pipe was Lone Star and the date of manufacturing of the pipe was 1961. The length of the segment involved was 18 miles. This EMAT tool was run primarily for assessment of SCC, so the ERW seam anomalies were only a secondary objective. To speed up the assessment for SCC, the vendor was asked to report only the most severe indication within each joint of pipe. In some cases, seam anomalies were found in conjunction with pipes that were examined for SCC indications. It is possible that these anomalies would have been reported if not for another more severe anomaly on the same pipe.

Comparisons between ILI Dimensions and Field-Measured Dimensions

The vendor declined to estimate the depths of seam anomalies for this tool run. Instead only the length and location of each called seam anomaly were provided. An attempt was initially made to put seam anomalies in bins by depth, but for reasons unknown to the investigating team, this was not pursued. The field examinations of the seams consisted of visual examination, magnetic particle inspection (MT), and ultrasonic inspection (UT).

The list of anomalies indicated by the ILI and the findings in the field is presented in Table 25.

Table 23. List of ERW Seam Anomalies Indicated by the EMAT ILI

Anomaly	AS INDICATED BY ILI		AS MEASURED IN FIELD		
	Anomaly Type	Length, inches	Actual Max Depth (%)	Significant Feature Length, inches	Field Investigation Comments
1	Linear Class 3 with coating imperfection	2.40	N/A		Suspended 0.050" deep from ID
2	linear anomaly w/coating imperfection	4.40	24%	7.0	internal stringer
3	Seam Indication II	3.10	18%	4.8	ID connected high/low
4	Seam Indication II	3.50	24%	10.0	ID connected high/low
5	Seam Indication II	2.80	14%	5.0	ID connected high/low
6	Linear indication		34%	4.0	lack of fusion from OD
7	Seam indication II	2.80	36%	1.0	(2) ERW LOF 1" long each separated by 1"
8	Seam Indication II strong signal	2.80	59%	1	lack of fusion from OD, one single
9	linear class 1 associated with coating imperfection	2.20	30%	1.0	ID connected anomaly the be cut out with 17050
10	linear class 2 associated with coating imperfection	1.70	41%	1.3	single ERW fusion defect on OD
11	Seam Indication, strong signal	3.00	15%	1	Dent 3" diameter dent 0.09" deflection at ERW; seam indiaction OD connected 1" long
12	poss. longseam influence	3.70	44%	3	possible lack of fusion from ID, one single
13	poss. longseam influence	4.10	44%	3	possible lack of fusion from ID, one single
14	poss. longseam influence	4.10	44%	3	possible lack of fusion from ID, one single
15	poss. longseam influence	4.90	50%	3	possible lack of fusion from ID, one single
16	poss. longseam influence	3.70	44%	3	possible lack of fusion from ID, one single
17	Linear Class 3 poss. manufacturing anomaly	2.80	34%	4.50	Single internal stringer
18	Linear Class 3	2.80	38%	1	Long seam indication
19	Linear Class 2; possible manufacturing defect	2.80	34%	1	Long seam indication
20	Linear Class 2; possible manufacturing defect		21%	1	Long seam indication
21	Linear Class 2; possible manufacturing defect	3.30	44%	1	Long seam indication

The list of anomalies found in the field but not indicated by the ILI is presented in Table 26.

Table 24. List of Anomalies Found in Field but Not Indicated by the EMAT ILI

Anomaly	Actual Max Depth (%)	Significant feature Length, inches	Field Investigation Comments
1	26%	1.50	Intermittent pits
2	20%	2.00	OD connected LOF
3	30%	1.5	OD connected LOF
4	36%	2.5	OD connected LOF
5	31%	1.0	OD connected LOF
6	32%	1.5	OD connected LOF
7	29%	1.5	OD connected LOF
8	30%	1.0	OD connected LOF
9	38%	1.5	OD connected LOF
10	30%	1.0	OD connected LOF
11	24%	2.5	OD connected LOF
12	21%	0.5	OD connected LOF
13	20%	1.0	OD connected LOF
14	15%	0.5	OD connected LOF
15	15%	1.0	OD connected LOF
16	18%	1.0	OD connected LOF

The comparison between lengths measured in the field to those indicated by the EMAT ILI (21 anomalies) is shown in Figure 40. There is no correlation between the reported lengths and the actual lengths.

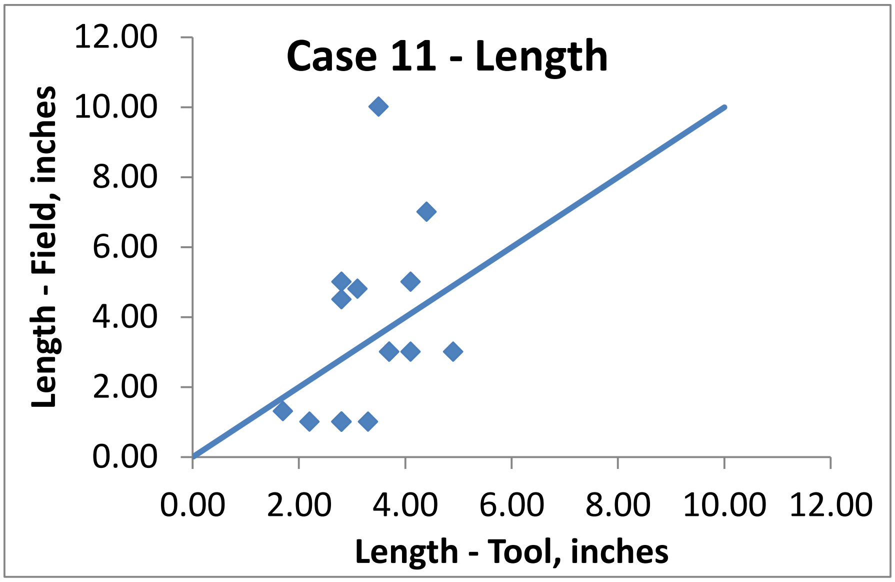

Figure 40. Lengths Measured in the Field Compared to Those Indicated by the EMAT ILI

In the absence of ILI depths, predicted failure stresses can be calculated based only on field measurements of the lengths and depths of the anomalies. This was done for two sets of anomalies found by field scans of the seams. One was for the anomalies that had been indicated by the ILI, and the other was for the anomalies that had not been indicated (recalling that the vendor may not have reported it if there was a larger SCC anomaly on the same joint). There were 21 ILI anomalies and 16 anomalies not indicated by ILI that were found and characterized in the field. The predicted failure stress levels for the 21 ILI anomalies ranged from 92.2% of SMYS to 118.5% of SMYS. The predicted failure stress levels for the 16 anomalies not called ranged from 106.6 % of SMYS to 119.0 % of SMYS. These failure stresses are shown graphically in ascending order in Figure 41.

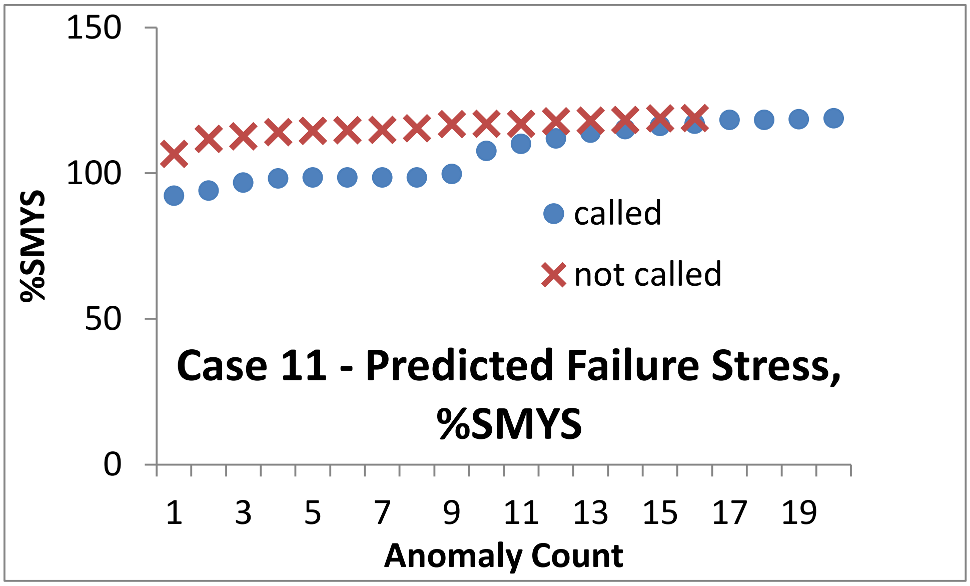

Figure 41. Predicted Failure Stress Levels for Anomalies Based on Field Measurement with MT and UT

It appears that the ILI anomalies were generally more of a threat to pipeline integrity than the anomalies not indicated by ILI, although none of them appeared to be a significant threat.

Conclusions Regarding the Case 11 ILI Crack-Tool-Run

In this particular situation the EMAT ILI appeared to be able to locate ERW seam anomalies. However, to be used efficiently for ERW seam inspection, the tool will have to be improved such that depths of anomalies can be determined and that lengths can be determined more accurately.

Case 12

Pipeline Attributes and Inspection Parameters

Case 12 pertains to a 139-mile liquid pipeline comprised of two different kinds of ERW pipe: 20-inch-OD, 0.230-inch-wall, X52, DC-ERW pipe manufactured by Youngstown Sheet and Tube Company and 20-inch-OD, 0.219-inch-wall, X52, HF-ERW pipe manufactured by U.S. Steel. The pipeline was installed in 1968.

This pipeline was inspected in 2009 using a CMFL tool, a caliper tool, and ultrasonic wall loss tool, and an ultrasonic crack-detection tool. Thirty-six features identified by the CMFL ILI and 52 features identified by the ultrasonic crack-detection ILI were examined in the field. Of these 88 features, 72 were repaired by sleeves. The pipeline was then subjected to a hydrostatic test in 2010 to confirm its maximum operating pressure and to assess defects below the detection threshold of the 2009 ILI tools.

Nine pipe samples from six different joints containing ILI indications that were repaired by sleeves prior to the hydrostatic test were cut out for further evaluation by Laboratory C after the hydrostatic testing was completed. A description of each sample is listed in Table 27. Twelve anomalies identified by the ultrasonic crack detection ILI were included in these samples. Two anomalies (dents) identified by the caliper tool were included in the samples. No anomalies identified by the CMFL ILI were included in the samples. Because no assessment of the anomalies detected by the CMFL ILI was made by the investigating team, the Case 12 analyses involved only data acquired by the ultrasonic crack detection ILI.

Table 25. Descriptions of the 9 Samples That Had Been Sleeved Prior to the 2010 Hydrostatic Test That Were Removed for Examination

<table>
<tr><th>Sample</th><th>Manufacturer</th><th>ILI Tool</th><th>ILI Tool Feature Type</th></tr>
<tr><td>1-A</td><td>U.S. Steel</td><td>Ultrasonic crack detection tool</td><td>Crack-Like</td></tr>
<tr><td>1-B</td><td>U.S. Steel</td><td>Ultrasonic crack detection tool</td><td>Crack-Like</td></tr>
<tr><td rowspan="5">1-C</td><td rowspan="5">U.S. Steel</td><td>Ultrasonic crack detection tool</td><td>Crack-Like</td></tr>
<tr><td>Ultrasonic crack detection tool</td><td>Crack-Like</td></tr>
<tr><td>Ultrasonic crack detection tool</td><td>Crack-Like</td></tr>
<tr><td>Ultrasonic crack detection tool</td><td>Crack-Like</td></tr>
<tr><td>Ultrasonic crack detection tool</td><td>Crack-Like</td></tr>
<tr><td>2</td><td>U.S. Steel</td><td>Ultrasonic crack detection tool</td><td>Crack-Like</td></tr>
<tr><td>3-A</td><td>U.S. Steel</td><td>Ultrasonic crack detection tool</td><td>Crack-Like</td></tr>
<tr><td>3-B</td><td>U.S. Steel</td><td>Ultrasonic crack detection tool</td><td>Crack-Like</td></tr>
<tr><td>7-A</td><td>Youngstown</td><td>Ultrasonic crack detection tool</td><td>Crack-Like</td></tr>
<tr><td rowspan="2">7-B</td><td rowspan="2">Youngstown</td><td>Caliper</td><td>Dent (bottom-side)</td></tr>
<tr><td>Caliper</td><td>Dent (bottom-side)</td></tr>
<tr><td>7-C</td><td>Youngstown</td><td>Ultrasonic crack detection tool</td><td>Crack-Like</td></tr>
</table>

The laboratory examinations of these 9 samples consisted of scanning both the OD and ID surfaces of pipes along the seams with magnetic particle inspection (MT) to locate anomalies. These scans located 48 crack-like anomalies, 36 of which were not indicated by the ILI crack-tool and 21 of which were not found via the field NDE. The nature and size of each anomaly was determined by means of breaking open each anomaly to expose it on fracture surfaces and by making metallographic specimens across many of them. The 50 anomalies (48 crack-like and 2 dents) are listed in Table 28 & Table 29. The modifier “Amb” on “Crack-Like” means that the analyst could not decide whether the anomaly was external or internal. “LOF” stands for lack of fusion. The laboratory classification of hook cracks as “stringer” hook cracks refers to those formed at strings of inclusions as opposed to hook cracks formed from laminations.

Table 26. List of Anomalies Found by Laboratory Examination (first 25)

Sample (Indication)	ILI Tool Feature Type	Field NDE Feature Type	Lab Feature Type
1-A (1)	Amb Crack-Like	---	Int Under-Trim
1-B (1)	Amb Crack-Like	---	Int Hook Crack
1-C (1)	---	Ext LOF	Ext Stringer Hook Crack
1-C (2)	---	---	Ext Stringer Hook Crack
1-C (3)	---	---	Ext Stringer Hook Crack
1-C (4)	---	---	Ext Stringer Hook Crack
1-C (5)	---	Int LOF - Potential Hook Crack	Int Hook Crack
1-C (6)	---	Int LOF - Potential Hook Crack	Int Hook Crack/Stepped
1-C (7)	Ext Crack-Like	Ext LOF	Ext Stringer Hook Crack
1-C (8)	---	Int LOF	Int Hook Crack/Stepped
1-C (9)	---	Ext LOF	Ext Stringer Hook Crack
1-C (10)	---	Ext LOF	Ext Stringer Hook Crack
1-C (11)	---	---	Int Hook Crack
1-C (12)	---	---	Int Hook Crack
1-C (13)	---	Int LOF	Int Hook Crack
1-C (14)	---	Int LOF - Potential Hook Crack	Int Hook Crack
1-C (15)	---	---	Ext Stringer Hook Crack
1-C (16)	---	---	Ext Stringer Hook Crack
1-C (17)	---	Ext LOF	Ext Stringer Hook Crack
1-C (18)	---	---	Ext Stringer Hook Crack
1-C (19)	---	---	Ext Stringer Hook Crack
1-C (20)	Int Crack-Like	Int LOF	Int Hook Crack
1-C (21)		---	Int Hook Crack
1-C (22)	---	---	Int Hook Crack/Stepped
1-C (23)	---	---	Ext Stringer Hook Crack

Table 27. List of Anomalies Found by Laboratory Examination (second 25)

Sample (Indication)	ILI Tool Feature Type	Field NDE Feature Type	Lab Feature Type
1-C (24)	---	---	Ext Stringer Hook Crack
1-C (25)	---	---	Ext Stringer Hook Crack
1-C (26)	---	Ext LOF	Ext Stringer Hook Crack
1-C (27)	---	Int LOF	Int Hook Crack
1-C (28)	---	Ext LOF	Ext Stringer Hook Crack
1-C (29)	---	---	Int Hook Crack
1-C (30)	---	Ext LOF	Ext Hook Crack
1-C (31)	---	Ext LOF	Ext Stringer Hook Crack
1-C (---)	---	LOF - Potential Hook Crack	Int Under-Trim
1-C (32)	Int Crack-Like	LOF - Potential Hook Crack	Int Hook Crack
1-C (33)	---	---	Ext Hook Crack
1-C (34)	---	Ext LOF	Ext Hook Crack
1-C (35)	---	---	Int Hook Crack
1-C (36)	Amb Crack-Like	Int LOF LOF - Potential Hook Crack	Int Hook Crack
1-C (37)	---	---	Int Hook Crack
1-C (38)	Amb Crack-Like	LOF	Int Hook Crack/Stepped
2 (1)	Int Crack-Like	Int LOF - Potential Hook Crack	Sloping Lamination
3-A (1)	Ext Crack-Like	LOF	Int Hook Crack
3-A (1)	---	Mid-Wall Lamination	Mid-Wall Lamination
3-A (2)	---	Mid-Wall Lamination	Mid-Wall Lamination
3-B (1)	Amb Crack-Like	---	Int Hook Crack
7-A (1)	Amb Crack-Like	Int LOF	Ext Under-Trim
7-B (1)	Dent	Dent w/Cracks	Dent
7-B (2)	Dent	Dent w/Cracks	Dent
7-C (1)	Int Crack-Like	---	Int Under-Trim/Over-Trim

Findings of Laboratory Measurements and Metallurgical Examinations

Most of the 50 features found in the ERW seams were hook cracks. Both internal hook cracks and external hook cracks were identified. The 50 features as categorized by the laboratory examinations (including breaking open anomalies and metallographically sectioning anomalies) are illustrated in Figure 42.

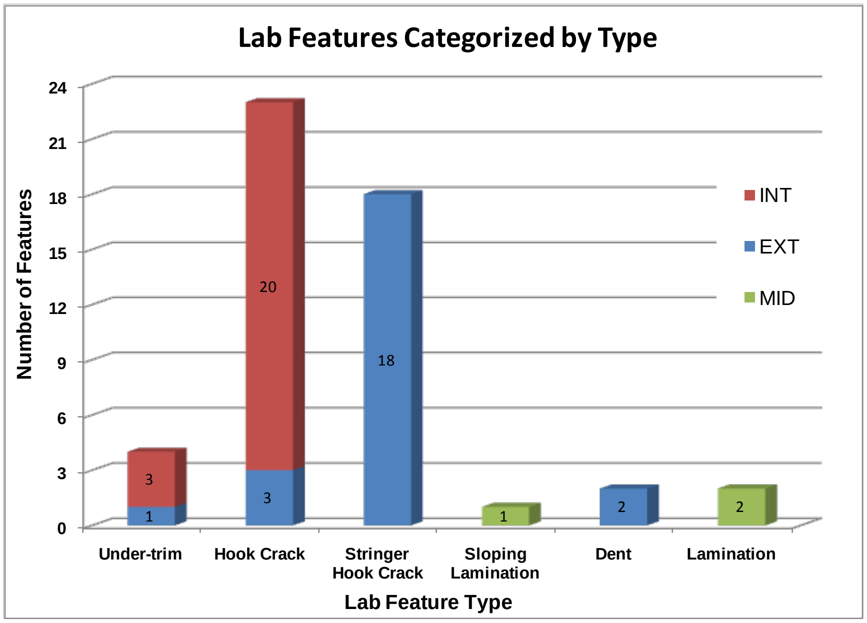

Figure 42. Total Lab Indications Categorized by Feature Type

Several crack features appeared stepped. It is possible multiple laminations/inclusions across multiple planes were at one time separate features that extended into a single feature. Ductile tearing of the material between the adjacent defects could have occurred during a high-pressure event like a hydrostatic test. One crack showed signs of such growth. Indication 38 from Sample 1-C exhibited what looks like ductile crack extension, possibly from a prior hydrostatic test. No sign of fatigue crack growth was seen on the fracture surfaces of this anomaly after it was broken open and examined by means of a scanning electron microscope. No other feature showed evidence of fatigue crack growth.

The graphs discussed throughout the remainder of this case focus on the accuracy of the ultrasonic crack-detection ILI, as well as field inspection results, in terms of crack identification, classification and sizing.

The classification of crack-like features by the ultrasonic crack tool ILI correlated well with the actual feature type determined by destructive testing. Approximately 70 percent of the features classified as crack-like were actually cracks in the ERW seam (Figure 43). The single sloping lamination in Figure 43 was the indication from Sample 2 that had characteristics of a hook crack, but was not connected to the either the inside surface or the outside surface.

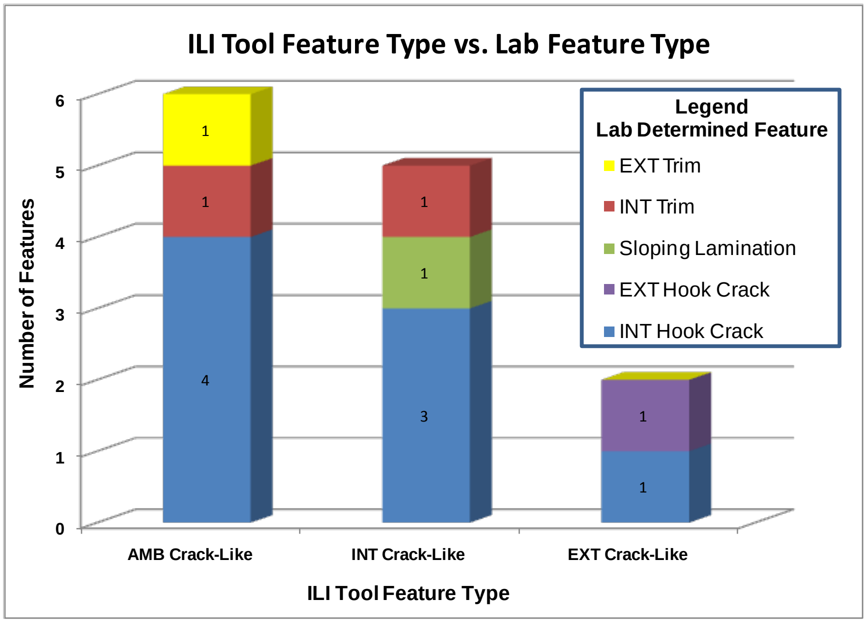

Figure 43. ILI Tool Feature Type vs. Lab Determined Feature Type

Maximum depths of 25 cracks were directly measured and are categorized below in terms of percent wall thickness (Figure 44). The majority of the cracks identified in the lab but not detected by ILI were less than 10 percent deep. Indication 27 from Sample 1-C was the one feature in the 30 percent to 40 percent depth range not detected by ILI. This was due to the length of Indication 27 being below the ILI length detection capabilities. Figure 45 is based on the same data set as Figure 44 but further defines the features by surface location. The deepest cracks investigated were open to the inside surface.

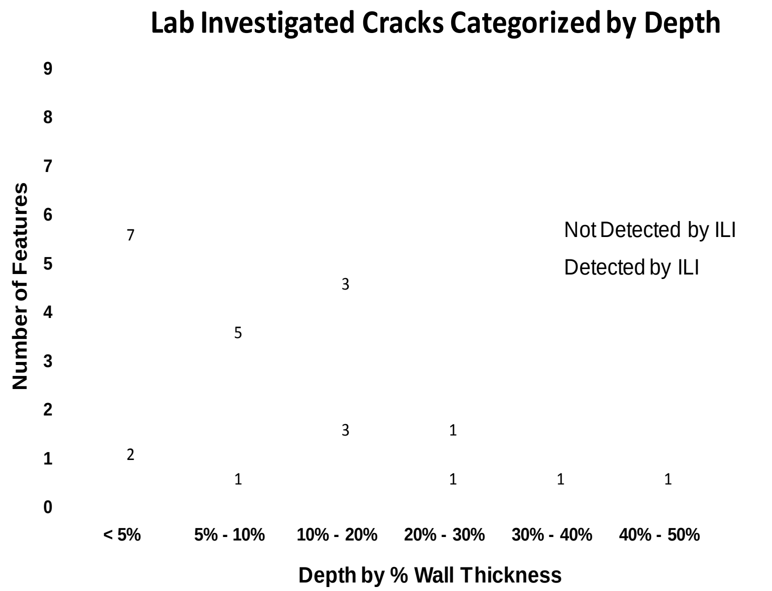

Figure 44. Lab Investigated Cracks Categorized by Depth and Detection

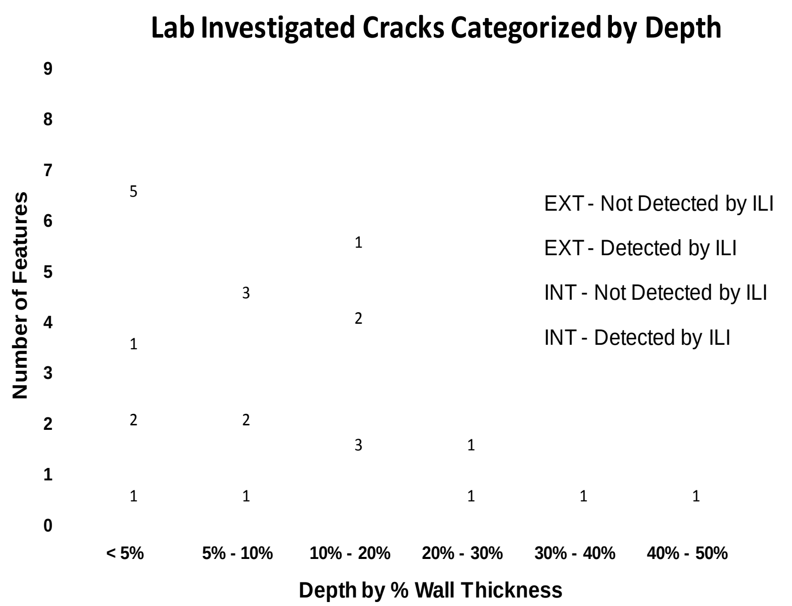

Figure 45. Lab Investigated Cracks Categorized by Depth, Detection and Surface Location

The lengths of 40 cracks were measured and are categorized below in Figure 46. The majority of the cracks not detected by ILI were less than 1.0 inch. The longest cracks, those greater than 4 inches, were open to the inside surface of the pipe.

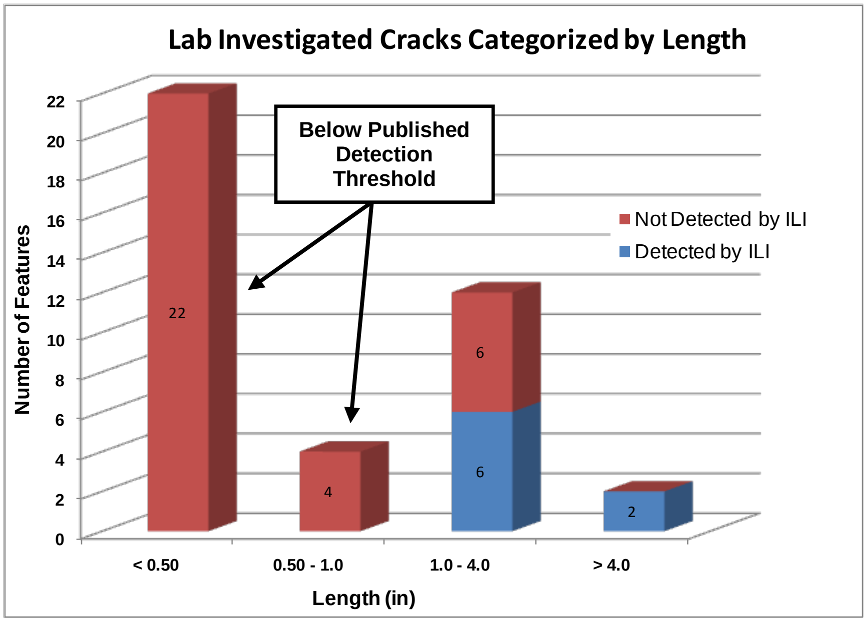

Figure 46. Lab Investigated Cracks Categorized by Length and Detection

The minimum detectible crack size in weld material for the ultrasonic crack tool used in this case is 1.2-inch-long, 0.04-inch-deep (if the anomaly is located in base metal), and 0.08-inch deep (on the basis of the crack being located in the weld zone). For this particular tool run, it is apparent that the third-party analysts (not the vendor's analysts) regarded 0.04 inch as the depth-detection threshold for anomalies in the weld as well as for anomalies in the base metal. Another representation of the results that compares both length and depth is shown in Figure 47. Four cracks detected by ILI were below the published detection threshold (Figure 47). The majority of the crack indications detected by ILI were internal hook cracks (Figure 48). Only one feature met the minimum detection criteria for length and depth but was not identified by ILI. This feature was Indication 6 from Sample 1-C. Indication 6 was a non-uniform crack with multiple peaks and valleys. It is possible that this feature was not detected by ILI since the peak depth was not continuous along the entire length of the defect. Rather the crack had two separate areas where the minimum depth criteria were met but not the minimum length criteria (one approximately 0.20 inch long and another approximately 0.75 inch long).

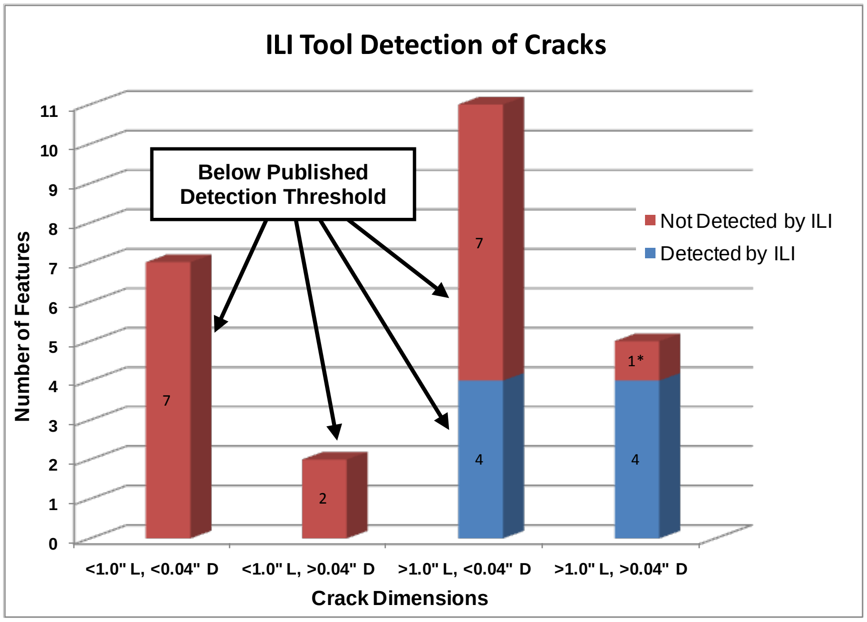

Figure 47. ILI Tool Detection of Cracks by Length and Depth Combinations

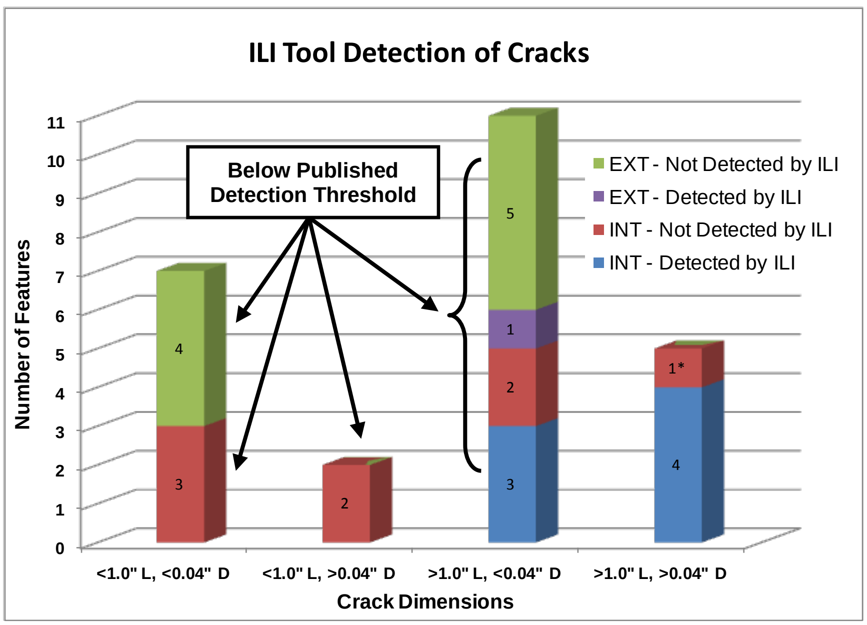

Figure 48. ILI Tool Detection of Cracks by Length and Depth Combinations and Surface

The unity plot below compares the predicted depth by ILI to the actual depth of features determined to be cracks (Figure 49). The ultrasonic crack-tool depths are reported in terms of ranges, less than 0.04 inch or 0.04 inch to 0.08 inch. The depth ranges are represented by the error bars. The diamond-shaped points are the mid-points of the ranges. The plot suggests that the ILI accurately sized 50 percent of the features in terms of depth. In general, the ILI trended towards over-stating depth. The depth of one feature was under-stated, Indication 38 from

Sample 1-C. Indication 38 was the deepest crack investigated (50% of the wall thickness) and had a tight crack tip. The ultrasonic technology does not have a minimum detection criterion for crack width. However, if the crack were under compression by residual stresses at the time of inspection the crack tip could have had essentially no width and would have not been detected by ILI. It cannot be proved that this was the scenario for Indication 6, so the data point remains as a single under-stated depth by ILI.

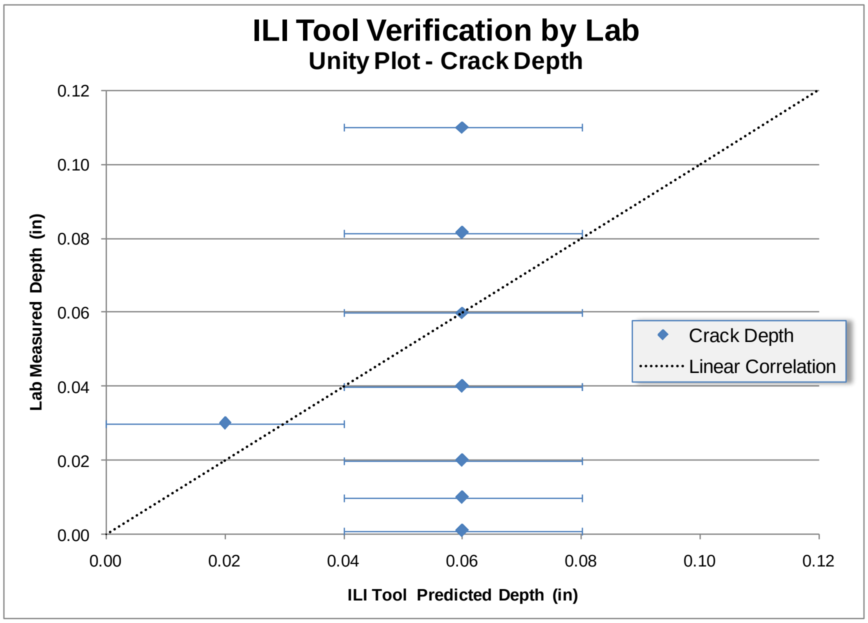

Figure 49. Crack Depth Unity Plot – Lab Measured Depth to ILI Predicted Depth

The unity plot below compares the length predicted by ILI to the actual length of features determined to be cracks (Figure 50). Stated length tolerance for the ultrasonic crack-detection tool used in this case is plus or minus 0.40 inch for cracks less than or equal to 4.0 inches long or 10 percent of the total length for cracks greater than 4.0 inches long. The appropriate tool tolerances for the crack features are represented by error bars. When tool tolerance is considered in this manner, the ILI accurately predicted length for 88 percent of the cracks detected. When only anomalies that met the minimum depth criteria for detection are considered, the ILI accurately predicted length for 100 percent of the cracks detected.

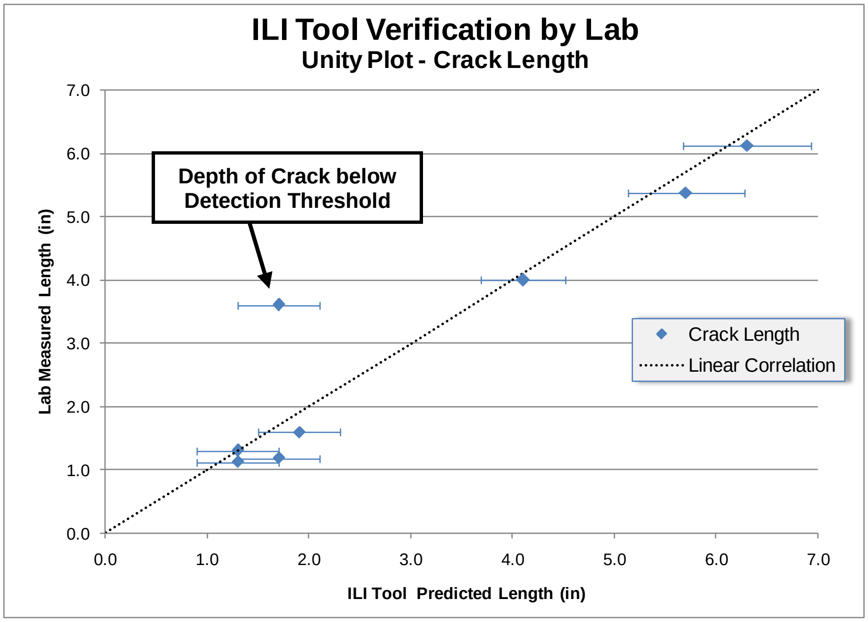

Figure 50. Crack Length Unity Plot – ILI Predicted Length to Lab Measured Length

Field measurements of depth and length compared to actual depth and length are shown in Figure 51 and Figure 52, respectively. The depth data suggest that the field NDE generally over-stated depth of crack features. The length data are quite scattered suggesting that field NDE length results are not reliable.

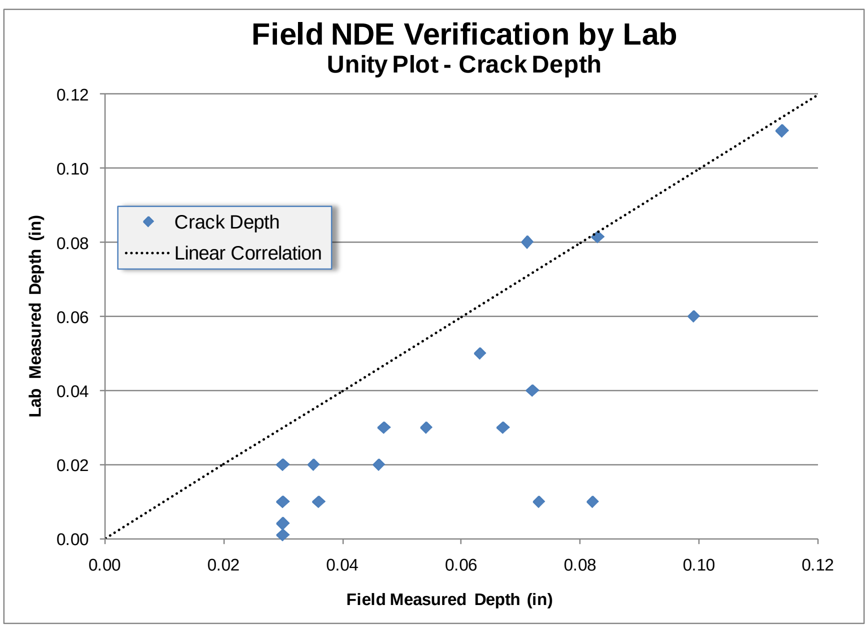

Figure 51. Crack Depth Unity Plot – Field Measured Depth to Lab Measured Depth

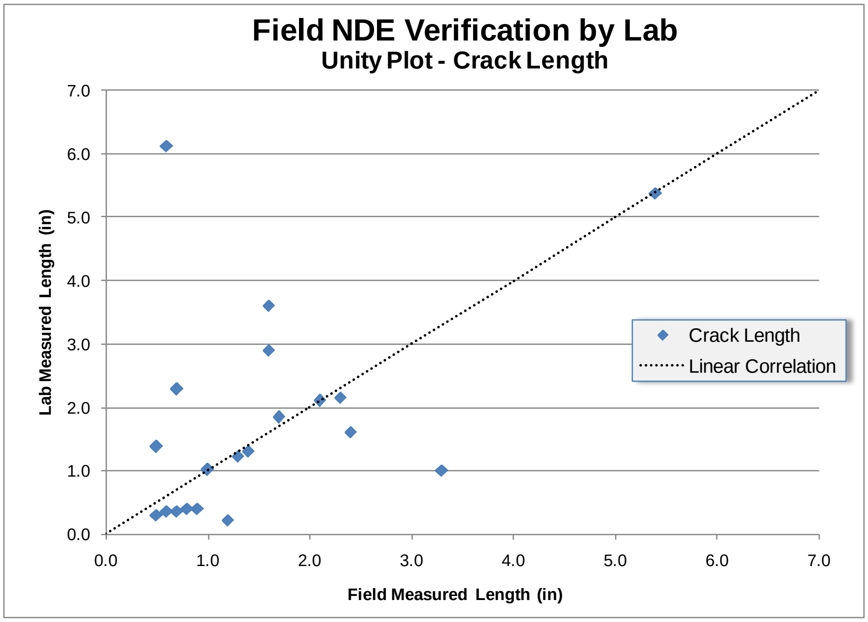

Figure 52. Crack Length Unity Plot – Field Measured Length to Lab Measured Length

Comparisons between ILI Findings and Hydrostatic Test Results

The pipeline was subjected to a hydrostatic test in 2010 to establish its maximum operating pressure and to assess defects below the detection threshold of the 2009 ILI tools. The hoop stress levels in the "spike" test[4] ranged from 86.8% of SMYS to 96.5% of SMYS.

Four leaks and one rupture occurred during hydrostatic testing. All four of these failures occurred in pipe manufactured by U.S. Steel.

The three leaks were discovered during the hold time for the required test at 1.25 times the maximum operating pressure of the pipeline. It is suspected that the anomalies began leaking during the spike test. All three leaks were associated with longitudinal ERW seam weld penetrators. Penetrators are short areas of lack of fusion that extend entirely through the wall. They are oxide-filled and can be caused to leak if the oxide deteriorates or is broken by stretching of the anomaly under hoop stress. The lengths of the penetrators are well below the length detection threshold of ILI crack-detection tools.

The rupture initiated during the spike test at a lamination (actually a void) located in the base metal. The hoop stress level at the time and location of the rupture was believed to be as high as 114% of SMYS because the segment was accidentally over-pressurized. The lamination was

[4] A spike test is a short-duration (usually no more than 30 minutes) pressurization to the pipeline to a level in excess of 1.25 times the maximum operating pressure of the pipeline. In this case the spike test pressure was on the order of 1.33 times the maximum operating pressure.

detected by the ultrasonic wall measurement tool but was not repaired prior to the hydrostatic test.

The fact that no defect failed in the 2010 hydrostatic test at a pressure level below the spike test pressure level suggests that the crack-detection ILI did not miss any significant defect.

Conclusions Regarding the Case 12 Tool Runs

As a result of the evaluations of 50 anomalies removed from the Case 12 pipeline, it was found that:

- The majority of the indications turned out to be hook cracks.
- The classification of feature type by the ILI correlated reasonably well with the actual feature type.
- The ILI-predicted flaw depths were accurate for 50 percent of the crack-like features with a trend towards over-stated depth.
- The ILI-predicted flaw lengths were accurate for 88 percent of the crack-like features.
- Field NDE generally over-stated the depths of crack-like features.
- The field NDE depths and lengths correlated poorly with actual depths and lengths.
- One out of 25 investigated crack-like features met the minimum detection criteria for length and depth yet was not reported by ILI.
- One feature exhibited evidence of crack growth, a 50-percent-through-wall internal hook crack. It is believed that the growth was caused by a few large cycles, mainly the commissioning test and subsequent retests rather than by in-service pressure cycles.
- No feature exhibited confirmed high cycle, in-service fatigue.

It can be concluded that the ultrasonic crack-detection ILI performed reasonably well but not sufficiently well enough to inspire complete confidence (one crack that met the threshold detection limits was not reported). The examination of the actual physical sizes of defects in this case shows that field NDE measurements were not reliable and were not a sufficient means for validating the results of an ultrasonic crack-detection tool run.

Case 13

Case 13 involves an ILI and follow-up testing, both of which are described in a published paper.[5] The 23-mile-long gas pipeline is comprised of 20-inch-OD, 0.375-inch-wall, Grade B, DC-ERW pipe manufactured by Youngstown in 1943. The assessment of this pipeline was undertaken in 1999 to validate its integrity so that its operating stress level could be increased from 30% of SMYS to 50% of SMYS. A CMFL tool was run through the pipeline with the intent of finding ERW seam defects. The plan called for examining anomalies identified by the ILI using field NDE to establish that a seam anomaly existed at each location indicated by the ILI. At selected locations corresponding to what were believed to be the most injurious anomalies, the pipe was cut out of the pipeline to be sent to the operator's laboratory for direct physical measurement of the length and depth of the anomaly. The intent was to verify both the capabilities of the ILI and the field NDE. ILI runs to detect metal loss and mechanical damage were also made, but the focus for the purpose of this document is the CMFL tool run. The ILI assessments were followed by a hydrostatic test of the entire pipeline to 1.5 times the maximum operating stress to validate the new operating stress level.

The anomalies found by the CMFL ILI were classified in a manner similar to that discussed under Cases 9 and 10. The types of anomalies were classified as "A" meaning that the anomaly had all of the characteristics of a crack-like feature, "B" meaning that the anomaly had some of the characteristics of a crack-like feature, or "seam anomaly" meaning a non-crack-like anomaly associated with metal loss in the seam such as excess trim. The CMFL data indicated that there were 190 "reportable" anomalies, that is, anomalies that exceeded 1-inch in length and 10% of the wall thickness in depth. Five of the anomalies were reported as Type A anomalies, 10 were reported as Type B anomalies, and 175 were reported as Seam Anomalies. The Type A and Type B anomalies were subjected to further examination. The findings of the examinations of these anomalies are summarized in Table 30. Besides the descriptions of the 15 Type A and Type B anomalies, Table 30 also contains an anomaly that was found at the laboratory that was not found by either the CMFL ILI or the field NDE.

[5] Rogers, G.B., Rapp, S.C., and Matocha, G.M., "*Integrity Evaluation of an Older Vintage ERW Pipeline*", IPC 2002-27052, Proceedings of IPC'02, 4th International Pipeline Conference, September 29 – October 3, 2002, Calgary, Alberta, Canada

Table 28. Summary of Type A and Type B CMFL ILI Anomalies

Anomaly Number	CMFL Tool			Field UT		Metallographic Examination		
	Anomaly Type	Length, inches	Depth to Thickness Ratio	Length, inches	Depth to Thickness Ratio	Anomaly Type	Length, inches	Depth to Thickness Ratio
1	B	2.0	0.44	1.5		Excess Flash		
2	B	2.6	0.29	2.5	0.10	hook crack	2.4	0.40
3	A	3.8	0.41	2.0	0.10	hook crack	5.3	0.50
4	B	2.5	0.35	2.5	0.05	not ERW pipe		
5	B	3.9	0.30	3.5	0.32	Excess Trim		
6	A	7.0	0.49	7.0	0.30	not examined		
7	A	7.0	0.26			LOF	5.30	0.40
8	B	2.6	0.34	2.6	0.20	hook crack	2.1	0.30
9	B	4.2	0.21	4.0	0.25	hook crack	3.5	0.50
10	A	4.2	0.34	0.8	0.10	Excess Flash		
11	B	2.1	0.47	3.3	0.48	Excess Flash		
12	B	3.8	0.52	4.5	0.20	not examined		
13	B	2.0	0.62	2.0	0.10	not examined		
14	A	1.3	0.40			hook crack	1.0	0.15
15	B	1.1	0.52			Excess Flash		
16	not called			not found		HAZ crack	1.0	0.15

The abbreviation LOF in Table 30 stands for lack of fusion, and the abbreviation HAZ stands for heat-affected zone (of the ERW seam).

The data on anomaly type in Table 30 illustrate one difficulty with this CMFL ILI. The ILI tended to indicate crack-like conditions where the actual anomaly was either extra or missing metal (i.e., excess flash not trimmed away and excess trim). This tendency is likely to cause unnecessary excavations for anomalies which really have no significant detrimental effect.

Comparisons between ILI (Tool) dimensional findings and the laboratory dimensional findings (Met) are shown in Figure 53 and Figure 54. “Met” is short for metallurgical examination, one of the means used to verify the nature and sizes of the anomalies. In these cases the examinations consisted of both metallographic sectioning of anomalies and breaking open samples to expose the anomalies on fracture surfaces.

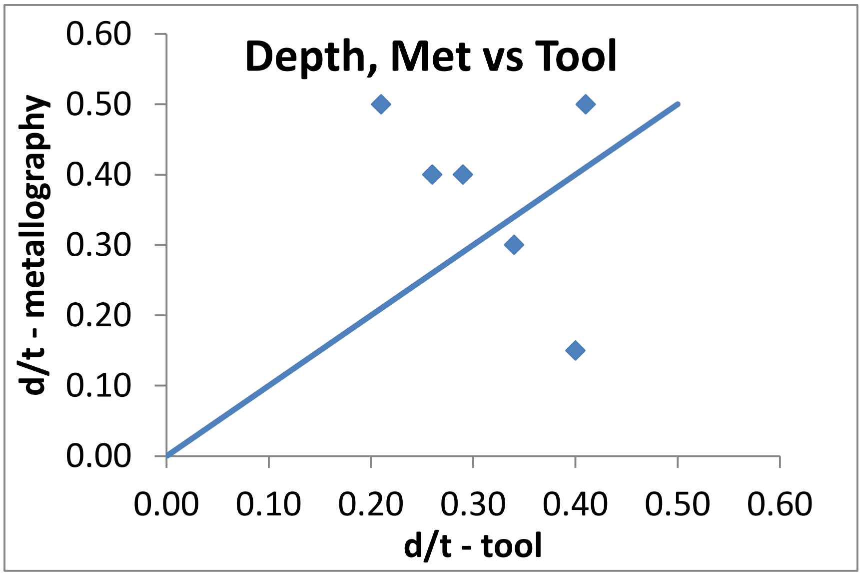

Figure 53. Comparisons of Depths Found by Metallography with Those Found by CMFL Tool

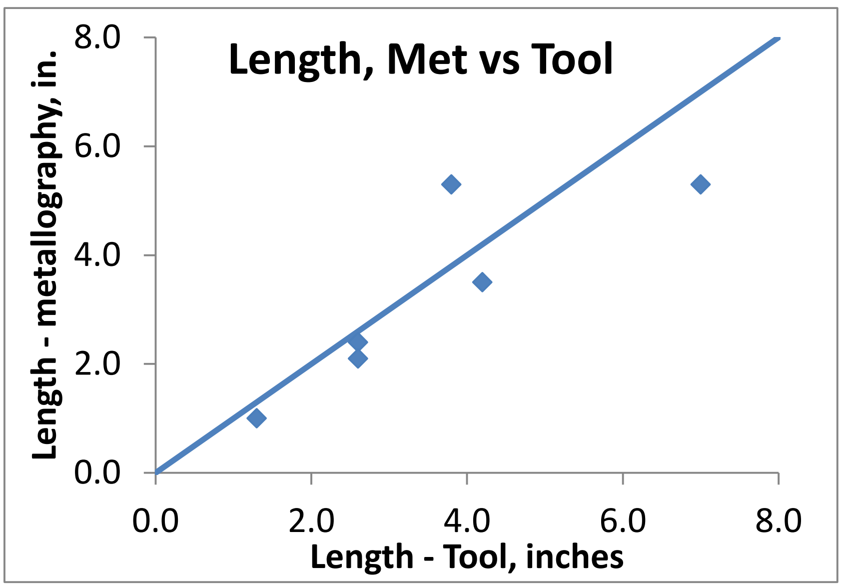

Figure 54. Comparisons of Lengths Found by Metallography with Those Found by CMFL Tool

As seen in Figure 53, there is no correlation between the actual depths and those indicated by the ILI. In several cases the ILI depth significantly underestimated the depth of the anomaly. The ILI lengths, however, seemed to correlate well with the actual lengths of the anomalies as shown in Figure 54.

The comparisons between field NDE dimensional measurements and the actual anomaly dimensions as determined in the laboratory are shown in Figure 55 and Figure 56.

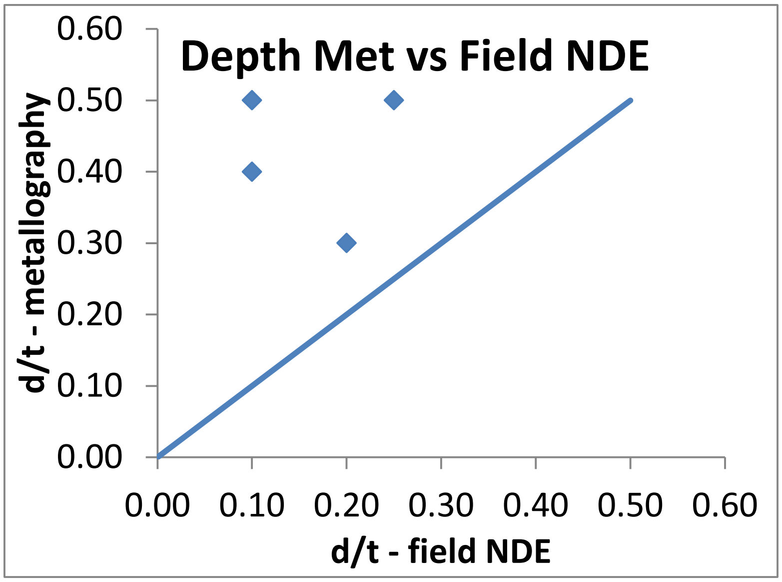

Figure 55. Comparisons of Depths Found by Metallography with Those Found by Field NDE

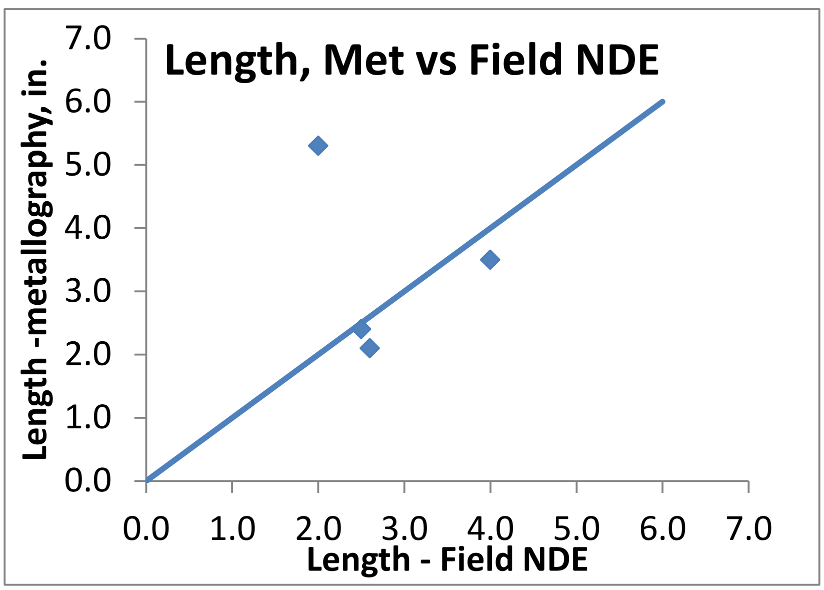

Figure 56. Comparisons of Lengths Found by Metallography with Those Found by Field NDE

It is seen in Figure 55 that the field NDE significantly under-estimated the depths of the anomalies. Except for one anomaly, as shown in Figure 56, the lengths determined by the field NDE correlated fairly well with the actual lengths of the anomalies.

The results of the hydrostatic test of the pipeline conducted in 2010 after the CMFL tool run are presented in Table 31.

Table 29. Hydrostatic Test Results

Failure Number	Hydrostatic Test Failures					CMFL Tool Findings		
	Mode	Defect Dimensions		Type of Defect	Failure Stress, %SMYS	Anomaly Type	Indicated Dimensions	
		Length, inches	Depth to Thickness Ratio				Length, inches	Depth to Thickness Ratio
1	Rupture	1.55	0.89	LOF	78.5	Seam Anomaly	2.8	0.30
2	Rupture	11/1.5	0.50	CW/LOF	77.8	not found		
3	Rupture	7.50		CW	73.5	not found		
4	Leak	1.56		LOF		Seam Anomaly	1.9	0.47
5	Rupture	3.88	0.67	LOF	76.0	not found		
6	Rupture	2.75	0.50	LOF	70.8	not found		
7	Rupture	1.50	0.67	LOF	74.9	not found		
8	Leak	0.81	0.75	LOF		not found		
9	Leak	0.75	0.91	LOF		not found		

It is seen that 6 ruptures and 3 leaks occurred during the test to a nominal stress level of 75% of SMYS. All 9 failures were attributed to original manufacturing defects: cold welds (CW)[6] and lack of fusion (LOF). It is stated in the paper that the test stress level in the 2010 test exceeded any level to which the pipeline had previously been exposed. That includes the manufacturer's hydrostatic test which would most likely have been a 5 or 10 second test to a stress level of 60% of SMYS.

Seven of the defects that failed in the test were not reported by the CMFL ILI. It is particularly significant that five of the anomalies that caused test failures were not reported by the CMFL ILI even though the length and depth dimensions of the anomalies exceeded the threshold detection limits of the tool. The failure of the ILI to identify these defects probably is associated with its inability to detect very tight crack-like defects. Typically the vendors of CMFL-tool services specify that detection is not certain for flaws with width openings less than 0.004 inch.

The hydrostatic test results can be used to illustrate another significant fact, namely, that a commonly used model for predicting the failure stress levels of axial flaws in pressurized pipes is not reliable for predicting failure stress levels for these types of ERW seam defects. The model chosen for this illustration is the Modified Ln-Sec Elliptical C-Equivalent model which has been extensively validated for predicting failure stress levels in ductile pipe materials. In this case the model was used in conjunction with an assumed Charpy energy level of 1.0 ft lb to represent the extremely low toughness of the bondline region of the seam. The comparisons of

[6] It is noted that the authors of the paper distinguish between cold welds and lack of fusion, though not everyone does. In their view a cold weld is an area of poor or no bonding that may not be an open crack. In contrast, their definition of lack of fusion pertains to a no-bond region that is coated with oxide because it was an open crack. The investigating team has tended to lump both of these phenomena under the term "cold weld".

the predicted to actual failure stress levels for the 5 defects where dimensions and failure stress levels were available are shown in Figure 57.

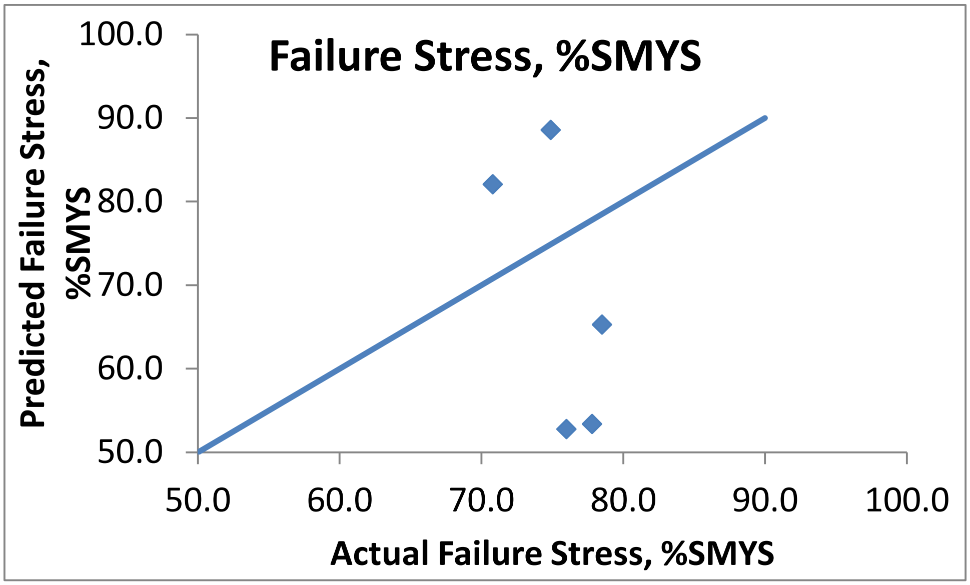

Figure 57. Comparisons of Predicted Failure Stress Levels to Actual Failure Stress Levels for the Test Failures

There is no correlation between the predicted and the actual failure stress levels. It is suspected that none of the other ductile flaw assessment models would perform any better. This situation arises because of the extremely brittle behavior exhibited in conjunction with failures of defects in and around ERW seams, especially LF-ERW and DC-ERW seams. The problem this creates for using ILI tools for ERW seam integrity assessment is that even if the tools were capable of accurately predicting the sizes of defects, it would not be feasible to prioritize the defects for remediation based on the predicted failure stress levels or fatigue lives. A better approach to defect assessment is needed for flaws in or around ERW seams.

Conclusions Regarding the Case 13 Tool Runs

The authors of the technical paper on the Case 13 results concluded the following:

- The use of the CMFL ILI minimized the number of failures in the subsequent hydrostatic test.
- The use of the ILI provided greater confidence in the integrity of the pipeline and its capacity to be upgraded.
- The ILI did not find all detrimental anomalies.
- The ILI tended to underestimate the sizes of anomalies that it did detect.

- The ILI performed better with "volumetric" anomalies such as hook cracks than it did with tight cracks such as cold welds and lack of fusion.
- Field NDE is no more able to size anomalies accurately than is the CMFL ILI.
- Conservatism should be applied in determining which anomalies should be addressed.
- The technology will improve with experience.

The investigating team concurs with these conclusions and adds that there is a need for a better means to predict failure stress levels of defects in and around ERW seams, particularly LF-ERW and DC-ERW seams.

DISCUSSION

The 13 cases of ERW seam integrity assessments described in this document involved three different types of in-line inspection (ILI) technologies:

- Ultrasonic angle-beam inspection for crack detection,
- Circumferential magnetic-flux leakage (CMFL) inspection for detecting axially-oriented anomalies, and
- Electromagnetic Acoustic Transducer (EMAT) inspection for crack detection.

The inspections covered 741 miles of liquid, HVL, and natural gas pipelines comprised of low-frequency-welded ERW (LF-ERW) pipe, direct-current-welded ERW (DC-ERW) pipe, and high-frequency-welded ERW (HF-ERW) pipe.

To facilitate the discussion of the findings of the analyses of these 13 cases, a table that appeared near the beginning of this document (Table 3) is reproduced here as Table 32. This table summarizes the attributes of the inspected pipelines.

Table 30. Summary of the 13 Cases of ERW Seam Inspections

Case Number	Year Installed	Manufacturer	Liquid or Gas	Diameter, inch	Wall Thickness, inch	Grade	Seam Type	Miles	Year of ILI	Type of ILI
1	1953	Youngstown	Liquid	16	0.281	X52	DC ERW	29.9	2007	Ultrasonic crack-detection tool
2	1966	Bethlehem	Liquid	16	0.312	X52	LF ERW	53.9	2007	Ultrasonic crack-detection tool
3	1961	Page Hersey	Liquid	12.75	0.219 & 0.250	X52	LF ERW	54	2008	Ultrasonic crack-detection tool
4	1986	Stelco	Liquid	12.75	0.25 & 0.375	X56	HF ERW	64	2008	Ultrasonic crack-detection tool
5	1961	Alberta Phoenix	Liquid	12.75	0.250	X52	LF ERW	40	2008	Ultrasonic crack-detection tool
6	1961	Prairie Pipe	Liquid	12.75	0.250	X52	LF ERW	16	2008	Ultrasonic crack-detection tool
7	1953	Youngstown	Liquid	16	0.250	X42	DC ERW	21.8	2007	Ultrasonic crack-detection tool
8	1961	Lone Star	HVL	12.75	0.250	X52	LF ERW	120.3	2005	Ultrasonic crack-detection tool
9	1961	Lone Star	HVL	12.75	0.250	X52	LF ERW	120.3	2008	Circumferential MFL
10	1956	Lone Star/A.O. Smith	Gas	16	0.250	X52	LF ERW	64	2007	Circumferential MFL
11	1960	Lone Star	Gas	16	0.260	X52	LF ERW	18	2009	EMAT
12	1968	Youngstown/U.S. Steel	Liquid	20	0.230/0.219	X52	DC ERW/HF ERW	139	2009	Ultrasonic crack-detection tool
13	1943	Youngstown	Gas	20	0.375	Grade B	DC ERW	23	1999	Circumferential MFL

Nine of the cases involved inspections of liquid and HVL pipelines by means of an ultrasonic crack-detection tool. Such tools are seldom used in gas pipelines because of the need for liquid to couple the transducer signals to the pipe wall. Only by running such a tool in a slug of liquid within a “pig train” can the technology be used in a gas pipeline. Not all gas pipelines can accommodate such pig trains, so it is rare to find a case where an ultrasonic tool has been run in a gas pipeline.

Three cases involved inspections of two gas pipelines and one HVL pipeline by means of a circumferential MFL (CMFL) tool. These tools are not advertised as crack-detection tools because the minimum advertised flaw opening that they can reliably detect is 0.004 inch or 0.008 inch depending on the vendor, much more that the opening one expects for a tight crack such as a lack of fusion defect. The belief is that the CMFL tools can find such ERW seam anomalies as misaligned edges, over-trim, under-trim, selective seam corrosion, and some hook cracks.

One case involved inspection of a gas pipeline by means of an EMAT tool. The EMAT tool is intended to be a crack-detection tool. It does not require a liquid couplant, so it can be run in a gas pipeline without the introduction of a slug of liquid.

The statistics of anomalies discovered and investigated in the 13 cases are summarized in Table 33.

Table 31. Summary of Anomalies Found and Investigated in the 13 Cases

Case Number	Type of ILI	Number of Anomalies	Number of Anomalies per Mile	Number of Anomalies Examined in the field	Number Examined/Total Number of Anomalies, %
1	Ultrasonic crack-detection tool	60	2	12	20.0
2	Ultrasonic crack-detection tool	73	1	12	16.4
3	Ultrasonic crack-detection tool	2738	51	275	10.0
4	Ultrasonic crack-detection tool	387	6	16	4.1
5	Ultrasonic crack-detection tool	1668	42	29	1.7
6	Ultrasonic crack-detection tool	1409	88	21	1.5
7	Ultrasonic crack-detection tool	61	3	23	37.7
8	Ultrasonic crack-detection tool	1353	11	101	7.5
9	Circumferential MFL	548	5	46	8.4
10	Circumferential MFL				
11	EMAT				
12	Ultrasonic crack-detection tool			52	
13	Circumferential MFL	190	8	15	7.9

It is seen in Table 33 that the numbers of anomalies found varied widely. A more meaningful number is the number of anomalies per mile. This number varied from 1 per mile to 88 per mile. The wide variation in anomalies per mile could be a function of the seam quality in each pipeline or it could be a function of the sensitivity level of each ILI or a combination of both. Similarly, both the number of anomalies subjected to field examination and the number subjected to examination as a percent of the total number of anomalies are shown in the table. The number examined as a percent of the total number is the more important of the two, because it speaks to the degree to which the field examination findings may be representative of the condition of the whole pipeline. It is seen that the percent examined varied from as low as 1.5% to as high as 38%. For some of the cases, these numbers were not available because in those cases only limited data were made available.

The various means of verifying the nature and characteristics of the anomalies are summarized in Table 34 for the 13 cases.

Table 32. Summary of Methods Used to Verify the Nature of the Anomalies (Cases 1-8)

Case Number	Type of ILI	Means of Verification	Comments
1	Ultrasonic crack-detection tool	Field NDE and hydrostatic test 5 years after the tool run.	Most Field NDE depths exceeded tool-called depths, in one case, by a lot. Field NDE lengths tended to exceed tool-called lengths.
2	Ultrasonic crack-detection tool	Field NDE only	Most Field NDE depths exceeded tool-called depths. Field NDE lengths agreed in most cases with tool-called lengths
3	Ultrasonic crack-detection tool	Field NDE/grinding, metallurgical examinations and burst tests	Most tool-called depths exceeded Field NDE depths. Laboratory measurements tended to show that the Field NDE in this case was reasonably accurate. Agreement between tool-called lengths and field NDE lengths was highly variable.
4	Ultrasonic crack-detection tool	Field NDE/grinding	Most tool-called depths exceeded Field NDE depths. Most field NDE lengths exceed tool-called lengths
5	Ultrasonic crack-detection tool	Field NDE/grinding	Most tool-called depths exceeded Field NDE depths. Tool-called lengths tended to be similar to field NDE lengths with a few exceptions.
6	Ultrasonic crack-detection tool	Field NDE/grinding	All tool-called depths exceeded Field NDE depths. Most field NDE lengths exceeded tool-called lengths.
7	Ultrasonic crack-detection tool	Field NDE only	Most tool-called depths exceeded Field NDE depths. Most tool-called lengths exceeded field NDE lengths.
8	Ultrasonic crack-detection tool	Field NDE followed up with phased-array UT scanning and burst testing and metallurgical examinations	Most tool-called depths exceeded Field NDE depths. Agreement between tool-called lengths and field NDE lengths varied widely. 21 burst tests exhibited failure stress levels ranging from 101 to 159% of SMYS. Origin of failure coincided with tool-called anomaly in 8 of the tests.

Table 33 (continued). Summary of Methods Used to Verify the Nature of the Anomalies (Cases 9-13)

Case Number	Type of ILI	Means of Verification	Comments
9	Circumferential MFL	Field NDE followed up with phased-array UT scanning and burst testing and metallurgical examinations	No correlation between tool-called anomaly dimensions and those found by Field NDE. On 28 samples of pipe nearly 300 indications found during phased-array UT scans had not been indicated by the tool.
10	Circumferential MFL	Field NDE not made available for this investigation. Burst tests of removed samples (the only data made available for this investigation).	Burst stress levels ranged from 84 to 128% of SMYS. Tool-called depths tended to underestimate the actual depths of the defects at the origins. The tool-called lengths agreed pretty well with the actual lengths. The tool did find one tight crack, a cold weld.
11	EMAT	Field NDE only	The tool did identify some types of ERW seam anomalies.
12	Ultrasonic crack-detection tool	Field NDE followed up by laboratory UT scans and metallurgical examinations of 50 anomalies, 12 of which had been called by the tool. A follow-up hydrostatic test was conducted.	The tool-called depths and lengths agreed reasonably well with the laboratory determined values. Laboratory scans with MT found 36 small crack-like anomalies missed by the tool and 21 missed by Field NDE. The Field NDE tended to overcall depths and to erratically call lengths.
13	Circumferential MFL	Field NDE, metallurgical examination and a follow-up hydrostatic test	Tool-called depths did not correlate well with metallurgically-determined depths. Field NDE undercalled the actual depths but gave fairly good representations of length.

In all 13 cases, field NDE consisting of magnetic particle inspection and UT crack-depth measurements was conducted to verify that anomalies existed at locations indicated by the ILI and to assess the nature and sizes of the anomalies. It is seen that the depths of anomalies found by field NDE sometimes were deeper than those called by the tool, but in most cases the opposite was true. It is also seen that the lengths of anomalies found by NDE were sometimes longer than, in one case shorter than, and sometimes about the same as lengths indicated by ILI. The point is that the relationship between ILI dimensions and field-NDE-determined dimensions was inconsistent, and therefore, field NDE cannot be used by itself to verify the sizing accuracy of an ILI. In Cases 8 and 9, phased-array UT scanning of the exposed seams was carried out in addition to manual UT. It is clear that the phased-array scans identified numerous additional anomalies that were missed by the UT scans and the tools. However, among the anomalies found by both manual UT and phased-array UT, the agreement between ILI dimensions and phased-array-UT-determined dimensions was not any better than the agreement between ILI dimensions and manual-UT-determined dimensions.

It is noted that "grinding" was used in some cases along with field NDE to verify the depths of anomalies. It is assumed that this meant grinding until no further crack indication was observable and taking the depth of the grind to be the depth of the anomaly. Of course, this can only be done for external-surface-connected anomalies in an operating pipeline and then only to a limited depth. Codes such as ASME B31.4 and ASME B31.8 limit grinding on an operating pipeline to a maximum depth of 40% of the wall thickness and only if the length of the grinding in combination with the depth does not impair the serviceability of the pipeline at its current pressure. The information available in the data provided to this investigation was insufficient to allow an assessment of its effectiveness.

Other methods of verification applied in the 13 cases consisted of removal of pipe for metallurgical examinations and/or burst tests and conducting follow-up hydrostatic tests of the pipeline. These activities provided, by far, the best evidence of the effectiveness of the inspections. Metallurgical examinations consist of breaking open and/or metallographic sectioning of anomalies. This allows a direct measurement of the length and depth of the anomaly. The results can be used to assess not only the ILI but the field NDE as well. Burst tests expose the worst-case anomaly in the pressurized segment, and they provide a direct measure of the effect of the anomaly on the pressure-carrying capacity of the pipe. If the anomaly exposed in a burst test has clearly-defined dimensions, the effective toughness of the material in which the defect is embedded can be back-calculated. Follow-up hydrostatic testing either finds critical defects that the ILI failed to identify or it proves that the ILI missed no critical defects. Above all, it provides verification of the seam integrity of the pipeline in the event that the ILI does not.

The overall assessments of the effectiveness of the inspections for each of the thirteen cases are summarized in Table 36.

Table 34. Summary of Evaluations of Effectiveness of the Inspections (Cases 1-8)

Case Number	Type of ILI	Number of Anomalies Missed That Met the Threshold Dection Limits	Overall Evaluation of the Inspection
1	Ultrasonic crack-detection tool	The hydrostatic test proves that no serious anomalies were missed.	The inspection and follow-up field NDE were insufficient to conclude that the seam integrity had been verified. Seam integrity is assured by the hydrostatic test.
2	Ultrasonic crack-detection tool	0	The inspection and follow-up field NDE were insufficient to conclude that the seam integrity had been verified.
3	Ultrasonic crack-detection tool	Field NDE showed an 11.4-inch-long, 0.077-inch-deep anomaly that was not called by the tool	The facts that the Field NDE in this case was shown to be fairly accurate, and that the tool tended to overcall anomaly depths provides some confidence that the seam integrity was verified, but the missed anomaly prevents full confidence.
4	Ultrasonic crack-detection tool	Field NDE showed a 26.4-inch-long, 0.056-inch-deep anomaly that was not called by the tool	The inspection and follow-up field NDE were insufficient to conclude that the seam integrity had been verified.
5	Ultrasonic crack-detection tool	0	The inspection and follow-up field NDE were insufficient to conclude that the seam integrity had been verified.
6	Ultrasonic crack-detection tool	0	The inspection and follow-up field NDE were insufficient to conclude that the seam integrity had been verified.
7	Ultrasonic crack-detection tool	Two anomalies failed in a hydrostatic test 5 years after the tool run. There were no tool calls at the locations of these failures.	The inspection and follow-up field NDE were insufficient to conclude that the seam integrity had been verified. Seam integrity is assured by the hydrostatic test.
8	Ultrasonic crack-detection tool	No tool inidcation was present at the apparent origin of an in-service failure that occurred 2 years after the inspection. No tool calls could be linked to 3 of the 5 test failures that occurred in a test conducted 3 years after the inspection.	The burst tests showed that the tool often missed the most severe anomaly. The fact that a service failure occurred at an anomaly completely missed by the tool means that the operator can have no confidence in the inspection. Seam integrity is assured by the hydrostatic test.

Table 35 (continued). Summary of Evaluations of Effectiveness of the Inspections (Cases 9-13)

Case Number	Type of ILI	Number of Anomalies Missed That Met the Threshold Dection Limits	Overall Evaluation of the Inspection
9	Circumferential MFL	11 of 12 burst test origins were not identified by the tool. Only 5 of the 12 burst test origins were identified by the phased-array UT scans.	An adequate ERW seam inspection where tight cracks are present cannot be achieved by means of a CMFL tool without enhanced signal processing. The vendors state that axial flaws must have an opening of at least 0.004 inch to be detected.
10	Circumferential MFL	The burst tests revealed deep crack-like defects, the depths of which were significantly undercalled by the tool.	An adequate ERW seam inspection where tight cracks are present cannot be achieved by means of a CMFL tool without enhanced signal processing. The vendors state that axial flaws must have an opening of at least 0.004 inch or 0.008 inch to be detected.
11	EMAT	The use of EMAT technology in this case for ERW seam anomalies was a secondary objective, and therefore, no attempt was made by the vendor or the pipeline operator to carefully assess the results.	The EMAT technology was probably not given a thorough and fair test in this case, so one cannot conclude whether or not it can produce a satisfactory seam integrity assessment.
12	Ultrasonic crack-detection tool	One crack that met the minimum threshold detection size (1.2 inch in length, 0.04 inch in depth) was missed.	The tool missed one crack that should have been detected. In most cases the tool overcalled the depth, but it undercalled the depth of the deepest crack examined metallurgically. The tool-called lengths were reasonably accurate. The follow-up test found 3 penetrators that were missed by the tool because their lengths were below the length detection threshold of the tool. Because one anomaly was missed that should have been called , the operator cannot have full confidence in the integrity of the seams solely on the basis of the ILI crack-tool results. Seam integrity is assured by the hydrostatic test.
13	Circumferential MFL	The tool missed five anomalies the sizes of which exceeded the threshold criteria for length and depth. These five defects failed in the follow-up hydrostatic test at stress levels ranging from 71 t0 78% of SMYS.	An adequate ERW seam inspection where tight cracks are present cannot be achieved by means of a CMFL tool without enhanced signal processing. The vendors state that axial flaws must have an opening of at least 0.004 inch or 0.008 inch to be detected. Seam integrity is assured by the hydrostatic test.

As seen in last column of Table 36, there was no case for which the investigating team is willing to say that the inspection provided full confidence in the seam integrity of the assessed segment. There are various reasons for this.

1. For Cases 1, 2, and 4-6, the verification of the ultrasonic crack detection ILI effectiveness was solely dependent on field NDE. As discussed above, field NDE as typically practiced (that is without any blind calibration) is not reliable. Therefore, these verifications of ILI performance are insufficient to provide confidence in seam integrity.
2. For Cases 3, 7, and 12, anomalies were revealed by metallurgical examinations or follow-up hydrostatic that were missed by the ultrasonic crack detection ILI even though the lengths and depths of the anomalies exceeded the threshold detection limits of the tool.
3. For Case 8, a service failure occurred 2 years after the inspection that appeared to have originated at a seam anomaly large enough to have been detected by the ultrasonic crack tool. This clearly shows that the seam integrity was not assured by the ILI.

4. For Cases 9, 10, and 13, where a CMFL tool was used, it is clear that the CMFL ILI could not reliably find some crack-like defects that would likely impair the integrity of the ERW seam[7].
5. For Case 11, although the EMAT tool was shown able to find some ERW seam anomalies, there was insufficient information to evaluate the tool let alone prove its effectiveness.

Aside from the evaluations summarized in Table 36, it should be noted that the ILI categories of anomaly types (e.g., crack-like, notch-like, crack-field, seam anomaly, Type A, Type B, etc.) often mischaracterized what was found upon direct examination. This is best illustrated in Table 3, Table 7, Table 9, Table 10, Table 11, Table 12, and Table 18. Therefore, the usefulness of these categories for making excavation decisions is questionable.

The reviews of these 13 cases consistently point to two significant weaknesses in the use of ILI crack-detection tools for ERW seam assessment. One weakness relates to the ILI itself. The sizing accuracies for anomaly length and depth leave something to be desired. More importantly, defects with sizes exceeding the threshold detection limits of the tools were missed. The other significant weakness is related to the fact that field NDE measurements of the lengths and depths of anomalies are unreliable and should not be considered as a sufficient means to "prove-up" ILI crack-detection tool results unless the NDE methods have been carefully calibrated for the pipeline being inspected.

A third weakness in the use of ILI crack-detection tools for ERW seam integrity assessment that may not be obvious from the reviews of these 13 cases has to do with calculating failure stress levels and predicting remaining lives of anomalies found and sized by the ILI. These predictions along with ILI anomaly categories are typically used to prioritize field examinations of anomalies. As has been shown previously in another report on this project[8], the inability to determine the applicable strength and toughness in the ERW weld zone because of high variability of these properties along the seam means that predictions based on existing models are not dependable. Because of this and because of the previously mentioned weaknesses, the operator of an ERW pipeline really cannot have confidence that the seam integrity has been validated even though the lengths and depths of the detected anomalies are given, the failure stress levels and remaining lives have been calculated, and the ostensibly injurious anomalies indicated thereby have been repaired.

---

[7] These CMFL tool runs were done without "enhanced filtering" a technique which has been introduced by one pipeline operator. The presentation entitled "KMAP™ for Longitudinal Weld Threat Analysis" given by Noel Duckworth on behalf of Kinder Morgan at the PHMSA Pipeline Seam Weld Workshop in Arlington, VA on July 20, 2011 introduced a new procedure for improved analysis of CMFL data. The results mentioned in that presentation suggest the CMFL technology used with enhanced filtering could be significantly more effective than was demonstrated by the cases reviewed in this document.

[8] Subtask 1.4 report: Draft Report on ERW and Flash Weld Seam Failures, May 30, 2012.

It is worthwhile to consider ways in which the use of crack-detection ILI as currently practiced could be used as a useful indication of the seam integrity of the segment. One way would be to conduct a hydrostatic test of the pipeline in conjunction with (i.e., after) an ILI. The test would show whether or not serious anomalies had been either not detected at all or mischaracterized with respect to size even if detected. The higher the test-pressure-to-operating pressure without having seam failures, the more confidence one could have that no serious anomaly was missed or mischaracterized. If seam splits occur during the test, the visible attributes of the initiating anomalies and the associated failure pressures can be compared to the ILI attributes and the failure pressures calculated on the basis of the ILI attributes. While it seems like a hydrostatic test is a costly duplication of seam integrity assessment, an ILI tool run which does not result in high confidence that all injurious anomalies have been found and repaired does not constitute a validation of ERW seam integrity. As ILI crack detection improves, as it almost certainly will, hydrostatic testing in conjunction with a tool run may become unnecessary.

Another way to determine the reliability of crack-detection ILI without performing a hydrostatic test is to use field examinations with NDE methods to confirm the locations of anomalies and then to remove sufficient numbers of samples for destructive evaluation to validate the findings of the tool inspection. In this respect, destructive testing should consist of breaking open and/or sectioning defects to determine physical dimensions. Alternatively, the samples could be subjected to burst testing, so that the dimensions of the origin defect can be measured to assess the sizing accuracy of the ILI and/or field NDE measurements. The burst pressure would also be a useful benchmark of the effectiveness of the ILI run, and it would provide data for further evaluation of predictive models.

Alternatively, a pipeline operator may be able to verify seam integrity by grinding external-surface-connected anomalies to a depth and along a length consistent with safety at the existing internal pressure. If the anomaly is removed by such grinding, the depth and length of grinding necessary to eliminate the anomaly can be used to assess the accuracy of the ILI and/or the field NDE. Any anomaly for which grinding to a safe depth and length does not eliminate the anomaly would have to be repaired or removed. Any removed segment can then be subjected to burst testing and/or metallographic examination as described previously.

The facts that ILI technology continues to improve and that continued use of the tools is one of the best ways to evaluate them, strongly suggest that ILI crack-detection technology should continue to be accepted as one component of an ERW seam-integrity assessment. However, more rigorous verification of tool performance is needed. For future use of ILI for ERW seam integrity inspection, the use of one or more of the following verification procedures is recommended.

- A hydrostatic test of the pipeline can be conducted to assess the integrity of the ERW seams.
- A field-NDE calibration program can be carried out. This could consist of blind examinations of ERW seams on pieces of ERW pipe either taken from the pipeline to be inspected or from pipe of the same manufacturer and vintage. Some industry-sponsored entity could acquire and maintain sets of calibration pipes removed from active pipelines. The NDE on these samples could be calibrated based on destructive metallurgical examinations of the located anomalies. After all located anomalies have been examined and compared to the NDE findings, additional pipe samples could be subjected to pressure testing to a level of at least 100% of SMYS to assure that no injurious defects were missed. By doing this, the pipeline operator can have some assurance that the dimensions of anomalies found by the ILI that are evaluated by field NDE will be believable.
- Samples of pipe containing anomalies found by the ILI can be removed and subjected to metallurgical examination and/or burst testing. Direct examination of the dimensions of defects allows calibration of the dimensional accuracy of both the ILI and the field NDE. Samples not used for metallurgical examination can be subjected to burst testing to prove that no injurious anomaly was missed.

Eventually, as confidence in the capabilities of the technologies grows, the need for these verification procedures will diminish.

Finally, there is the question of what to do about the apparent inability of typical failure stress prediction models to accurately predict the failure stress levels of flaws in or adjacent to ERW seams. The problem may not be the models themselves; they certainly have been well-validated for flaws in ductile pipe parent metal. The problem is that the strength and toughness of the ERW weld zone are usually quite different from the parent metal and notoriously difficult to measure because of high variability from point to point along the seam. No model will be satisfactory until or unless the applicable strength and toughness are known. Efforts are underway on other tasks within this research project that may shed light on how to get the applicable strength and toughness and to assess models that could be applicable to the brittle behavior often associated with ERW seam failures. In the meantime, pipeline operators utilizing crack-detection ILI technology for ERW seam assessment should continue to use available models to prioritize excavations, but once the anomalies have been characterized, the focus should be on consideration of the dimensions and type of anomalies. Conservative repair criteria should be followed in the absence of certainty about the strength and toughness of the ERW seam.